Quantitative electron probe microanalysis of carbon in binary carbides

QUANTITATIVE ELECTRON PROBE MICROANALYSIS OF CARBON IN BINARY CARBIDES

Dr.Ir. G.F. Bastin and Ir. H.J.M. Heijligers

Laboratory for Physical Chemistry,
Eindhoven University of Technology
P.O. Box 513, 5600 MB Eindhoven
Netherlands.

Work performed in the period:
March 1983 - March 1984

First Edition: March 1st 1984.

Second Revised Edition: April 10th 1985.

Laboratory for Physical Chemistry
P.O. Box 513, 5600 MB Eindhoven

ISBN 90-6819-004-0 CIP

CIP-DATA KONINKLIJKE BIBLIOTHEEK, DEN HAAG

Bastin, G.F.

Quantitative electron probe microanalysis of carbon in binary carbides : work performed in the period: March 1983-March 1984 / G.F. Bastin and H.J.M. Heijligers. - Eindhoven : University of Technology. - Ill.
Publ. of the Laboratory for Physical Chemistry. - With ref.
ISBN 90-6819-004-0
SISO 542 UDC 541.1
Subject heading: microbeam carbon analysis.

page

CONTENTS

SUMMARY

Quantitative electron probe microanalysis has been performed in 13 binary carbides over a range between 4 and 30 kV, both for the metalcomponent as well as for carbon. The practical problems encountered in carbon analysis are discussed in detail and solutions to these problems are proposed. It is shown that in the case of very light elements like carbon it is no longer permitted to measure X-ray intensities at the position of the maximum of the emission peak as the shape of the carbon-K_α peak is found to be subject to strong alterations according to the type of chemical bond involved. As a consequence integral measurements have to be performed and it is shown that errors of 30-50% are easily made if this is neglected.

The present work has resulted in a total of 145 accurate intensity ratios with respect to pure element standards in the case of metals and 117 (integral) intensity ratios with respect to Fe_3C for carbon, which served as a reliable data file on which four current correction programs were tested on their performance.

Evidence is presented that the existing sets of mass absorption coefficients for carbon-K_α radiation are not fully consistent and a new set is therefore proposed, which is in better agreement with the experimental results.

Finally it is shown that the modified Gaussian $\phi(\rho z)$ approach (BAS-program), when used in conjunction with the new set of mass absorption coefficients, leads to unexpectedly good results: a relative root-mean-square value of 3.7%. This demonstrates that even for carbon very good accuracy can be obtained provided that proper care is exercised in the measurements and the proper procedures are followed.

I. INTRODUCTION

Since the development in the first half of the sixties of pseudocrystals with sufficiently large interplanar spacings to make the detection of very light elements (atomic number Z<10) possible, a large number (see e.g. Ref. 1-12) of papers have appeared on the subject of quantitative electron probe microanalysis of these elements.
Many of these publications have dealt with the practical problems encountered in this particular type of work, while others have discussed the applicability for the various matrix correction procedures then available or have led to the introduction of new procedures[1].
The result of all this is that the practical problems seem to have been well discussed while it is to a large extent still an open question which of the existing correction programs, if any, is capable to deal with e.g. the enormous absorption correction which often has to be applied in order to convert the measured intensity ratio (k-ratio) into concentration units. In this connection it is interesting to note that e.g. in B_4C at 30 keV the measured k-ratio for carbon has to be multiplied with about 20 in order to correct for absorption alone!
Recently, our own correction program[13,14] has been added to the list of existing programs and it has been indicated[14] that this particular program, based on the use of Gaussian $\phi(\rho z)$ (ionisation vs. mass depth) curves, might be well suited to the application on light element analysis.

Quite frankly it must be stated that the main reason for the uncertainty about the performance of the existing programs is undoubtedly the general lack of reliable data on which the programs can be tested.
One of the main objectives of the present work, therefore, has been to supply a sufficiently large data file of accurate measurements on which the existing correction programs (and future possibly improved programs) can be tested and compared. The second motive for the present investigation was the fact that a long-term investigation is going on in our laboratory into the diffusion of carbon in the ternary systems Ti-Fe-C and Ti-Co-C for which it was an absolute necessity to develop microanalytical techniques capable of measuring carbon quantitatively with a relative accuracy of better than about 3% .
For these reasons an extended series of measurements of carbon k-ratios were carried out on 13 binary carbides over a large kV-range. Somewhat special emphasis was thereby laid on the measurements in Ti-carbides.

II. PRACTICAL PROBLEMS IN LIGHT ELEMENT ANALYSIS

The practical problems encountered in the analysis of light elements can be summarized as follows:

1. First there is the problem of a low yield of X-rays, coupled with a relatively inefficient detection system. In order to overcome this problem, one would be inclined to increase the beam current in an effort to increase the count rate for carbon to acceptable levels. This, however, may automatically lead to
2. Dead-time problems for the metal lines if these are to be measured simultaneously, and to appreciable pulse shift problems. These problems are the result of the counter being choked by abnormally high countrates, and can be overcome by either measuring the metal and carbon separately, with obvious disadvantages, or by ressorting to higher orders of reflection for the metal.
3. The next problem is that of the frequent interference of higher order metal lines with the Carbon-K_α line.
   Notorious examples in this respect are metals like Cr and Zr. This problem is usually tackled by applying a rather sharp discrimination in the pulse height analyser of the detection system. This situation, however, bears the inherent risk of a magnification of the effect of small pulse shifts as a result of large differences in count rates between standard and unknown. Serious errors in the k-ratios may then result since differences in count rates between standard and unknown may well amount to two orders of magnitude.
4. A further problem is that of the measurement of the background. The usual procedure of measuring the background on either side of the peak and interpolating between these values, is absolutely out of the question in light element analysis as this may lead to dramatic errors (100% or more for low concentrations), especially in the present case of carbon analysis. This problem is closely connected with that mentioned under 3. and also with the problem of
5. Contamination. This is a consequence of hydrocarbons in the vacuum system being cracked at the point of impact of the electron beam, resulting in a carbonaceous deposit which yields an increasing carbon count rate with time. As the problems mentioned under 3-5 are obviously closely connected, they will be separately discussed in II.1.
6. The choice of a suitable carbon (containing)-standard presents another problem. As there are a number of allotropic forms of carbon available, like synthetic or

natural diamond, various types of graphites, or glassy carbon, it is difficult to arrive at a well-founded decision in favour of one of them.
It is a fact, though, that Weisweiler[5], in an extended series of papers (e.g. Ref. 4-6), arrived at the choice of glassy carbon, mainly because of its good electrical conductivity (contrary to diamond) and its isotropic behaviour (in contrast to the various grades of graphite which showed strong orientation-dependent characteristics). In many respects Weisweiler found that diamond was more an exception in the series of allotropic carbons!
In the present investigation we preferred the choice of cementite (Fe_3C) as a standard, mainly because the expected count rate for carbon is more or less comparable to that in most binary carbides which would rule out problems of pulse shift in cases of sharp discrimination. Moreover, cementite can easily be prepared and has a fixed composition (line compound).

7. The knowledge of the mass absorption coefficients is another difficult issue, Table II.1. shows the values according to different sources and it is obvious that differences of more than 100% are not uncommon. Needless to say that the large uncertainty in these data introduces an enormous uncertainty into the results of any correction program.
8. The choice of a proper correction program.
The crucial question is here whether the $\phi(\rho z)$ curve used is accurate enough to allow a correct procedure. This very important issue will be discussed in Chapter V, together with the numerical results of the various programs tested.
9. Perhaps the biggest problem discussed so far has to do with the fact that the K_α-line is produced by a K-L-transition. For very light elements ($Z<10$) the L-shell is not complete yet and includes the electrons involved in the chemical bond. This manifests itself in two ways:
   a. In appreciable shifts in the position of the maximum of the C-K_α emission peak[1,5,17]. This problem can easily be dealt with by retuning the spectrometer when moving from the standard to the unknown.
   b. In considerable changes in peak shapes.
   This is no doubt the most serious problem discussed so far and although detailed descriptions of C-K_α-emission peaks in various carbides have been given as early as 1964[17] this most important effect has since then been grossly neglected with only two exceptions[5,18]. The first concerns the work of Weisweiler on a large number of binary carbides, unfortunately restricted to only one accelerating voltage; while the second concerns the work of Love et al. on oxygen analyses.
   The immediate result of changes in peak shapes is that the intensity

Table II.1.

Mass absorption coefficients for Carbon-K_α X-rays according to various sources.

Absorber	He(74)[15]	Ru(79)[1]	He(82)[16]	K&S[9]	WW[6]	Present Work
B	37020	37020	37000	33000	31000	41000
C	2373	2373	2350	----	2535[a]	2373
Si	36980	36980	36800	31000	33000	37000
Ti	8094	8094	8090	6900	7500	9400
V	8840	9236	8840	7500	8500	10100
Cr	10590	10482	10600	7700	9500	10950
Fe	13300	13300	13900	9100	10800	13500
Zr	31130	31130	21600	20600	20600	24000
Nb	33990*	24203	19400	15800	15800	23200
Mo	32420*	15500	16400	12500	12500	19200
Ta	18390	20000	18400	8500	8500	15350
W	18750	21580	18800	10000	8700	16400

*Extrapolated over absorption edge[1].

[a]Value for glassy carbon; 2150 for diamond.

can no longer be measured at the maximum of the emission peak, as is usually done for medium to heavy elements in the tacit assumption that the peak height is proportional to the integral intensity. While this assumption is generally valid in the latter case it is completely wrong in the case of very light elements. Instead it is absolutely necessary to measure the intensities in an integral fashion. Although this is obviously a tedious operation for a wavelength-dispersive spectrometer, the problem can to some extent be overcome by the introduction of so-called Area/Peak (A/P) factors. The A/P factor will be defined as the ratio between the Area (Integral) k-ratio and the Peak k-ratio for a given binary carbide with respect to a given standard (in our case usually Fe_3C) and for a given spectrometer. The idea is now that once the A/P factor has been determined, future measurements can simply be carried out on the peak and multiplication with the appropriate A/P factor will yield the correct (integral) k-ratio. The accurate measurements of A/P factors will be discussed in Chapter III.

II.1. Contamination and Background problems

As already indicated before carbon contamination in the microprobe can be a very serious problem, especially if low concentrations of carbon have to be measured quantitatively. The sources for this effect are innumerable because virtually anything the specimen comes into contact with contains carbon, e.g. polishing agents (diamond), lapping oil, cleaning fluids etc. Besides there is the problem of hydrocarbons (diffusion pump oil) left in the high vacuum system. Under electron bombardment these hydrocarbons can be cracked at the point of impact of the electron beam, resulting in a rapid carbon build-up and correspondingly rapid increase of the carbon count rate. Several solutions to this problem have been proposed: The use of a cold (liquid nitrogen cooled) finger surrounding the point of impact on the specimen, the use of an air (or oxygen) jet in which case a fine stream of air is directed towards the point of impact of the electron beam, or a combination of both. Considering the importance of carbon contamination for the measurement of carbon it was decided at the beginning of the present investigation to start with a

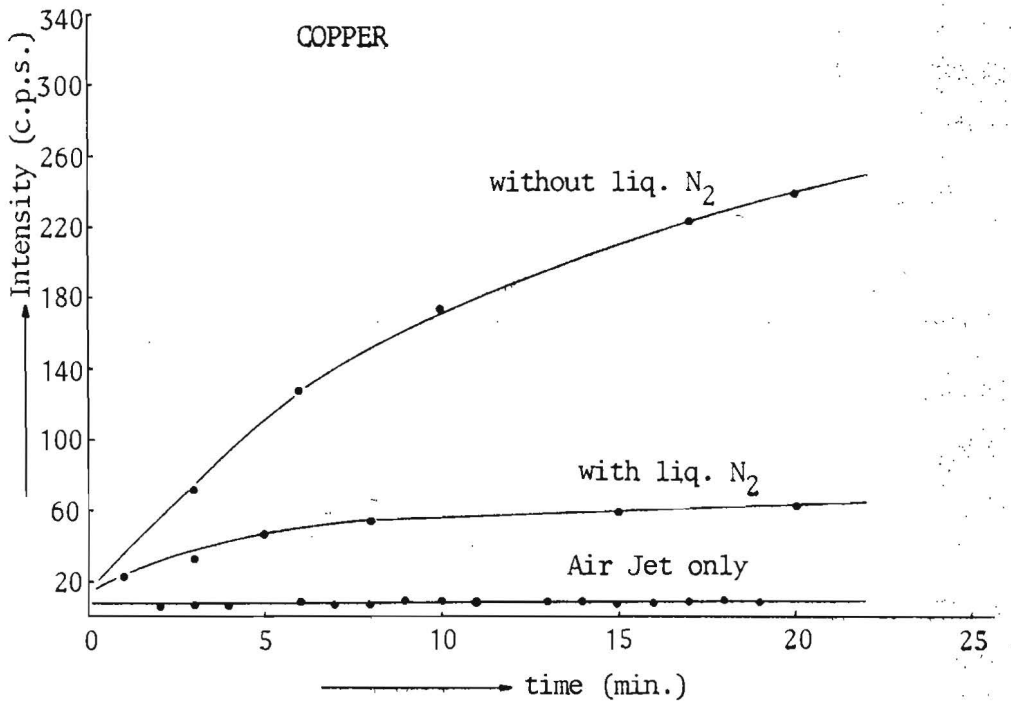

Fig. II.1. Carbon contamination rate on polished copper, without anti-contamination device, with cooling finger and with air jet. Conditions: 10 kV; 100 nA; Counter H.T.: 1700 V; Lower Level 0.6 V; Window 5.0 Volt; Gain: 64x5. Oil-diffusion pumped vacuum system.

separate investigation into the efficiency of the various anti-contamination devices, the influence of different pretreatments of the specimen and different experimental conditions in the microprobe.

Fig. II.1. shows the effect that the two anti-contamination devices have on the observed Carbon-K_α count rate on an alumina-polished copper specimen as a function of time.

It is obvious that in the long run (i.e. for very low concentrations which require long counting times) the use of an air jet represents the only efficien option in our case (JEOL Superprobe 733, oil diffusion pump).

Experiments with different gases to replace the air, the use of which reduces the life time of the filament considerably, showed that although noble gases like helium or neon do have some beneficial effect, they cannot compete with air (or oxygen). It is noticeable, though, that the use of an air jet leads to a slightly reduced specimen current, in the order of 1%, in spite of the fact that the beam current, measured immediately after the final lens, is kept the same. Thus, it should be kept in mind that measurement of standard and unknown should be carried out under exactly the same circumstances, also for the metal! This effect is probably caused

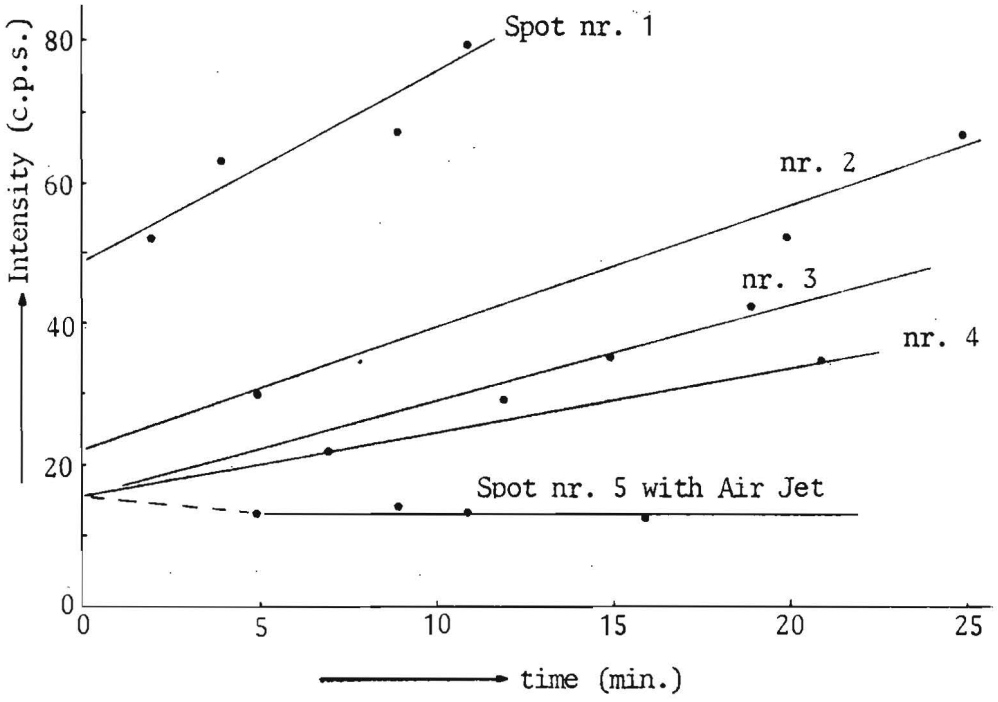

Fig. II.2. Effect on contamination rate on copper of increasing periods of time elapsed since the introduction of the specimen in the microprobe. Same conditions as in Fig. II.1. Spots 1-4 with cooling finger.

by a small fraction of the electrons being prevented from reaching the specimen by the presence of a cloud of air.
Fig. II.2 shows the effect of contamination rate, again on copper, after increasing periods of time have elapsed since the introduction of the specimen into the microprobe. Apparently the introduction is accompanied by an initial increase of contamination, probably caused by the release of hydrocarbons from the specimen mount and the operation of a number of grease-covered O-rings. With increasing time the contamination rate is decreased (Spots 1-4). Here too, however, the air jet is the most efficient device (Spot 5).

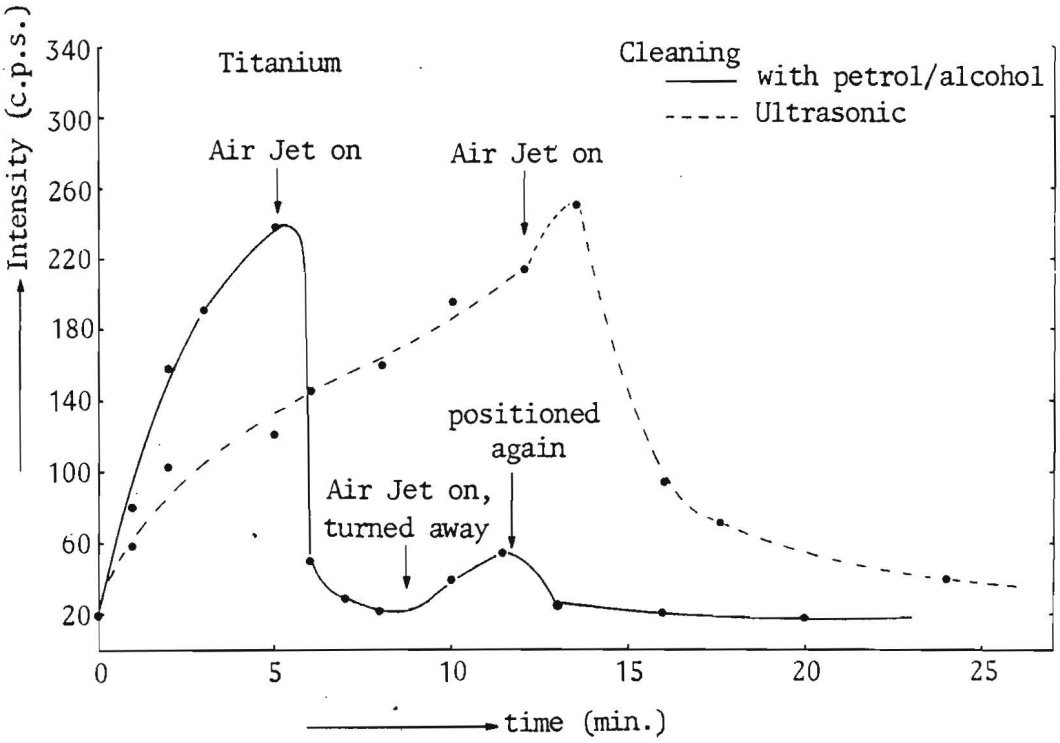

Fig. II.3. Effect of different pretreatments of the specimen on the contamination rate on Titanium. Same conditions as Fig. II.1.

The effect of different cleaning procedures is illustrated in Fig. II.3 for titanium. Ultrasonic cleaning of the specimen must clearly be preferred over the more conventional cleaning with light petrol and alcohol. Again, however, the powerful action of the air jet is obvious. Especially the observation that on spots, already heavily contaminated, the air jet is capable of reducing the carbon count rate quickly again to a constant and very low level, is quite impressive.

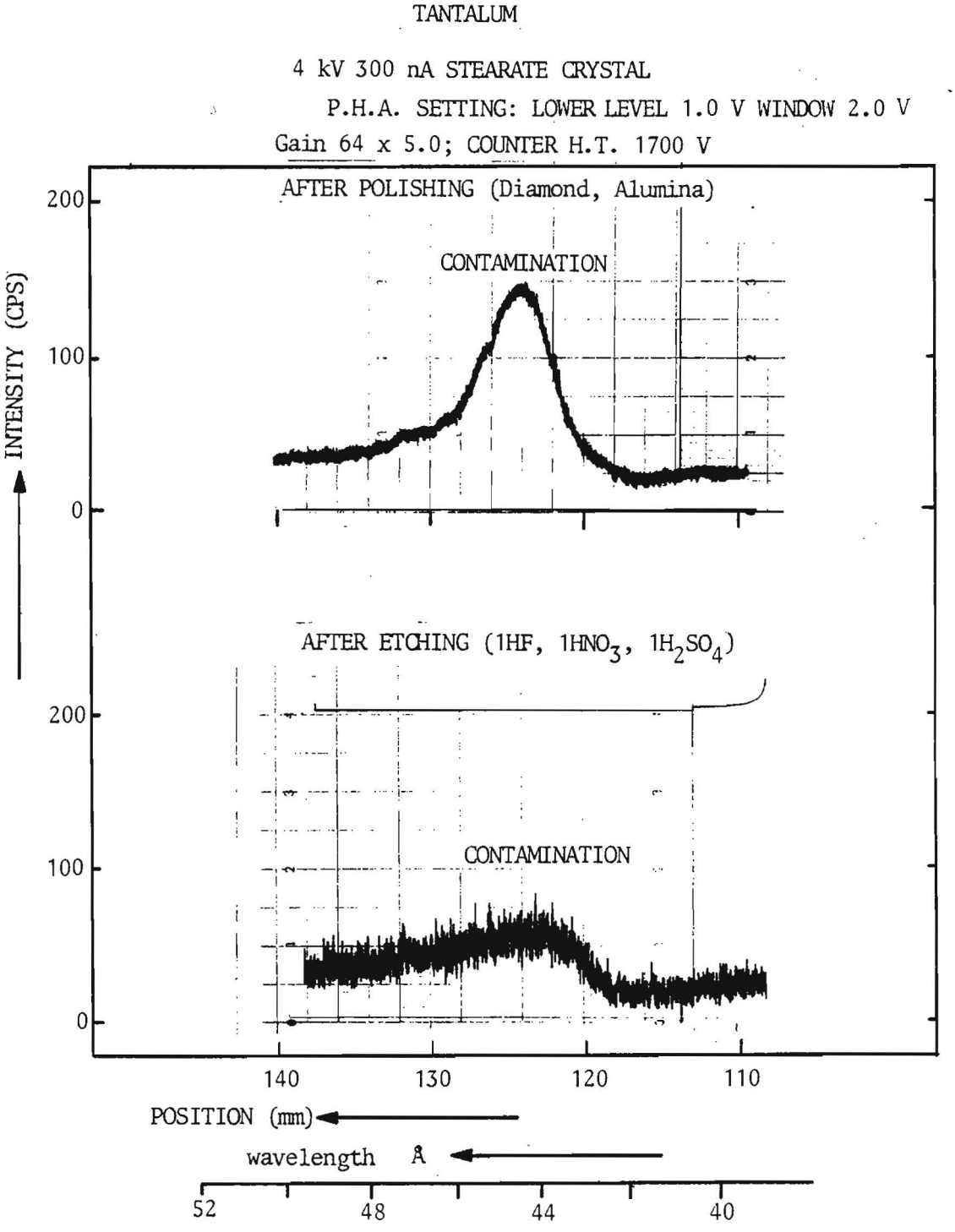

Fig. II.4. Influence of the polishing procedure on the contamination rate on a Tantalum specimen; Top, after polishing with diamond and alumina; Bottom, after etching with 1 HF, 1HNO_3, 1 H_2SO_4 by volume. Air jet switched on.

At this point some remarks must be made on the quality of the specimen and the specimen mount. The latter must be perfectly moulded and completely pore free. It has been observed on many occasions that the use of not-well-moulded specimens can result in incredibly high contamination rates because of the release of carbon-containing agents from porous areas. In such cases even the air jet can no longer be relied upon, and the only solution is to remount the specimen. For the same reason one must be very suspicious of pore-containing specimens. These can only be used after meticulous cleaning (ultrasonic), followed by a thorough degasing treatment, preferably in high vacuum for long times.

Another artefact can be introduced by the polishing techniques used, especially in the case of relatively soft metals. A conspicuous example of this effect is given in Fig. II.4 for Tantalum. In spite of the fact that final polishing has been done with alumina, it must be concluded that considerable amounts of diamond dust are still present in the surface. After etching with a 1:1:1 mixture (by volume) of concentrated HF, HNO_3 and H_2SO_4, which revealed the grain structure of the metal, the observed carbon peak has been drastically reduced. At the same time, however, it is obvious that the carbon count rate is not completely reduced to zero, not even with the use of the air jet. Apparently some contamination is always present and this effect has to be taken into account! As this problem is closely connected with that of background determination, it will be discussed later on in this section.

Next a number of experiments were carried out in order to determine the influence of the micro-probe conditions, like focused or defocused beam, scanning rectangular areas of variable sizes etc. on the contamination rate. To this end a silicon <111> single crystal was selected as this could easily be polished and the danger of rubbing diamond into the surface, like in the case of tantalum, could be considered negligible.

The general conclusions of this investigation can be summarized as follows:

1. It is always observed that the carbon count rate immediately after the positioning of the beam on a new spot is higher than after 30 seconds (Air jet on!). This conclusion is generally valid for all materials investigated (metals as well as carbides).

   A quite similar behaviour is usually found for the absorbed current; synchronously with the decrease in carbon count rate a decrease in absorbed current is observed.

   Apparently it takes some time, usually 30 seconds to 1 minute, even with the air jet on and fully focused beam, to attain a stable and

stationary situation. This should always be borne in mind in the analysis of carbon.

2. The time, necessary to obtain a stable and minimum count rate is dependent on the accelerating voltage; the lower the kV, the longer the time that is required.
3. The more the electron beam is defocused, the longer it takes to attain an equilibrium (and minimum) count rate.

The same conclusion applies when the beam is scanned over rectangular areas. Some of these features are summarized in Table II.2.

Table II.2.

Carbon contamination experiments on <111> Si-single crystal.
Time required to obtain a stable and minimum carbon count rate.
Conditions: 10 kV; 300 nA; Stearate Crystal.
P.H.A. Settings: Counter H.T.: 1700 V; Gain 64x5; Lower Level: 1.0 V; Window 2.0 V.

	BEAM MODE									
	SPOT						SCANNING			
Beam diam. (μm) or length of sides scanned (x 1.85 μm)	Foc.	10	20	30	40	50	1x3	2x5	5x5	10x10
4 kV; without anticont. device Time (min.)	1*	2	3	3	4	4				
with air jet	1/4	1/3	2/3	1½	3	4	1/3	2/3	1½	2
6 kV; with air jet Time (min.)									1/3	1

* Without decontamination device the absorbed current decreased during one minute from 228 nA to a minimum of 218 nA and then gradually increased over a 3 minute period to a stable level of 221 nA.
At the same time the carbon count rate dropped from an initial value of 125 cps to 95 cps and increased then to a constant level of 155 cps.

10 kV 300 nA; STEARATE CRYSTAL
P.H.A. SETTING: LOWER LEVEL 0.6 V, WINDOW 5.0 V
COUNTER H.T. 1700 V, GAIN 64x5.0

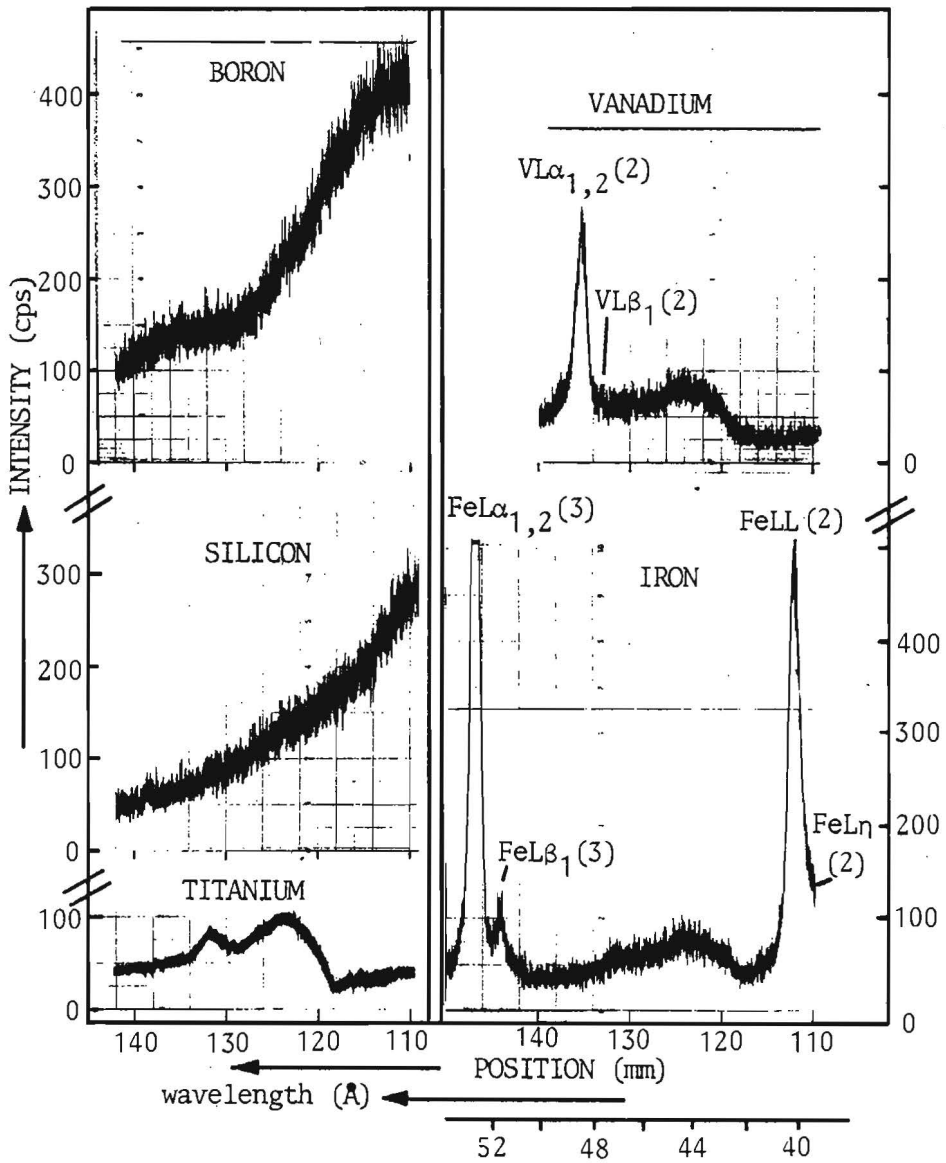

Fig. II.5. Backgrounds recorded in the spectral region of the Carbon-K_α peak on various elements. The Carbon-K_α peak itself is to be expected at about 124 mm.

10 kV 300 nA STEARATE CRYSTAL

P.H.A. SETTING: LOWER LEVEL 1.0 V WINDOW 2.0 V

GAIN 64x5.0; COUNTER H.T. 1700 V.

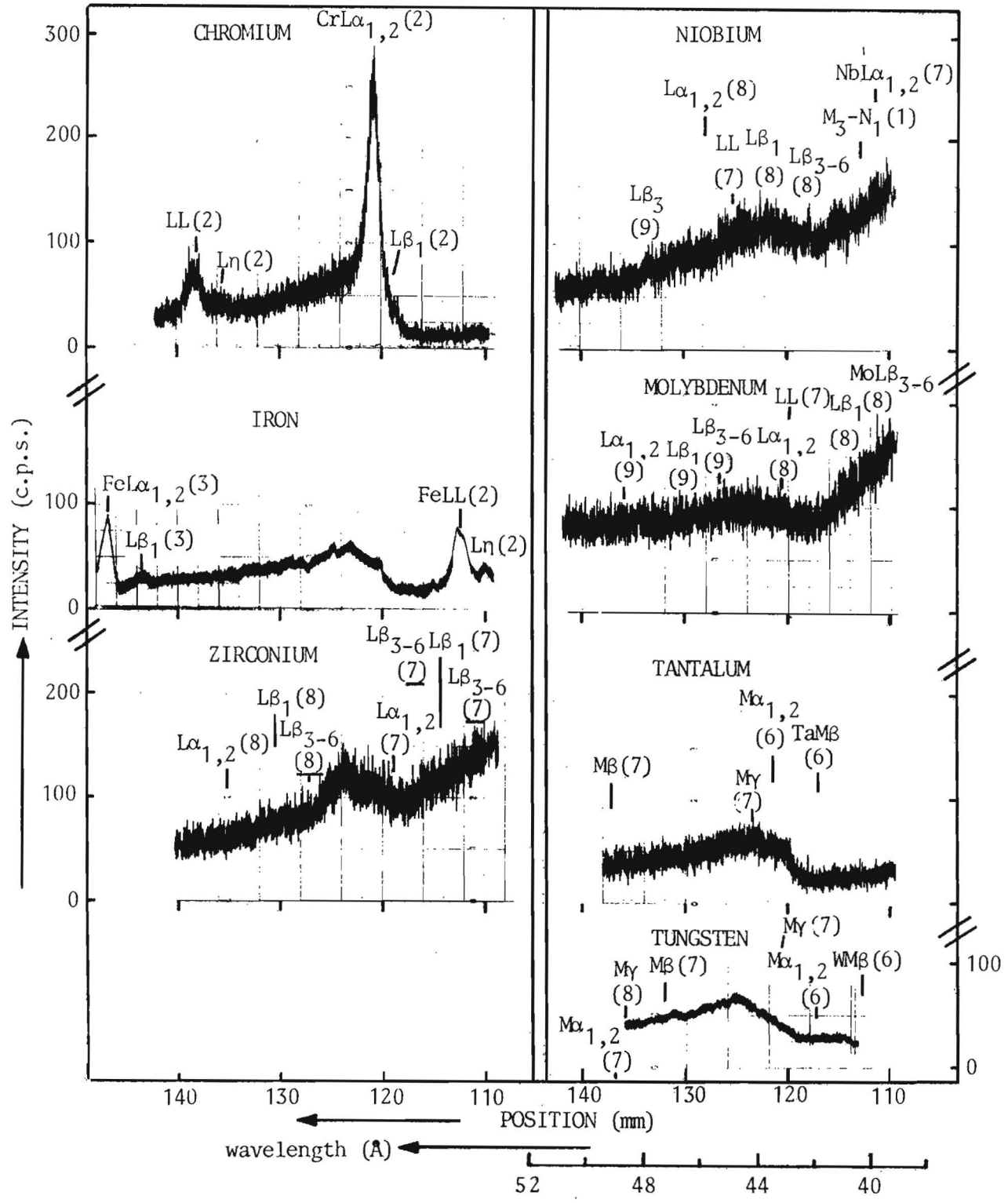

Fig. II.6. Backgrounds recorded in the spectral region of the Carbon-K_α peak on some of the heavier elements. Note the sharper discriminator settings.

As a quite general conclusion it can be stated that the best anti-contamination procedure consists of the use of a highly localized power density (high kV, best possible focus) combined with the use of an air jet (or any other oxygen-containing gas).
The oxygen is apparently necessary in some kind of "combustion" process which is capable of cleaning even heavily contaminated spots (see Fig. II.3). This process, however, only takes place at the exact point of impact of the electron beam and it has been observed on many occasions that even with the use of an air jet the wide surroundings of the spot become heavily contaminated after long periods of time. Long dwell times on the specimen in order to select suitable locations for analysis must therefore be avoided.

Another aspect of contamination is that it does not take place to the same extent on various elements.
Fig. II.5 illustrates these differences for 5 different elements. While the effect on boron and silicon is virtually absent at a first glance, it can be clearly noticed on the transition metals Ti, V and Fe. Perhaps this has something to do with the heat conductivity of the element in question which can be expected to be low for B and Si, leading to a better "burn-off" of the carbon. The reverse probably applies to the metals. Perhaps also some kind of catalytic action of the metal may play a role in the process of cracking and subsequent deposition of carbonaceous material.
In any case the different effects of contamination on different elements have to be taken into account, certainly when low concentrations of carbon have to be analyzed, in which case a correct background measurement is crucial. This, in turn, is closely connected with the problem of interference of higher order metal lines.

Fig. II.5 and II.6 clearly illustrate the topics discussed so far. Some kind of carbon contamination peak (at about 124 mm) is visible on almost all elements, in spite of the air jet. Furthermore it can be seen that the background in the vicinity of the carbon peak can have all kinds of appearances: from kinked (Boron) to curved (Silicon) to highly irregular and unpredictable in the case of the heavier metals. The last effect is caused by the very frequent interference of higher order metal lines (see e.g. Zirconium).
It is obvious that in the case of carbon the background is composed of three components:

a) A continuous background (see B and Si).
b) Remnants of higher order metal lines (see e.g. Cr), which are not fully discriminated away.

c) Residual contamination.

As a result the background can no longer be measured on both sides of the peak and interpolated in the conventional way, which has been done by Weisweiler[5]. Instead the only correct procedure consists of measurements at the carbon peak on perfectly polished (possibly etched) carbon-free samples of the constituent elements. The correct background value is then found by composing the values for the constituent elements on the basis of their weight fractions. The measurements on a carbon-free element with atomic number 6 can be avoided by interpolation between values for Boron and Silicon, or by using a compound like BN. This procedure is similar to the one proposed by Ruste[1].

While the wrong procedure would yield only small errors (a few %) in the present case of binary carbides with their high count rates and relatively high peak-to-background ratios, it would be fatal if carbon contents below 1% had to be analyzed.

III. EXPERIMENTAL PROCEDURES

The requirements for accurate micro-probe measurements demand the availability of 100% dense (at least over sufficiently large areas), homogeneous samples of binary carbides of known composition. As such specimens cannot be obtained commercially and the use of powders is out of the question, it was decided to prepare them in our own laboratory. The only exception concerns a single crystal of α-SiC (high purity, fully transparant and colorless), which was kindly supplied to us by Philips Research Laboratories in Eindhoven (Mr. G. Verspui).

III.1. Preparation and characterization of carbides

The majority of the carbides were prepared by repeated argon-arc melting of mixtures of elemental powders (purity better than 99.9%), pressed before into pellets. After melting the specimens were given a two-week homogenizing treatment at 1200°C in evacuated silica capsules, although these efforts must probably be considered futile in the light of the desperately slow diffusion rates of carbon in binary carbides[18] at these temperatures. Carbides of Ta and W could not be prepared in this way, conform literature findings[18]. In these cases layers of WC and TaC could be grown up to 20 μm thickness on the metal substrates in a R.F. furnace using a graphite + purified hydrogen environment at temperatures of 2000°C during 70h. In the same way massive specimens of W_2C, with thicknesses up to 150 μm could easily be prepared. Any solved hydrogen was removed afterwards by a vacuum annealing treatment at 900°C.

Table III.1 gives a complete survey of the carbides together with their compositions. The latter have been determined in most cases by conventional combustion techniques (LECO Corp. Equipment).

As already explained in the introduction, we had a special interest in TiC. Therefore we had this carbide (weighed-in composition 16.4 wt% carbon) analyzed at three different laboratories, with widely varying results, as Table III.2 shows.

The oxygen and nitrogen contents were typically 0.2-0.4 wt%.

At first sight these somewhat shocking differences might be explained by assuming that in spite of the homogenizing treatment apparently gross inhomogeneities still exist. This possibility, however, is not in agreement with our own microprobe measurements on this specimen which for Ti-K_α radiation showed a maximum deviation of $\pm$ 1½% in the k-ratio over the full area (about 6x5 mm^2)

Table III.1.

Survey of binary carbides used in the present investigation, with their compositions in wt% carbon.

B_4C	20.19	ZrC	8.55
α-SiC	29.95[1]	NbC	8.55
TiC	18.40	Mo_2C	5.58
VC	16.00	HfC	n.a.[3]
$Cr_{23}C_6$	5.78[1]	TaC	6.00[2]
Cr_7C_3	9.10	WC	6.13[1]
Cr_3C_2	13.30[1]	W_2C	3.16[1]

[1]These carbides were assumed to have the stoichiometric composition; in those cases where narrow homogeneity regions[18] are possible (chromium carbides) microscopic evidence like presence of second phases was used to fix the final composition.

[2]In this case the X-ray diffraction pattern, together with the characteristic golden color typical for near-stoichiometric TaC[18] was used to fix the composition.

[3]Not analyzed because of gross inhomogeneities.

Table III.2.

Results of Carbon analyses (wt%) on TiC, according to different laboratories.

LECO Corp. (demonstration)[1]	16.5 (second time 18.5)
Aachen Univ. of Techn. (Germany)[2]	18.4 (three times)
Philips Res. Labs. Eindhoven[3]	15.6
" "	14.8
" "	18.2
" "	17.1
" "	16.6
" "	16.0
" "	17.9

[1]The help of Mr. P. v.d. Dool of LECO Corp. Heerlen (Netherlands) is gratefully acknowledged.

[2]Thanks are due to the Chemistry Dept. of Aachen Univ. of Techn., through Dr. P. Karduck (Aachen, Germany).

[3]Analyses kindly performed by Mr. P. Vullings, Anal. Lab. of Philips' Research Labs. (Eindhoven, Netherlands).

of the specimen. Besides, the calculated composition (carbon "by difference") according to most correction programs was found to agree rather closely with the bulk analyses of Aachen Univ. of Techn. Their value, therefore, was finally adopted as the most probable composition, the more so as they also analysed several line compounds correctly. A last indication to put most faith in their results was found in the analyses of ZrC and NbC which are both virtually at the substoichiometric edge of the homogeneity region[18] (see Table III.1). In both cases microscopical evidence, like small Zr precipitates in the first case and Nb_2C precipitates in the second case, substantiated their conclusions.
Perhaps the large discrepancies could be explained on the basis of varying amounts of free carbon which always present a real danger in carbides[18]. Moreover it must be realised that in combustion analysis of carbon no distinction is made between free and bound carbon, whereas in microprobe analysis one is inclined to select dense, pore-free areas, free of inclusions or precipitates. Perhaps this explains to a great deal the differences between a bulk-analysis technique and a local (micro-probe) technique. A further problem for any combustion technique seems to be a total lack of suitable carbon standards in the proper composition range; the maximum concentration available is about 4 wt% C. This would render the extrapolation process towards high carbon contents somewhat uncertain.

The cementite (Fe_3C) which was used throughout this investigation as the carbon standard, was prepared by arc-melting of an Fe (4 wt% Carbon) alloy, followed by a week homogenizing at 1000°C in evacuated sealed silica capsules. This procedure usually yielded large platelets of cementite. In many cases also cementite in the shape of needles (about 20 µm diameter) were used. These were supplied to us by T.N.O. Apeldoorn, Netherlands by Mr. A.P. von Rosenstiel. Microanalyses showed the carbon contents of both types of specimens to be identical.

In the final stages of the investigation a number of measurements have been made with respect to glassy carbon as a standard. This specimen was kindly supplied by Mr. P. v.d. Straten (Philips Research Laboratories, Eindhoven, Netherlands).

III.2. Polishing and Cleaning procedures

After cutting of the carbide specimens with a diamond wheel they were embedded in copper-containing resin, grinded up to 600 Grit on silicon-carbide papers followed by 30 and 15 µm diamond disks. Polishing was carried

out successively with 6 and 3 μm diamond paste on a nylon cloth, 1 μm diamond paste on a soft cloth and finally with γ-alumina (0.05 μm) on a soft cloth.

In order to avoid inevitable problems with polishing of materials exhibiting large differences in hardness, the metals, cementite and carbides were prepared in separate mounts. After a satisfactory polish all specimens and standards were taken out again and assembled in a final mount, followed by a slight repolish on γ-alumina. This arrangement guaranteed a perfectly plane and parallel mount which is a vital requirement in view of the importance of the take-off angle for ultrasoft X-radiation. Final cleaning was carried out ultrasonically with alcohol followed by freon.

Usually the carbides and standards (including the metals) were arranged in groups around the central cementite standard. Thus a typical mount would e.g. contain a central piece of cementite, one B_4C specimen and a SiC-crystal, and pieces of pure boron and silicon. Likewise all chromium-carbides were grouped in one mount and also measured in the same run. In the same way, related carbides like TiC and VC, ZrC, NbC and Mo_2C, and TaC and WC were mounted groupwise and measured accordingly.

III.3. Check on the operating conditions of the microprobe

After the necessary condition for an accurate and well-known take-off angle was fulfilled, the other experimental circumstances had to be checked and these include the correctness of probe voltage, stability of beam current, proper functioning of the air jet etc.

All measurements were performed on a fully automated JEOL 733 Superprobe, equipped with 3 crystal-spectrometers and an energy-dispersive system (TRACOR NORTHERN 2000). The automation system was also supplied by TRACOR NORTHERN. The first spectrometer, specially for light elements, was equipped with a lead-stearate crystal on which all carbon analyses were performed, and a TAP crystal. The counter was of the gas-flow type; countergas argon-10% methane. The two other spectrometers contained a PET and an LiF crystal each, while the counters were of the sealed-Xenon type.

The correctness of the accelerating voltage was checked using the short wave-length cut-off measured on the screen of the C.R.T. of the multi-channel-analyzer in the EDX system. Deviations from the nominal voltage could not be detected and must therefore be assumed to be less than 20 eV, even for the lowest voltage (4 kV) used.

The stability of the beam current was found to be excellent; deviations of less than 1% over periods of up to 16 hrs were quite usual. Moreover, as the instrument was equipped with an automated beam current detector which measured the beam current before each measurement and corrected the standard count rates accordingly, any uncertainty resulting from small variations in beam current must be ruled out. Also switching from one kV to another could be carried out very fast: the instrument was found to be perfectly stable again within a few minutes.

The functioning of the air jet has been discussed in Chapter II. Tests with this device showed that a stable and minimum carbon count rate was guaranteed even over periods exceeding 16 hours on the same spot. It has been stated before that this only applies to the exact point of impact of the electron beam on the specimen. The wide surroundings (up to several tens of microns) still become contaminated as the presence of a kind of brown halo clearly indicates.
These experiments also prove, by the way, that the stability of the beam with respect to position is excellent over such long periods of time. If this would not have been the case any wandering of the beam would have manifested itself in an abrupt increase of carbon count rate because of the beam moving into the halo. This is further substantiated by microscopic investigation of the spot which showed a perfectly round and clear circle in the centre of a brown halo with gradually fading edges towards the outside.

III.4. Measurements of Area/Peak factors

The Area/Peak factors for Carbon-K_α radiation were measured by recording the integral C-K_α emission profile for Fe_3C (standard) as well as the unknown. The spectrometer was therefore scanned stepwise (0.03-0.05 mm; corresponding to 0.011-0.018 Å) over the spectral range of interest. At each successive point a large number of counts were accumulated and stored in successive channels of the multi-channel-analyzer. After completion the data were stored on floppy disk. In the beginning also Area/Peak factors for the metal lines were measured in the same run. Thus, a typical measuring sequence, e.g. for B_4C, would be: First a spectrum of Carbon in Fe_3C, then Carbon in B_4C, followed by a spectrum of Boron in B_4C and finally one of Boron in pure Boron after which the same cycle was repeated several times on different locations of the specimens. Typically, counting times per step were 5-10 seconds and the time required for a full spectrum was 1½ hours. All these measurements were carried out automatically over night.

The stored spectra were then processed to obtain the nett (area) integral and peak intensities from standard and unknown by subtracting the linearly interpolated background over the relevant region of interest. In some cases, notably the chromium carbides (see Fig. II.6.) it was considered necessary to exercise more care in the background subtraction. Here a profile recorded on pure chromium under identical conditions was also recorded. All values were then multiplied by the calculated k-ratio for Cr-L_α radiation for the carbide in question (using Henke's[16] mass absorption coefficients) and stripped from the appropriate carbon spectrum in the carbide after which the usual procedure was continued. For some carbides (SiC,TiC and ZrC) the Area/Peak factors have been measured between 4 and 20 keV (i.e. almost the full range covered in the present investigation) both for Carbon as well as the metal lines. As the Area/Peak factors turned out to be essentially independent of kV, contrary to earlier expectations[5,6], the other measurements were concentrated at kV's between 4 and 12 where the Peak-to-Background ratio for Carbon in many carbides is a maximum, with the emphasis on values around 10 kV.

The accuracy of each individual measurement can be estimated as better than 2%, which is corroborated by the observation that the Area/Peak factors for the metal lines, in spite of the relatively coarse step size for the sharp metal peaks, came out usually between 0.98 and 1.02. As an effect of chemical bond is not to be anticipated here one would expect a value of 1.00 which was indeed obtained when the step size was reduced. Hence, for the measurement of the Area/Peak factors of Carbon with its much broader peak the stepsize used is probably more than adequate and this justifies the estimated accuracy of better than 2%.

All together about 600 spectra were recorded and the final averaged A/P factors have an estimated accuracy of about 1%.

III.5. Measurements of Peak k-ratios between 4 and 30 keV.

In order to improve the statistics and to overcome the problems connected with slight inhomogeneities, inevitably present in most carbides, an extended series of accurate peak k-ratio measurements were carried out for the carbon and the metals over the range between 4 and 30 kV. These were, in the case of carbon, afterwards multiplied by the proper A/P factor to yield final Area k-ratios. In order to avoid excessive dead-time corrections for the metal lines (see Chapter II) the metals and carbon were measured separately.

The procedure used for the metals was as follows:
In a preliminary survey 6-10 suitable areas for analysis were located, the coordinates of which were stored in a points table in the computer. In the actual measurements the computer was instructed to move the specimen in 5 steps in a certain direction on each of the areas and to take point counts at each interval. In total a number of 30-50 measurements were thus performed for each carbide at each of the 9 kV's. The beam current was usually adjusted as to ensure a maximum count rate of 2500 cps, in order to avoid dead-time problems. Where possible (Ta, W) both M as well as L-lines have been measured. The air jet was not used for the metals.
A total number of 145 accurate k-ratios were thus accumulated (Ta_2C and Fe_3C included, HfC excluded). To give some idea about the homogeneity of the specimens it can be stated that the differences between the maximum and minimum count rates observed did very rarely exceed 3%. The standard deviation was usually better than 1%. The background was measured in the usual way, i.e. on either side of the peak and interpolated.

For the carbon a rather similar procedure was followed. In this case the air jet was of course used and the number of measurements increased to 10 areas with each 5 measurements. Besides, a waiting period of 30 seconds was programmed with the beam switched on (see Chapter II) for accelerating voltages higher than 6 kV and a 1-minute period for lower kV's, before the measurements were started. Measurements on B_4C, SiC, TiC and VC (and Fe_3C as standard) were performed with the same (relatively wide) discriminator settings of 0.6 Volt for the threshold and 5 Volt for the window. The window was narrowed to 2 Volt and the threshold increased to 1 Volt for the chromium-carbides and the carbides of the 5th and 6th period, in order to prevent interference as much as possible (See Chapter II, section 1). The Fe_3C standard was then, of course, measured under identical conditions. In all cases the counter high tension was 1700 Volt and the gain 64x5; counter slit open. Typical beam currents used were between 100 and 300 nA and the variations between extremes in count rates were usually within 6%.
Fig. III.1 gives an impression of a sequence of carbon measurements on ZrC, NbC and Mo_2C at 8 kV and 300 nA. The groups of 5 measurements distributed over 10 different areas are clearly visible, as are the beam current measurements. The differences in the position of the carbon peak were accounted for by a repeated, very slow peak search procedure which the program was instructed to carry out between measurements on standard and unknowns.

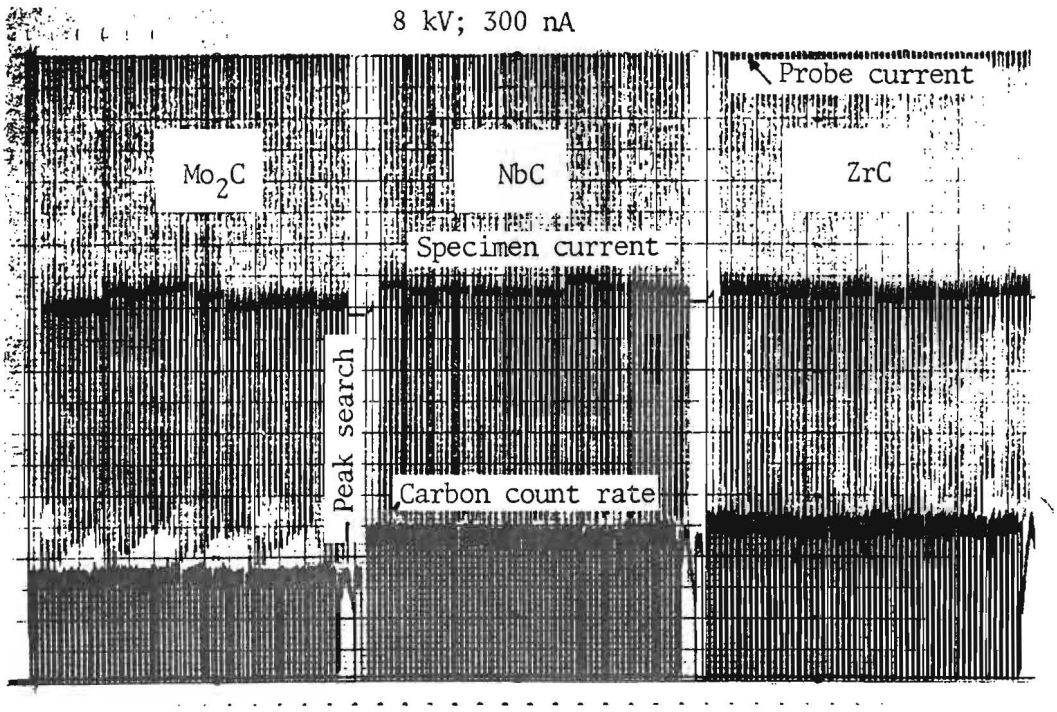

Fig. III.1. Strip-chart recording illustrating a number of peak k-ratio measurements of Carbon in ZrC, NbC and Mo_2C at 8 kV and 300 nA.

Special attention was paid to a correct determination of the background (See II.1). This was measured at the position of the maximum of the carbon peak on each of the constituent elements. That of carbon was obtained by a process of interpolation between the values for B and Si. Afterwards the background was composed on the basis of the weight fractions of the constituent elements and substracted from the gross intensities.
The final k-ratios obtained through this procedure differed only slightly (max. about 3%) from those obtained through a straight-forward interpolation between either side of the peak. This is because the former procedu affects both the unknown and the Fe_3C standard and much of the effects are lost in taking the ratio. Moreover, the Peak-to-Background ratio for most carbides is rather high.
Nevertheless, the former procedure certainly deserves preference and is in our opinion the only correct one. The second procedure would undoubtedly result in dramatic errors (several 100%) for carbon concentrations much below 1%.
All together a number of 117 accurate peak k-ratios with respect to Fe_3C (each value being the average of 50 measurements) were accumulated, which served after multiplication by the proper Area/Peak factor, as the data file on which the various correction programs could be tested.

IV. RESULTS

IV.1. Carbon Spectra in various Carbides.

Fig. IV.1. gives a survey of the spectra recorded from the various carbides. For demonstration purposes these have been recorded over a larger range than usual with a step size of 0.03 mm and counting times of 20 seconds per step. All were taken at 10 kV and 300 nA. Some general features are immediately obvious: Apparently the carbides of notoriously strong carbide forming elements like Ti, V, Zr and Hf tend to produce relatively narrow, unambiguous and highly symmetrical peaks while those of elements like Si, Fe and Mo tend to develop broader asymmetrical peaks which contain shoulders. In general the carbides belonging to the first group have a cubic crystal structure while most in the second group have hexagonal to orthorhombic structures.

Considering these spectra in detail it becomes almost self-explanatory why an intensity measurement carried out on the peak maximum has to fail. If, for example, the spectra of TiC and WC are compared it is clear that in the first case most of the intensity is concentrated in a relatively narrow area around the maximum of the peak while in the second case it is distributed over a much wider spectral region. As a consequence the former would be favoured over the latter. This leads us automatically to the next section:

Fig. IV.1. Carbon spectra recorded from various carbides and glassy carbon. 10 kV; 300 nA; Step size 0.03 mm; Counting time 20 seconds. Interval 110-138 mm.

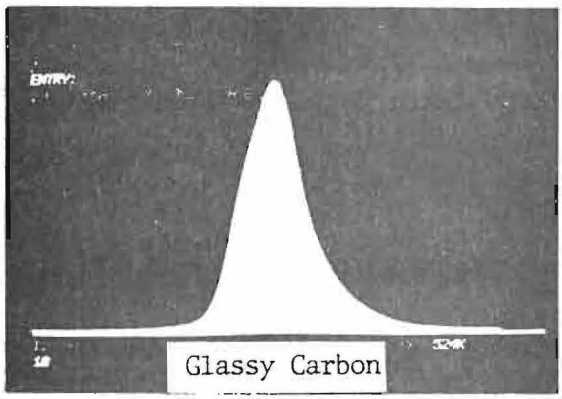
ENTRY:
Glassy Carbon

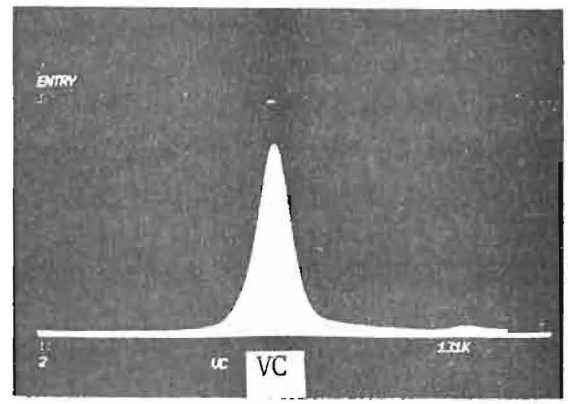
ENTRY
VC

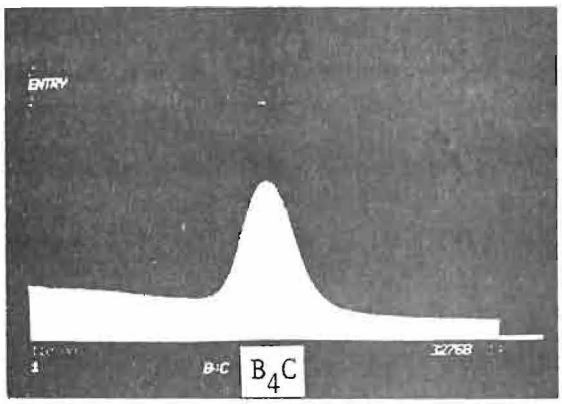
ENTRY
B4C
B_4C

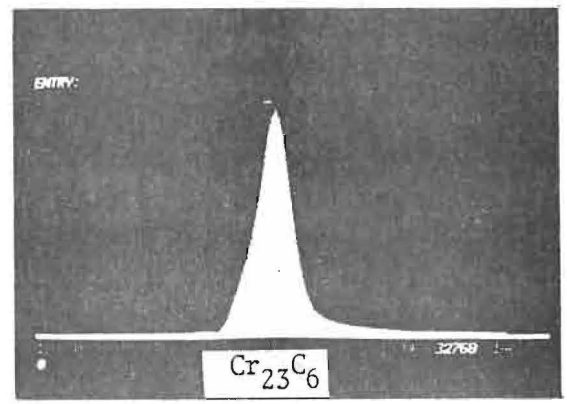
ENTRY:
$Cr_{23}C_6$

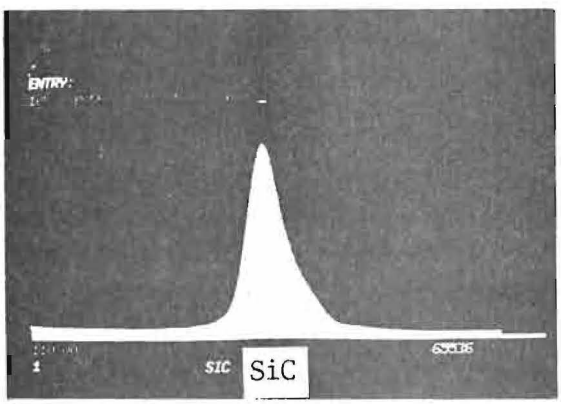
ENTRY:
SiC
SiC

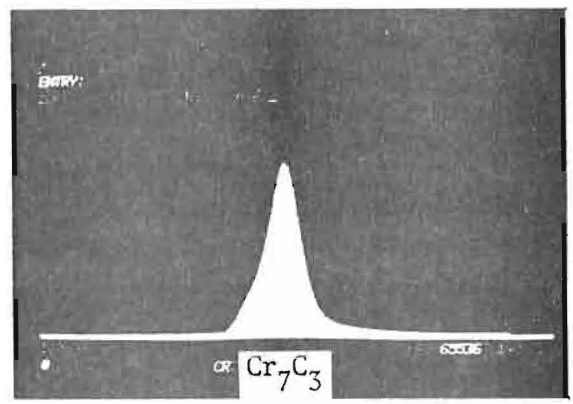
ENTRY:
Cr_7C_3

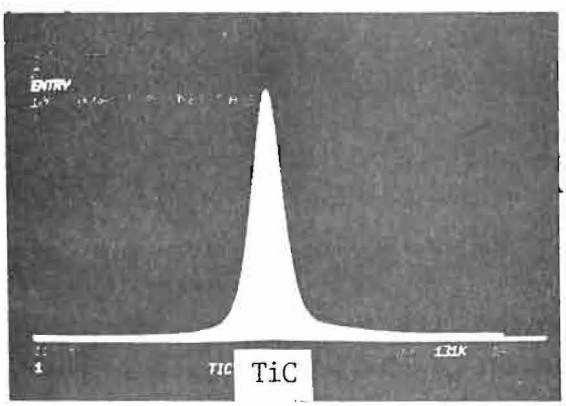
ENTRY
TiC
TiC

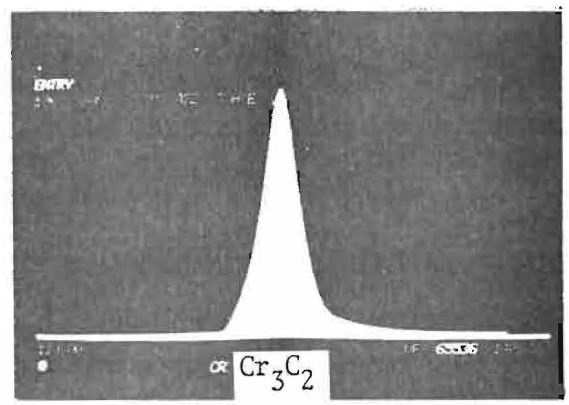
ENTRY
Cr_3C_2

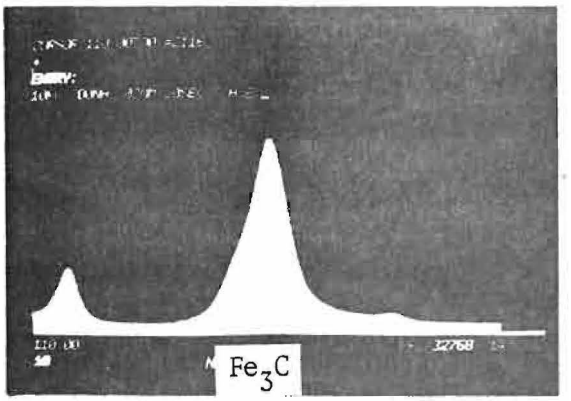

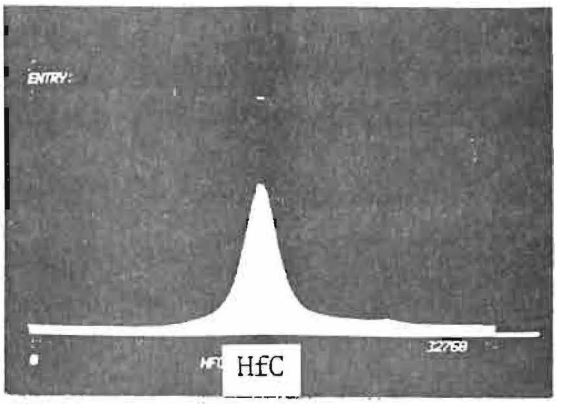

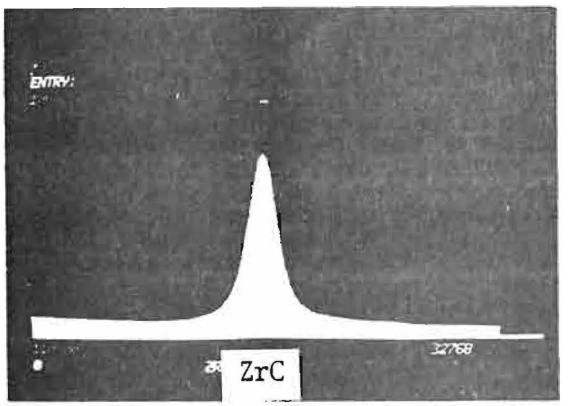

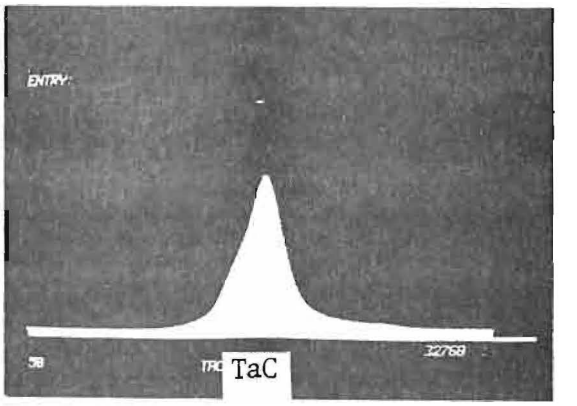

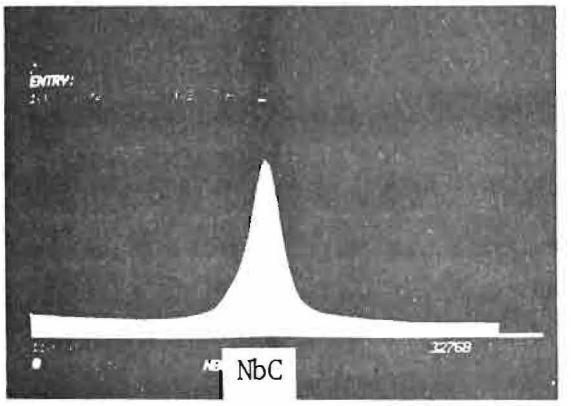

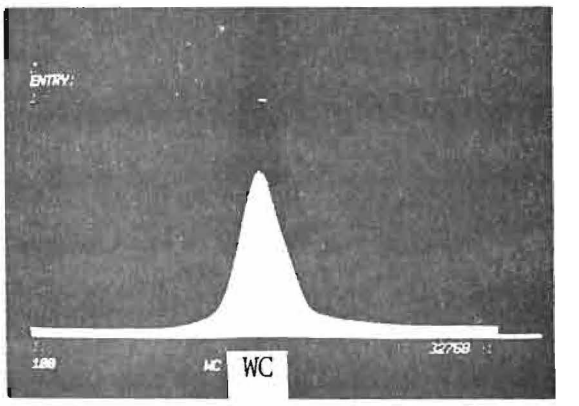

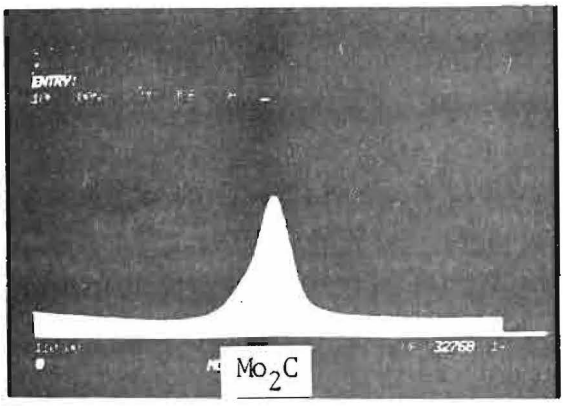

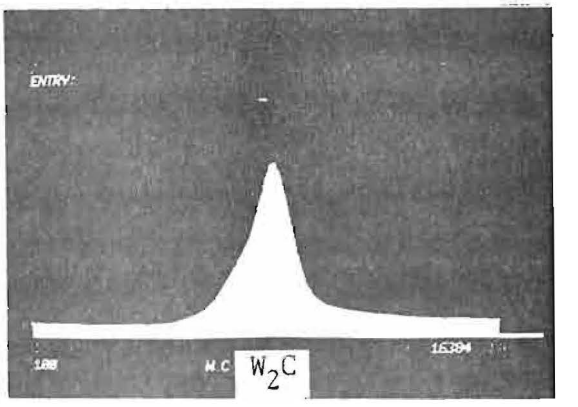

Fig. IV.1. (Continued).

IV.2. Area/Peak factors for Carbon.

From the preceeding section it has become clear that large errors can be made if k-ratios for carbon are measured at the peak. The magnitude of these errors depends of course on the choice of the carbon standard. For the present case of Fe_3C the Area/Peak factors are given in Table IV.1, together with some other relevant information. The examples for TiC and ZrC show that errors up to 30% are easily made. This would further be increased to even 50% if e.g. glassy carbon had been used as a standard. This is a result of the carbon peak of glassy carbon being even much broader than that of Fe_3C (See also Fig. IV.1) as is reflected by the A/P factor for carbon in Fe_3C relative to glassy carbon which has the value of 0.725 (average of 45 measurements).

Table IV.1.

Area/Peak factors for Carbon-K_α radiation in binary carbides with respect to Fe_3C.

Carbide	A/P factor	Peak Position (mm)	Wavelength (Å)	Structure
B_4C	1.048	124.25	44.477	Rhomb.
α-SiC (0001)	0.861	124.03	44.398	Hex
Fe_3C	1.000	124.25	44.477	orth.rhomb.
TiC	0.723	124.06	44.409	cub.
VC	0.773	124.22	44.466	cub.
$Cr_{23}C_6$	0.801	124.21	44.462	cub.
Cr_7C_3	0.803	124.19	44.455	Hex.
Cr_3C_2	0.825	124.12	44.430	orth.rhomb.
ZrC	0.715	123.88	44.344	cub.
NbC	0.787	124.17	44.448	cub.
Mo_2C	0.822	124.39	44.527	orth.rhomb.
HfC[1]	0.831	124.03	44.398	cub.
TaC	0.968	124.37	44.520	cub.
WC	0.974	123.87	44.341	Hex.
W_2C	1.021	124.57	44.591	Hex.

[1]Although the A/P factor has been measured, this carbide has been excluded from further measurements because of gross inhomogeneities.

A further conspicuous feature of Table IV.1 is the extreme shift in the peak position between WC and W_2C which actually represents the widest shift observed so far. In this case the location of the peak makes the identification of the carbide possible with almost absolute certainty.

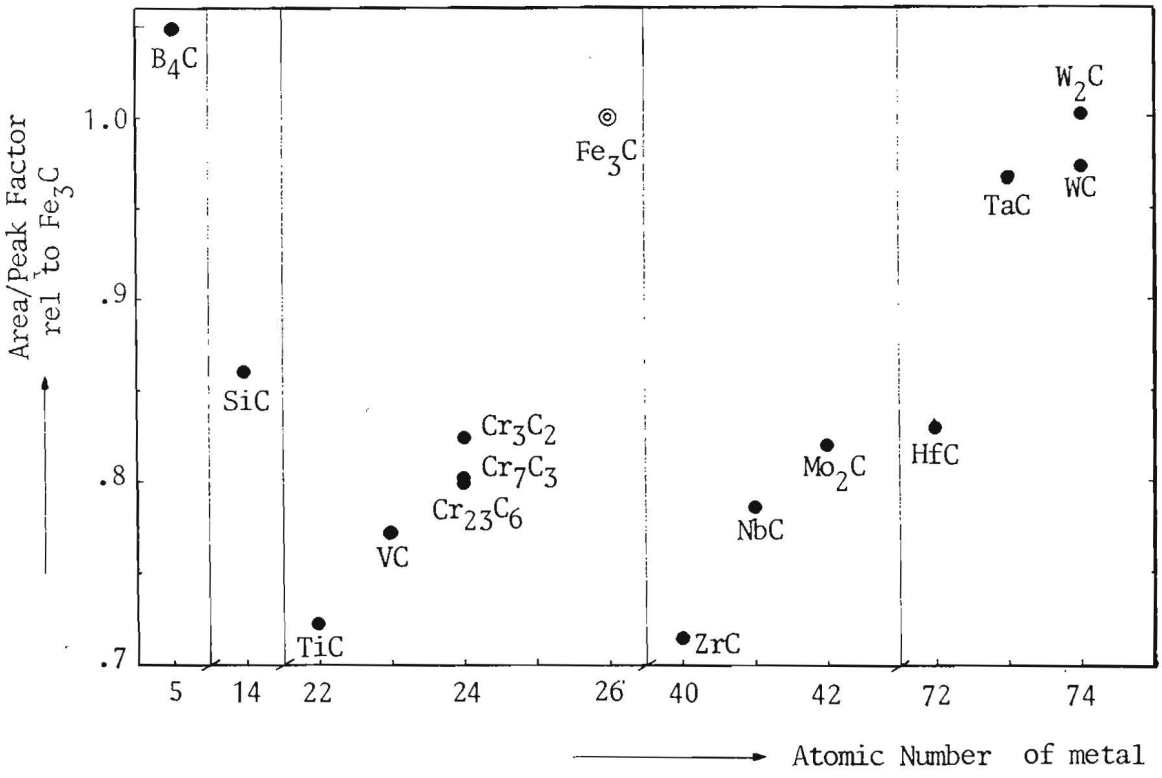

Fig. IV.2. Area/Peak factors for Carbon-K_α radiation of binary carbides relative to Fe_3C as a function of atomic number of the metal partner.
The value for Fe_3C is equal to one, by definition.

Fig. IV.2 gives a graphical representation of the measured A/P factor plotted vs. the atomic number of the metal partner. The obvious saw-tooth like appearance corresponds nicely with the beginning and ending of the periods in the periodic system. At this stage it would seem tempting to relate the peak shapes, peak position and A/P factors to the type of chemical bond involved as has been tried before by Weisweiler[5] for the former two cases. He has tried to relate the differences in electronegativity between the metal and carbon to the shape of the carbon emission peak: The larger these differences, the larger the tendency to develop only one maximum without shoulders. In his view carbides with a single maximum (TiC, VC, ZrC etc.) in their profiles have the highest bond energy (lowest enthalpy of formation)

and melting points higher than the constituent metals.
If, however, the wavelength is to be taken as a measure for the bonding stren
then the results in Table IV.1 are not fully consistent with such a view,
as the result for e.g. WC show.
Storms[18] in his book on binary carbides has also tried to find a relationship
between the stability of a carbide and the melting point of the metal involv
In very stable carbides the melting point of the carbide is raised far
above that of the metal (e.g. TiC, ZrC) whereas the reverse is true for less
stable carbides (WC, Mo_2C).
This is illustrated in Table IV.2 for some carbides from the IVth-VIth period

Table IV.2.
Stability of carbides as judged from their melting points compared to
that of the metals.

less stable, decrease of melting point. ⟶

Period					
IV	Sc	Ti	V	Cr	Mn
V	Y	Zr	Nb	Mo	Tc
VI	La	Hf	Ta	W	Re

⟵ more stable, increase of melting point.

This is discussed in terms of a competition between the strength of the
Metal-Metal bond and the Metal-Carbon bond which would be reflected in the
melting point of the carbide as compared to that of the metal.
As a whole the A/P factors in Fig. IV.2 seem to be consistent with such a vie
which to a large extent explains the saw-tooths.

Clearly, at this stage in the discussion three important questions
are still open:

- The first concerns the problem that many binary carbides can have rather wide homogeneity regions. TiC, for example can contain between 10 and 20 wt% carbon. Does the A/P factor have a constant value over this range or does it change? The answer can be found in Fig. IV.3.

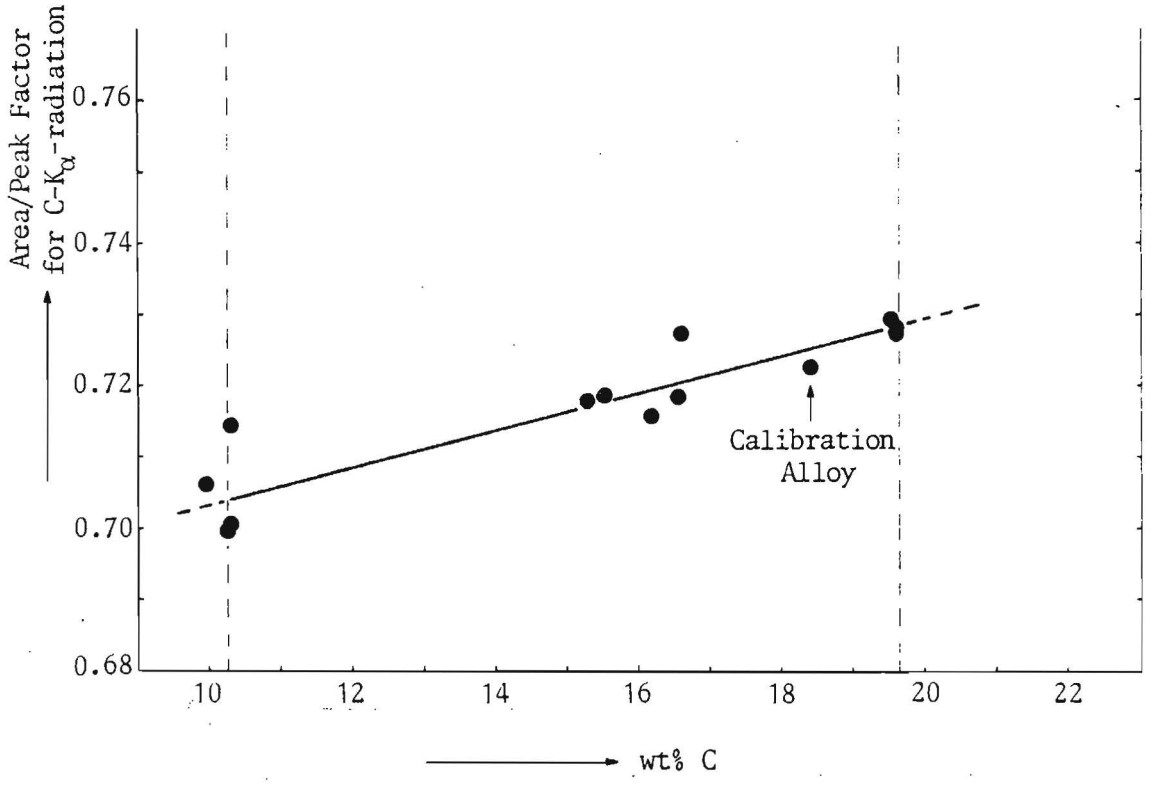

Fig. IV.3. Area/Peak factors for Carbon-K_α radiation relative to Fe_3C from a number of compositions inside the homogeneity region of TiC.

The A/P values for the extreme compositions have been measured in two-phased alloys (Ti-TiC eutectic and TiC-graphite eutectic) whereas the other compositions have been prepared in the same way as the calibration alloy and measured in our own laboratory using our own correction program (see Chapter V).
The results indicate that the A/P factor varies only slightly with composition and that for most practical purposes it could be assumed to be constant.

- The next question is: What happens to the A/P factor in the case of a mixed carbide; as many practical problems unfortunately are not restricted to binary carbides. If the A/P factor is discussed in terms of the typical metal-carbon bond involved, as has been done before, then one would expect that the A/P factor in a mixed carbide (A/B-C) could be composed on the basis of the atom fractions of the metals as these can be considered to be directly related to the number of A-C vs. B-C bonds.
This hypothesis was verified on two examples of W/Ti-carbides. Powders of these specimens were kindly supplied to us by Mr. A.P. von Rosenstiel (T.N.O. Apeldoorn, The Netherlands). Fortunately the constituent metal carbides represent the largest possible difference in A/P factors (Table IV.1)

After arc melting these specimens were fully dense and suitable for measurem
The compositions (W/Ti ratio) were determined by electron probe microanalysi
in our own laboratory.

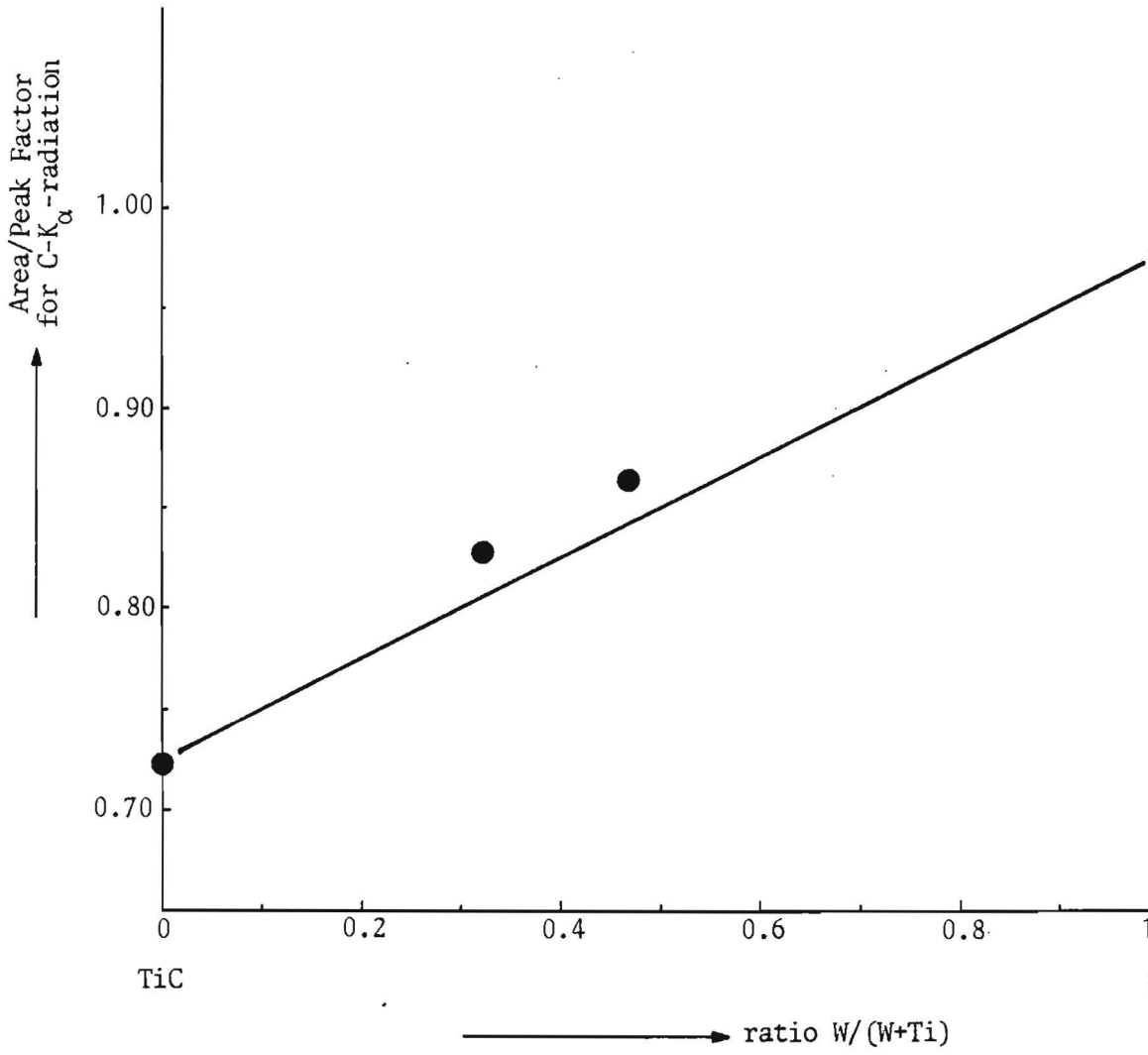

Fig. IV.4. Area/Peak factors for Carbon-K_α radiation relative to Fe_3C for two ternary W/Ti-carbides in relation to those of the constituent carbides.

As Fig. IV.4 indicates the calculated A/P factors are rather close to the measured ones. The carbon spectra are given in Fig. IV.5 (cf. Fig. IV.1).

- The last and vital question is: Are the measured A/P factors typical only for the specific microprobe with its specific crystal, spectrometer and Rowland circle, or are they of more universal value?

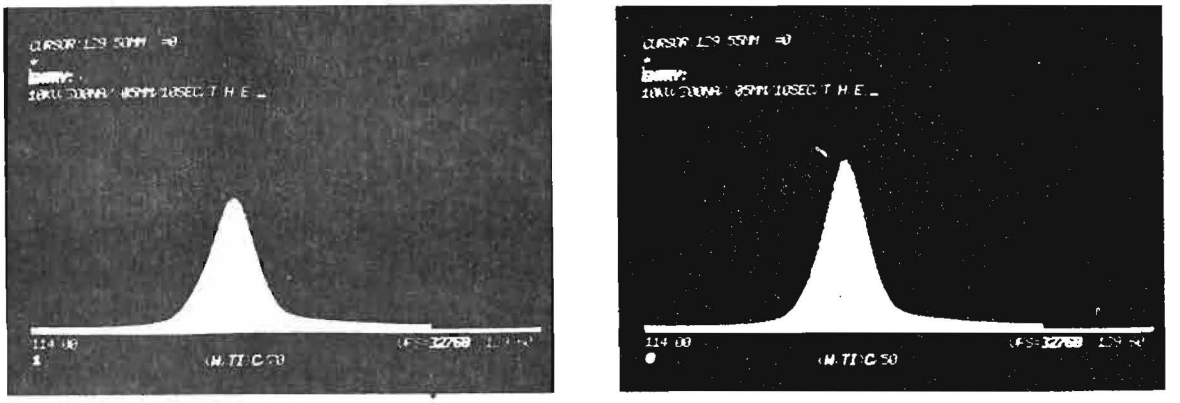

Fig. IV.5. Carbon spectra recorded from the two ternary W/Ti-carbides in Fig. IV.4. 10 kV; 300 nA; Step size 0.05 mm; Counting time 10 seconds, Interval 114-134 mm. Left hand side W-rich composition.

At first sight one would perhaps assume that the A/P factors would only apply to the particular instrument and conditions they have been measured on, in agreement with the observation that in a bad spectrometer more and more intensity is concentrated in a small region around the maximum. In a very good spectrometer, on the contrary, more and more fine-structure would be resolved leading to an extension of the peak. On the other hand, one has to bear in mind that all measurements are performed with respect to a standard and that in taking the ratio perhaps a lot of the spectrometer characteristics are divided out. There is some growing evidence in favour of the second opinion. Reports from TNO Apeldoorn, Netherlands (Mr.A.P. von Rosenstiel) where similar measurements are being carried out at the moment on the same specimens, indicate that preliminary results are very close to our values in spite of the use of completely different equipment (ARL microprobe). It is clear, however, that final conclusions in this respect, can only be drawn after similar measurements have been carried out on a number of widely varying instruments. The problem is only that A/P measurements are not too easy to perform if the microprobe is not automated. In that case one has to ressort to graphical integration of peaks recorded with conventional chart-recorders.

.1. Dependence of C-K_α X-ray emission on the crystallographic orientation of the specimen.

There is still one more vital problem and that has to do with the question whether the peak shape and the total (integral) emission of C-K_α radiation is dependent on the crystallographic orientation of the specimen. For symmetry reasons such an effect is not to be expected

for the many cubic carbides (Table IV.1.). It could be, however, perfectly conceivable for any of the non-cubic specimens. In order to investigate this effect a number of α-SiC crystals (hexagonal colorless platelets) were mounted in all kinds of orientations and their Area/Peak Factors were measured, both as a function of crystallographic orientation of the polished face exposed, as well as of the rotational position with respect to the electron beam.

The main result was that all orientations yielded exactly the same Area/Peak Factor as the value reported in Table IV.1.; i.e. the peak shape is not dependent on orientation. The same observations were made on a batch of β-SiC crystals (yellow, presumably cubic).

The only peculiar observation was that the α-SiC (0001) face, which was used in the APF measurements in Table IV.1. and in all subsequent Peak intensity measurements (see Sec. IV.3.), proved to be a rather exceptional orientation:

The integral intensity emitted from this face is approx. 5% higher than from any other crystallographic plane. At the same time the absorbed current was found to have the lowest value: approx. 2% smaller than in planes parallel to the hexagonal axis.

Most probably this effect must be explained on the basis of the typical layer structure of α-SiC. Apparently, electrons penetrating in directions parallel to the hexagonal axis (i.e. perpendicular to the layers) produce a shallower excitation volume, which is accompanied by a more pronounced backscatter process and, hence, a lower absorbed current. Due to the lower average penetration depth a larger number of X-ray photons is able to escape from this heavily-absorbing matrix. For all other directions the average depth of X-ray production is probably higher, so that more electrons are captured (higher absorbed current); yet, less photons are released.

Anyway, this anomaly must certainly be kept in mind when measuring poly-crystalline SiC, in which case it is advisable to adopt a correction factor of 1.05 for measurements made relative to a (0001)-α-SiC plane. Such an effect has never been found in Fe_3C, which has been measured as a standard numerous times. In all other cases the effect, if present, has gone unnoticed; the small crystal sizes, usually available, precluded a more detailed investigation. If such an effect would be present in e.g. Mo_2C, W_2C or WC, it must be assumed to be smaller than the measuring error.

IV.3. Peak k-ratios for metals and carbon

The peak k-ratios for metals and carbon have been measured over a very wide range of kV's; at 4, 6, 8, 10, 12, 15, 20, 25 and 30 keV. This has been done with a twofold purpose in mind:

- The first was, as already indicated in the introduction, to supply a firm reliable data base on which the present and future (possibly improved) correction programs can be tested.
- The second was to test the existing sets of mass absorption coefficients (Table II.1) on their internal consistency. This test has been carried out using the "Thin Film Model", introduced by Duncumb and Melford[12]. According to these authors the necessary conditions for this model are a high value of χ ($\equiv (\frac{\mu}{\rho})$. cosec θ), in which $(\frac{\mu}{\rho})$ is the mass absorption coefficient and θ is the take-off angle, and a high overvoltage ratio (E_o/E_c; E_o = accel. voltage, E_c = critical excitation voltage). These conditions are sometimes summarized in the requirement that $\chi >> \sigma$ (σ = Lenard coefficient, defined by $\sigma = \frac{4.5 \times 10^5}{E_o^{1.65} - E_c^{1.65}}$).

Certainly, if ever the conditions for this model would be expected to apply it would be in the present case of C-K_α radiation at accelerating voltages beyond 30 keV!

According to Duncumb and Melford under these circumstances the intensity of carbon-K_α radiation can be thought to originate only from a very thin film very close to the surface of the specimen and the intensity can be written as:

$I : : \phi(o) . \Delta(\rho z)$ in which $\phi(o)$ is the surface ionisation and $\Delta(\rho z)$ is the thickness of the thin film (in units of mass depth), which in turn can be considered to be inversely proportional to χ.

At very high overvoltages the so-called "limiting k-ratio" in our case could then be expressed by:

$$k = \frac{I_{MeC}}{I_{Fe_3C}} = \frac{\phi(o)_{MeC} \cdot (\frac{\mu}{\rho})_{Fe_3C} \cdot X_{MeC}}{\phi(o)_{Fe_3C} \cdot (\frac{\mu}{\rho})_{MeC} \cdot X_{Fe_3C}}$$

in which I is the intensity of carbon-K_α radiation, Me is the metal in the unknown carbide and X is the weight fraction of carbon. The values of $\phi(o)$ have been calculated using Love et al.'s[19] expression. The nice thing about this model (if it applies) would be that it predicts a limiting k-ratio which is independent of take-off angle and that it allows

the relationship between the mass absorption coefficients in standard and unknowns to be tested.

The measured peak k-ratios are presented in Fig. IV.6 a-o. Note that measurements of the metal lines on Fe_3C itself have been included as well as on Ta_2C, which was available in a 8 μm thick layer in a cross-section of the Ta/TaC specimen. The carbon measurements in the latter case have only been carried out on TaC in a plane parallel to the substrate. The numerical data of the peak k-ratio measurements are contained in appendix A.1-15. The relative intensities for C-K_α radiation in the various carbides are represented in appendix B.1-B.4. These are very useful for testing correction

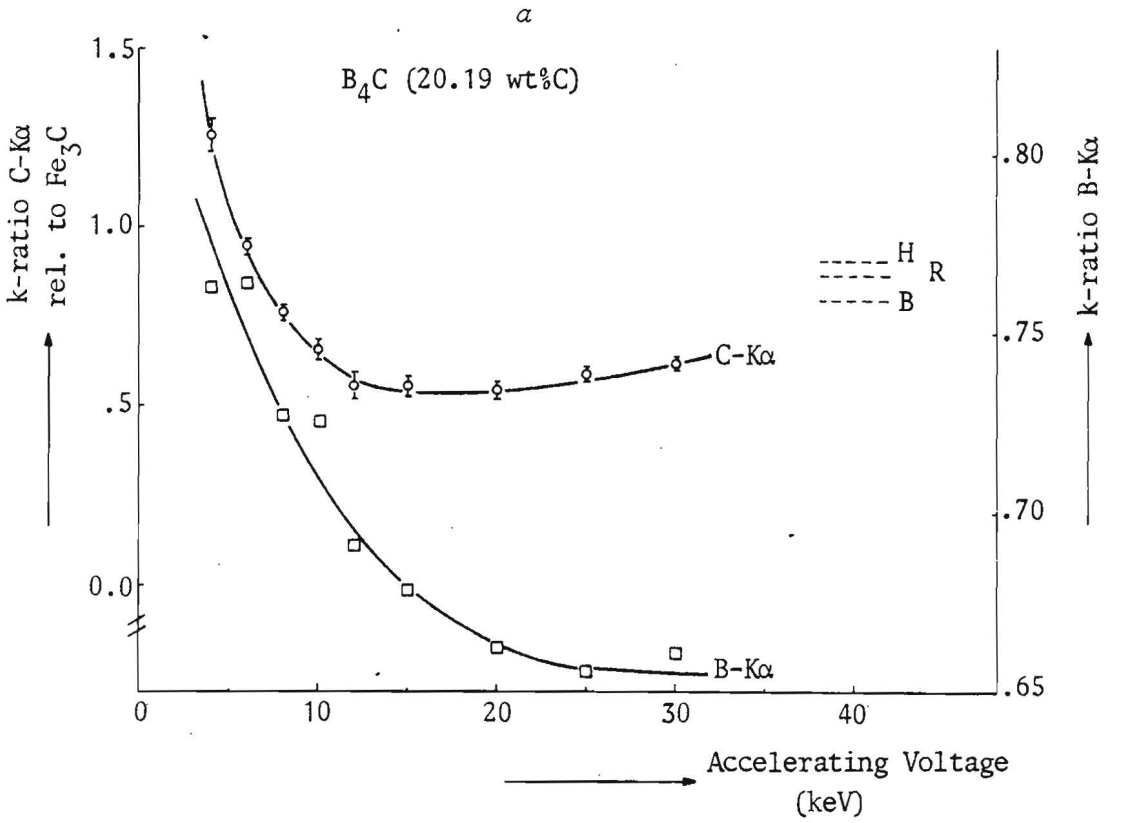

Fig. IV.6. a-o.

Peak k-ratios for the metals (with respect to pure element standards) and carbon (with respect to Fe_3C) as a function of accelerating voltage. The letters H, R, B refer to the limiting k-ratio calculated using the mass absorption coefficients according to Henke[16] (H), Ruste[1] (R) or present work (BAS) (B). Note the large differences in scale between the metal and carbon k-ratios.

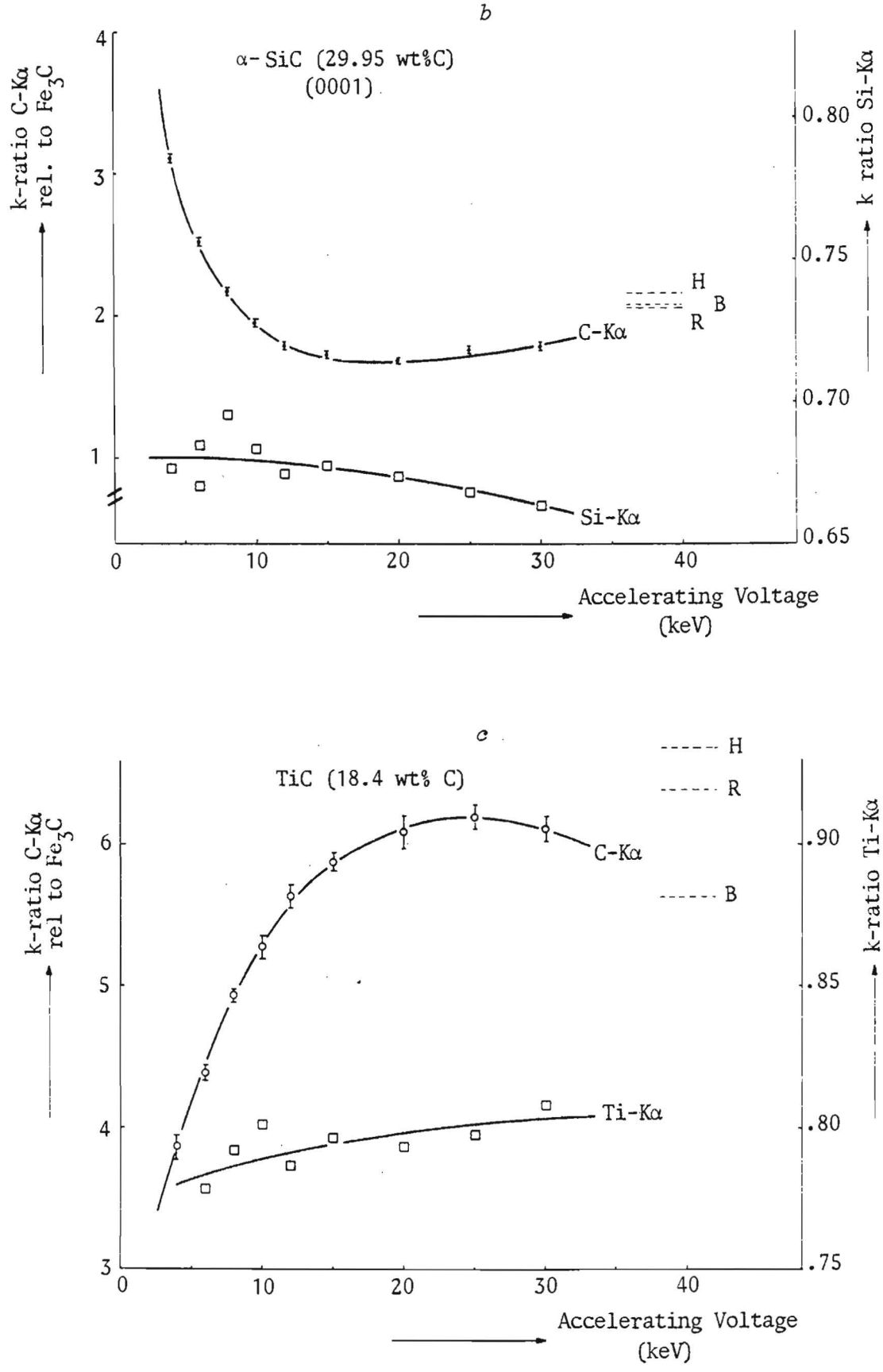
b
α- SiC (29.95 wt%C)
(0001)
k-ratio C-Kα
rel. to Fe_3C
k ratio Si-Kα
C-Kα
Si-Kα
H
R
B
Accelerating Voltage
(keV)
c
TiC (18.4 wt% C)
k-ratio C-Kα
rel to Fe_3C
k-ratio Ti-Kα
C-Kα
Ti-Kα
H
R
B
Accelerating Voltage
(keV)

Fig. IV.6.

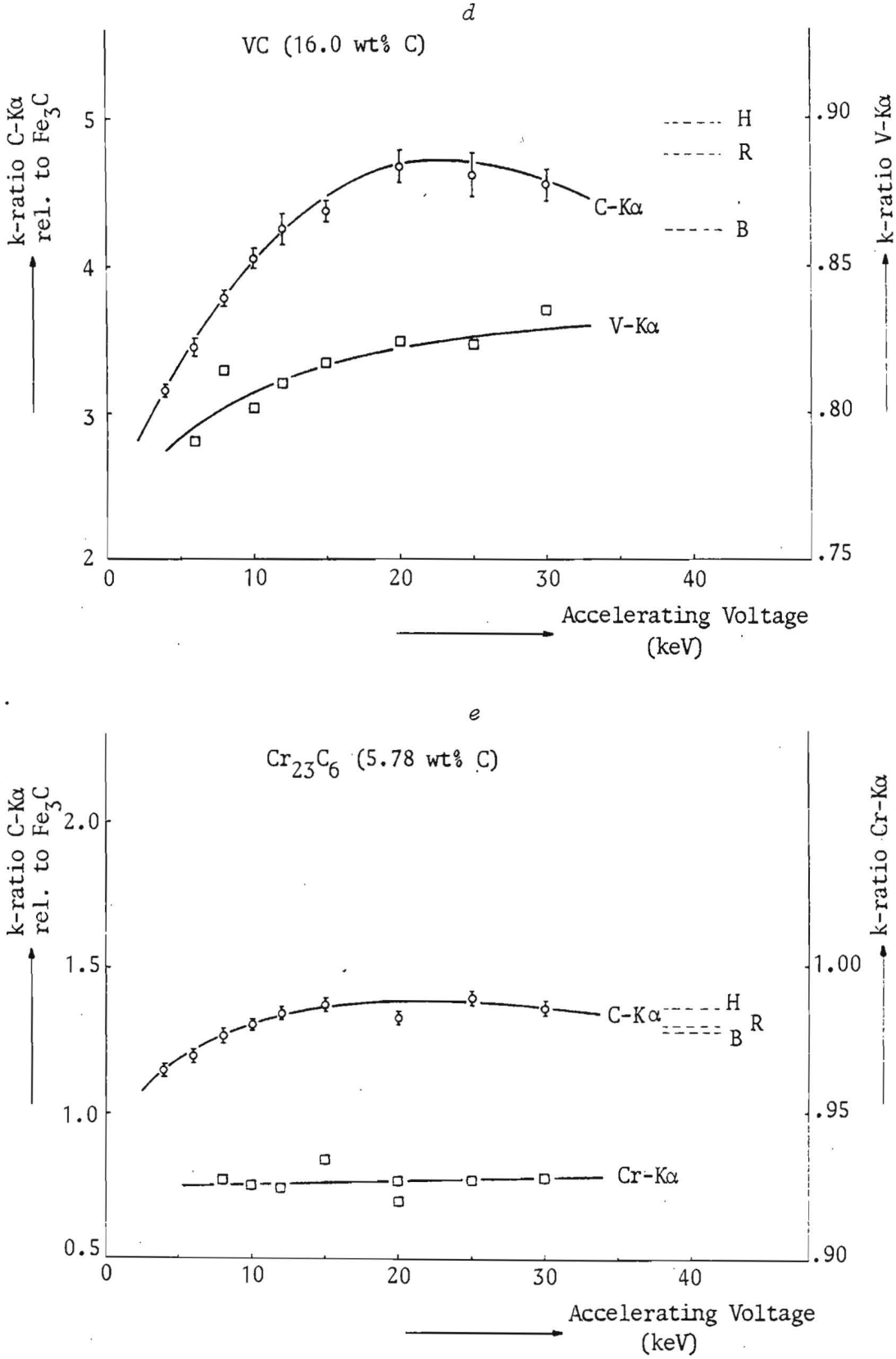
d
VC (16.0 wt% C)
k-ratio C-Kα rel. to Fe_3C
k-ratio V-Kα
C-Kα
V-Kα
H
R
B
5
4
3
2
.90
.85
.80
.75
0
10
20
30
40
Accelerating Voltage (keV)
e
$Cr_{23}C_6$ (5.78 wt% C)
k-ratio C-Kα rel. to Fe_3C
k-ratio Cr-Kα
C-Kα
Cr-Kα
H
R
B
2.0
1.5
1.0
0.5
1.00
.95
.90
0
10
20
30
40
Accelerating Voltage (keV)

Fig. IV.6.

f

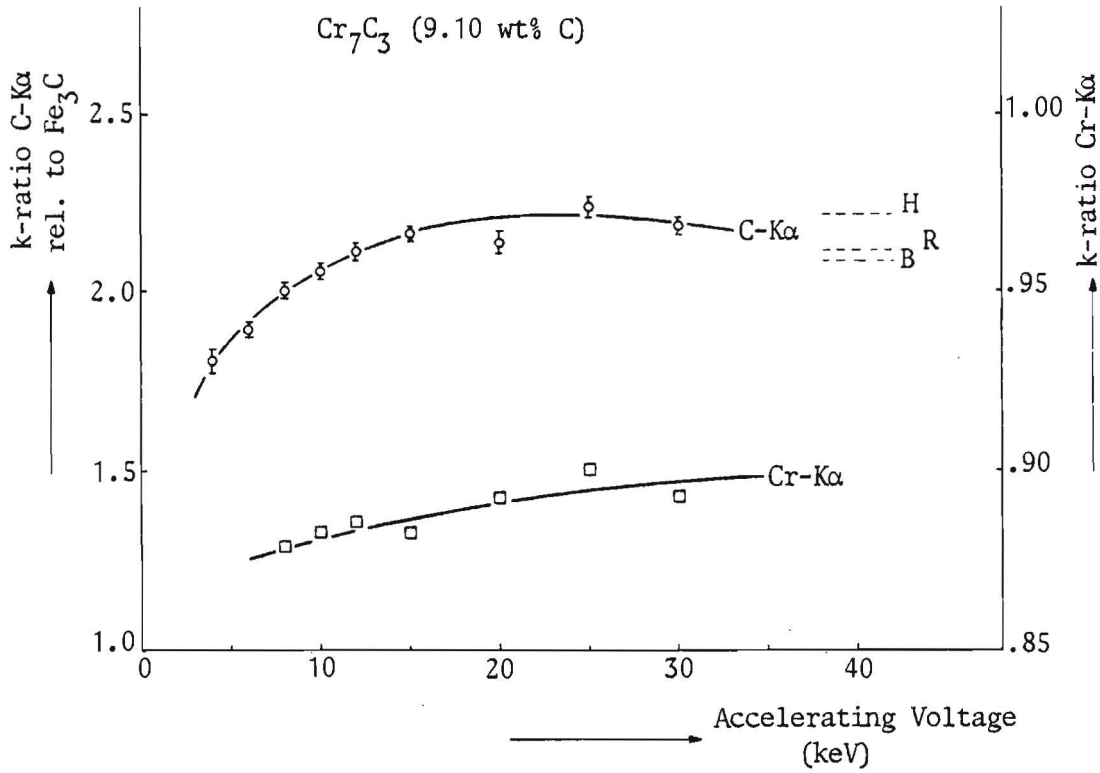
Cr_7C_3 (9.10 wt% C)
k-ratio C-Kα rel. to Fe_3C
k-ratio Cr-Kα
C-Kα
Cr-Kα
H
R
B
Accelerating Voltage (keV)

g

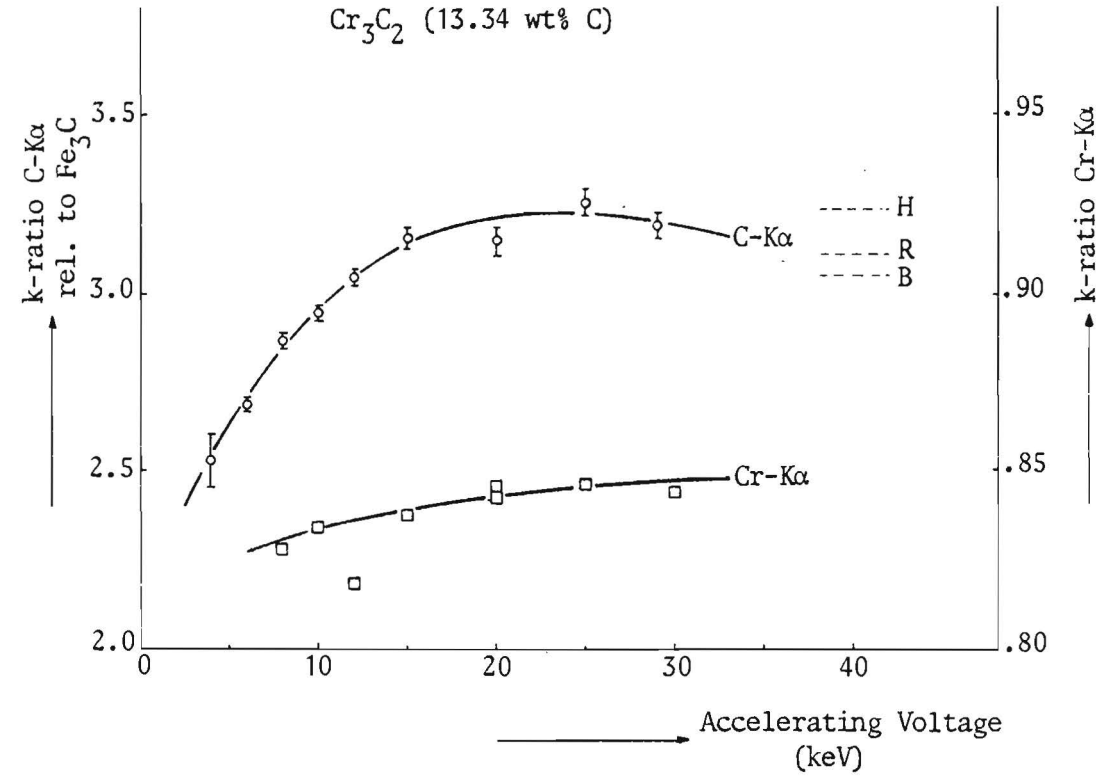
Cr_3C_2 (13.34 wt% C)
k-ratio C-Kα rel. to Fe_3C
k-ratio Cr-Kα
C-Kα
Cr-Kα
H
R
B
Accelerating Voltage (keV)

Fig. IV.6.

h

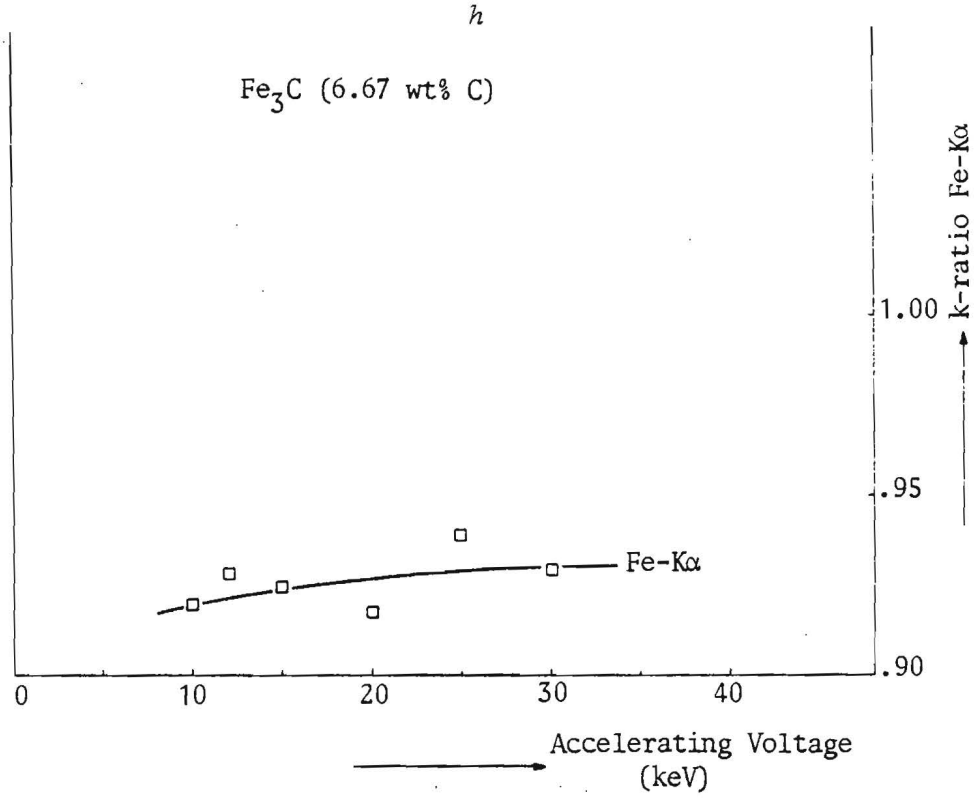
Fe3C (6.67 wt% C)
Fe-Kα
1.00
.95
.90
k-ratio Fe-Kα
0
10
20
30
40
Accelerating Voltage
(keV)

i

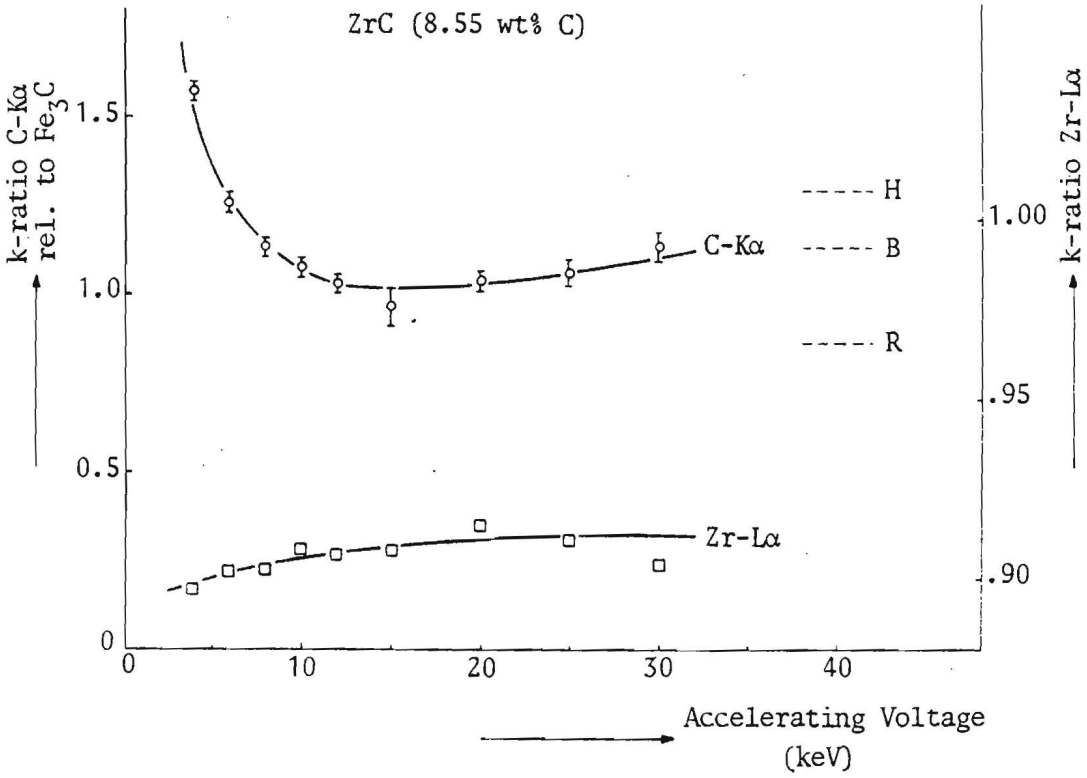
ZrC (8.55 wt% C)
k-ratio C-Kα
rel. to Fe3C
1.5
1.0
0.5
0
C-Kα
Zr-Lα
H
B
R
1.00
.95
.90
k-ratio Zr-Lα
0
10
20
30
40
Accelerating Voltage
(keV)

Fig. IV.6.

j

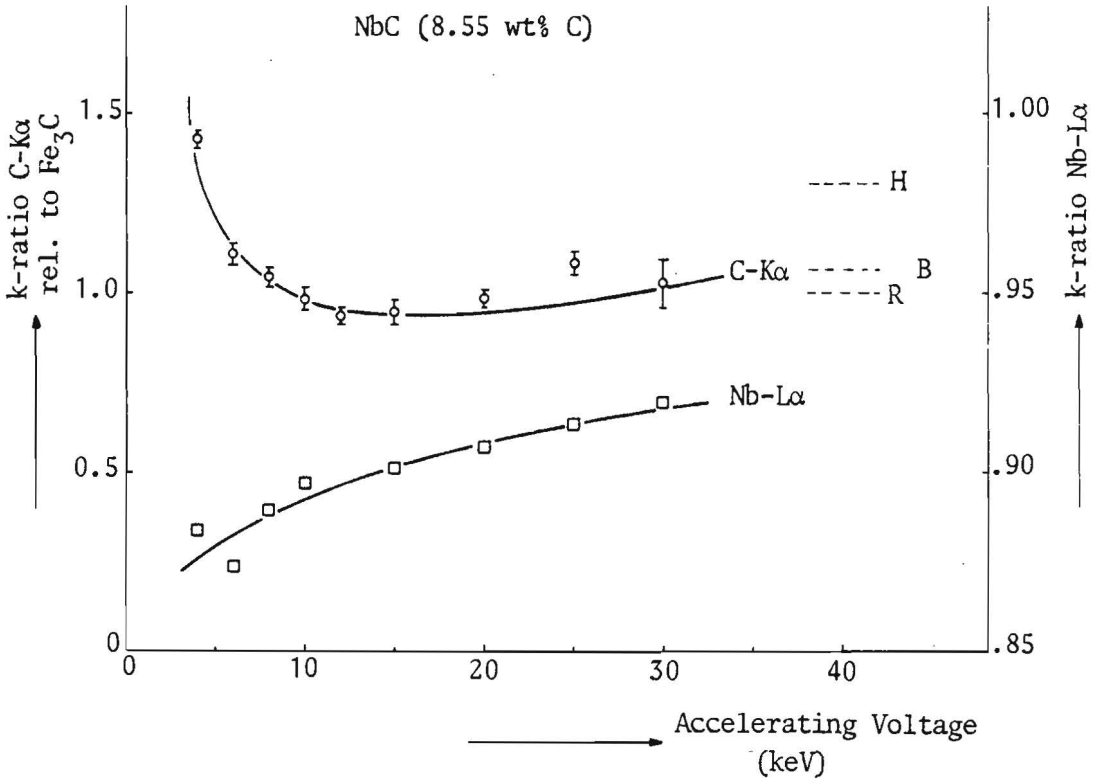
NbC (8.55 wt% C)
k-ratio C-Kα rel. to Fe_3C
k-ratio Nb-Lα
1.5
1.0
0.5
0
1.00
.95
.90
.85
H
B
R
C-Kα
Nb-Lα
0
10
20
30
40
Accelerating Voltage (keV)

k

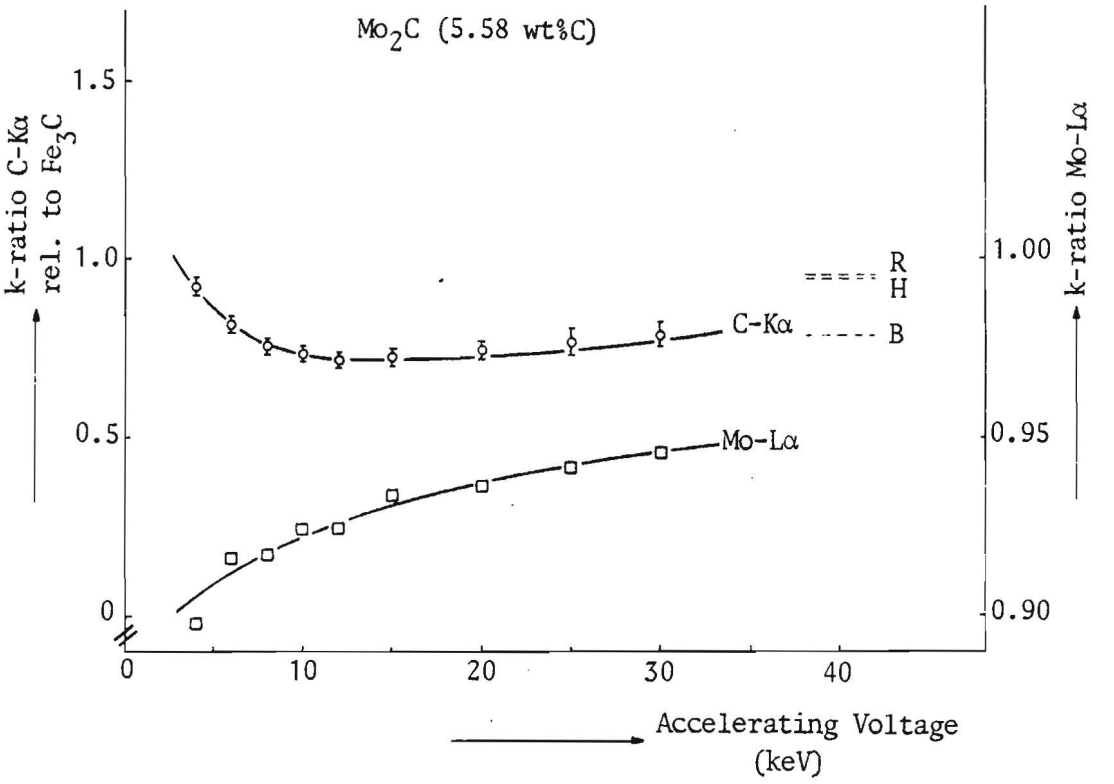
Mo_2C (5.58 wt%C)
k-ratio C-Kα rel. to Fe_3C
k-ratio Mo-Lα
1.5
1.0
0.5
0
1.00
0.95
0.90
R
H
B
C-Kα
Mo-Lα
0
10
20
30
40
Accelerating Voltage (keV)

Fig. IV.6.

l

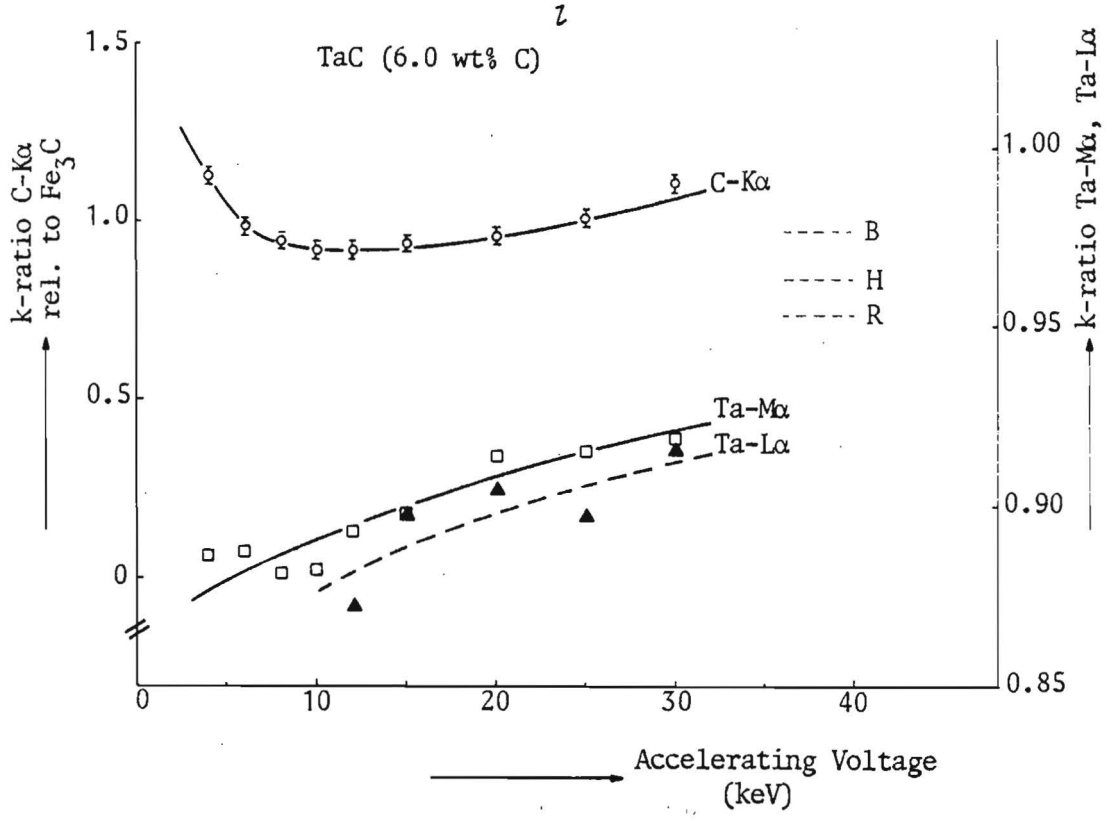
TaC (6.0 wt% C)
k-ratio C-Kα rel. to Fe3C
k-ratio Ta-Mα, Ta-Lα
C-Kα
B
H
R
Ta-Mα
Ta-Lα
1.5
1.0
0.5
0
1.00
0.95
0.90
0.85
0
10
20
30
40
Accelerating Voltage (keV)

m

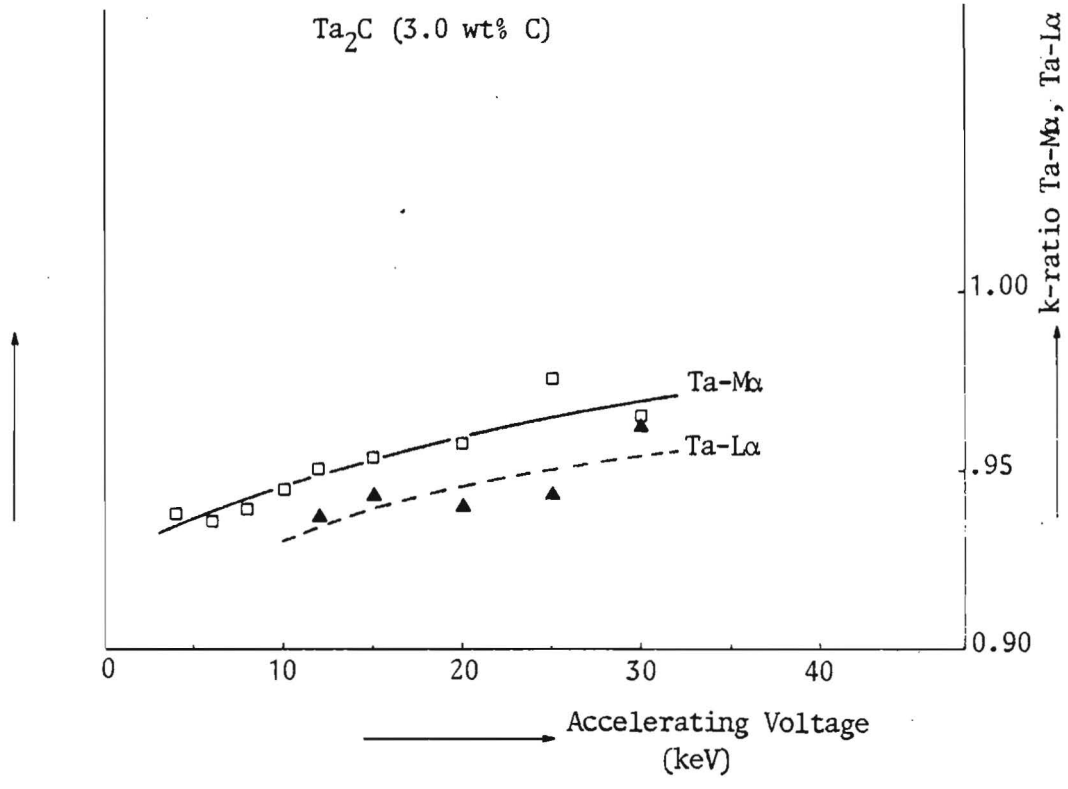
Ta2C (3.0 wt% C)
k-ratio Ta-Mα, Ta-Lα
Ta-Mα
Ta-Lα
1.00
.95
0.90
0
10
20
30
40
Accelerating Voltage (keV)

Fig. IV.6.

n

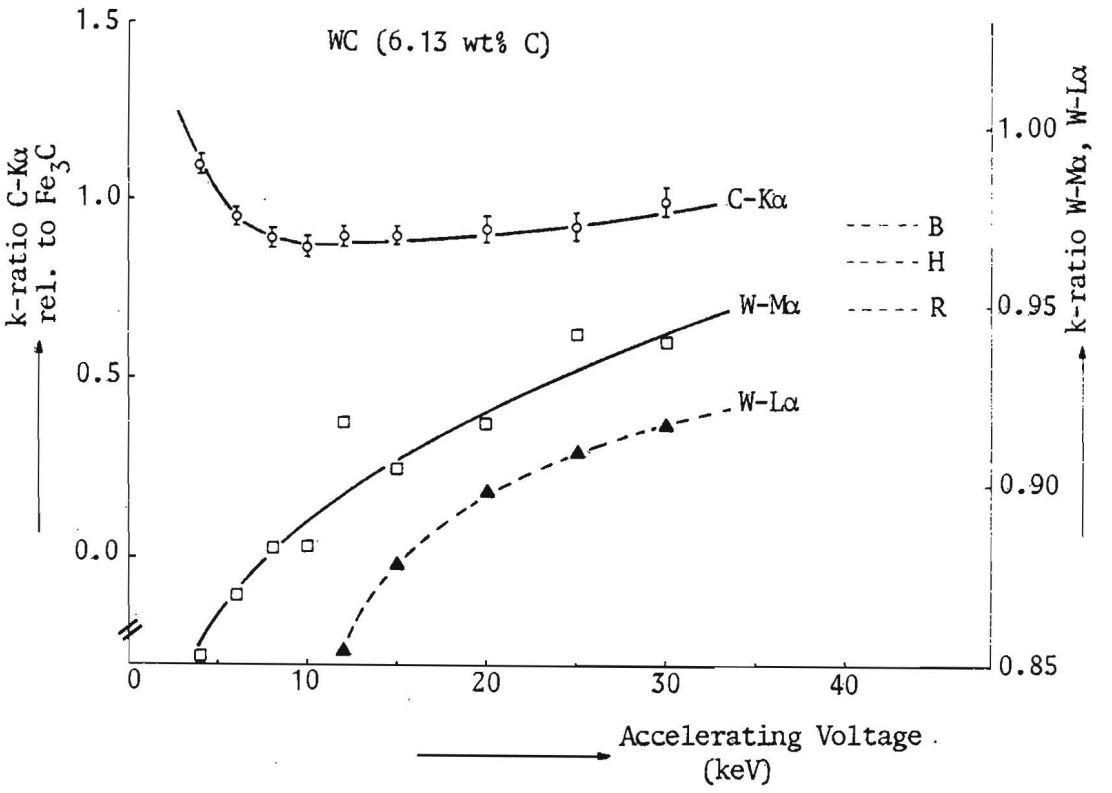
WC (6.13 wt% C)
k-ratio C-Kα rel. to Fe_3C
k-ratio W-Mα, W-Lα
C-Kα
W-Mα
W-Lα
B
H
R
1.5
1.0
0.5
0.0
1.00
0.95
0.90
0.85
0
10
20
30
40
Accelerating Voltage (keV)

o

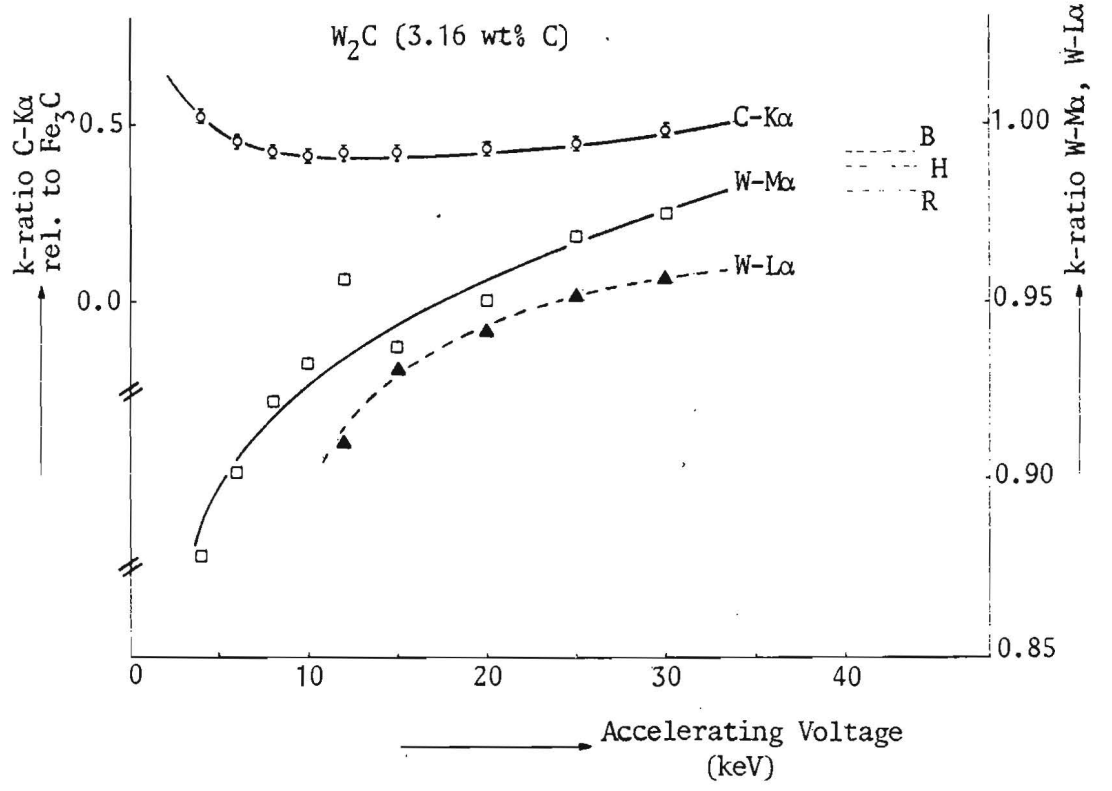
W_2C (3.16 wt% C)
k-ratio C-Kα rel. to Fe_3C
k-ratio W-Mα, W-Lα
C-Kα
W-Mα
W-Lα
B
H
R
0.5
0.0
1.00
0.95
0.90
0.85
0
10
20
30
40
Accelerating Voltage (keV)

Fig. IV.6.

programs. A close inspection of these figures immediately reveals two conspicuous features:

- In the first place it seems to be a general law that the k-ratio for carbon in systems with a stronger absorption than in the Fe_3C standard shows an initial decrease, followed by a kind of saturation, which is in turn followed by an increase again. Typical examples of this case are the carbides of B, Si and Zr.
  The reverse takes place when the absorption in the unknown is lower than in the standard, as for example the cases of TiC, VC and Cr_3C_2 indicate.
  Apparently it is too simple to expect the limiting k-ratio to attain a simple saturation level. In fact, if the present measurements were not pursued up to 30 keV one would easily have been misled by the saturation frequently observed between 10 and 20 keV with the result that the observed limiting k-ratios would be assumed to take completely wrong values! These effects are, of course, closely connected with the ways the relative intensities in the various carbides are observed to vary with kV. (See appendix B.1-B.4).
  If e.g. the cases of Fe_3C and B_4C are compared, it is immediately clear that between 5 and 10 keV the decrease in relative intensity in B_4C is much faster than in Fe_3C with the result that the k-ratio of C-K_α in B_4C decreases fast.
  Between 20 and 30 keV, however, the decrease in intensity in B_4C is much slower than in Fe_3C with the result that the k-ratio shows a tendency to increase again. Reverse reasoning must be applied to e.g. TiC with respect to Fe_3C.
- The second important observation concerns the fact that apparently the existing sets of mass absorption coefficients, indicated in the Figures by H (Henke[16]) and R (Ruste[1]) are not fully consistent and do not lead to good agreement between observed and predicted limiting k-ratios, certainly not if the measurements are extrapolated to voltages of 35-40 keV.
  This observation has partially been the reason for us to propose a new set of mass absorption coefficients (See Table II.1) which provide a better agreement with the extrapolated limiting k-ratio as Table IV.3 shows. Drastic changes are apparently necessary for B_4C, TiC, VC, ZrC, TaC and WC (See also Table II.1).

One final remark on the measurements must still be made and that is the observation that the measurements at 4 kV were sometimes difficult to reproduce. Undoubtedly this is a result of the fact that at such low kV's X-ray generation only takes place in an extremely superficial layer;

Table IV.3.

The extrapolated peak k-ratio at 35 kV for C-K_α radiation relative to Fe_3C, as compared to the limiting k-ratio predicted on the basis of different sets of mass absorption coefficients.

	observed	Limiting k-ratio based on mass absorption coefficients according to: Ruste[1]	Henke[16]	Present Work (BAS)
B_4C	0.69	0.87	0.90	0.79
SiC	1.90	2.06	2.16	2.09
TiC	5.70	6.39	6.68	5.63
VC	4.20	4.76	4.97	4.25
$Cr_{23}C_6$	1.35	1.30	1.36	1.28
Cr_7C_3	2.15	2.12	2.22	2.08
Cr_3C_2	3.18	3.11	3.24	3.05
ZrC	1.18	0.85	1.28	1.12
NbC	1.15	1.00	1.30	1.06
Mo_2C	0.82	0.96	0.95	0.79
TaC	1.17	0.74	0.83	0.97
WC	1.05	0.69	0.83	0.93
W_2C	0.52	0.32	0.38	0.42

hence one makes oneself extremely vulnerable to all kinds of surface effects, like artefacts introduced by polishing and cleaning procedures, small surface relief effects etc. We would not advise, therefore, carbon measurements to be performed at such low kV's; instead we would prefer the region between 8 and 12 kV; the more so as in this region most metal lines can satisfactorily be excited. Besides, one would only be inclined to choose very low kV's in order to avoid excessive absorption corrections, which no longer have to be avoided as the next chapter shows.

V. DATA REDUCTION AND COMPARISON OF CORRECTION PROGRAMS

Now that a reliable set of data is available it is time to turn to the last step in the procedure and that is the conversion of measured k-ratios into concentration units. To this end a number of correction programs are currently at ones disposal. After a brief introduction into the general features of a correction progam three of the most frequently used programs will be discussed and compared to our own program.

V.1. Introduction

In quantitative electron probe micro-analysis a number of corrections have to be applied to the measured intensity ratios between specimen and standard in order to convert them into concentration units. In the commonly accepted and widely used *"ZAF"* approach these corrections are usually split up into three separate factors, Z, A and F, respectively.

The Z-factor (related to the atomic number effect) deals with the differences in X-ray generation between specimen and standard and is in fact split up in two separate factors R and S which treat the effects of electron backscattering (R) and X-ray generation (stopping power S) in the target. Most of the existing computer programs available today are based on the atomic number correction of Duncumb and Reed[20] while a few employ the more rigorous but also much more complex Philibert/Tixier[21] procedure. As the differences between the two models are reported to be very small (see e.g. Beaman and Isasi[22]) the former is usually preferred.
Some years ago a new atomic number correction has been proposed by Love et al.[23] with the aim to overcome a number of limitations in the Duncumb/Reed model mainly anticipated in the use of low electron energies and low or high overvoltage ratios.

In calculating the A-factor an effort is made to calculate the differences in absorption of the generated X-rays between specimen and standard. The most extensively used method still seems to be the one based on the simplified Philibert[24] model in which the surface ionisation ($\phi(o)$) is assumed to be zero and the $\phi(\rho z)$ curve from a certain depth on is characterized by an exponential decay: $\exp(-\sigma\rho z)$, in which σ is the Lenard coefficient.

It has been shown on many occasions that the validity of this model is very limited and for strongly absorbing systems the full Philibert[24] model has to be preferred[3].
A very simple absorption correction model has been proposed by Bishop[25]. This model is based on the assumption that the ionisation is constant from the specimen surface up to a certain depth after which it falls abruptly to zero. One of the crucial parameters in this model is the mean depth of X-ray production for which Love and Scott[26] developed a suitable expression based o the results of Monte-Carlo calculations.
The resulting absorption correction seems to work surprisingly well[26] in spit of its astonishing simplicity.

The fluorescence correction (*F*-factor), finally, in most correction procedures is based on the model of Reed[27] and it is generally felt that the inaccuracies in the physical parameters used in it impose more limitations upon the procedure than the model itself.

A completely new correction procedure has recently been put forward by Brown et al[28,29]. Their approach can be described as a serious effort to describe the $\phi(\rho z)$ curves as accurately as possible. To this end equations have been developed which are indeed capable of producing $\phi(\rho z)$ curves in close agreement with actually measured ones. Based on these equatio a computer program was written and tested on about 500 microanalyses with reported excellent results: a standard deviation of 4.8%, compared to 6.8% for the so-called "established" ZAF procedure and 5.4% for the Love and Scot program.
A point of interest to note about the so-called Gaussian $\phi(\rho z)$ approach introduced by Brown and coworkers, is that no longer a separation has to be made between the *Z* and *A*-factors. Once the shape of the (Gaussian) $\phi(\rho z)$ curve is known, it is a quite straightforward matter to calculate the emitted intensity of X-radiation in standard and specimen.

Our efforts to reproduce the excellent results claimed by Brown et al., however, failed as we have reported before[13].
We found it necessary to introduce some alterations in the original equations and after re-optimizing[13] the set of equations using about 450 published microanalyses we were able to produce results quite similar to those of Love and Scott[26]. In a subsequent paper[14] we have compared our program (henceforth shortly called "BAS") to the Love and Scott ("LOS"). Ruste ("RUSTE") and established ZAF ("ZAF") programs. The results are summarized in Table V.1.a and b, which represent so to say "the state of the art"

Table V.1.a

Root-mean-square values* and averages obtained with four correction programs for 441 published microanalyses.

Program	Average	RMS(%)
BAS	0.9902	5.46
LOS	0.9929	5.56
ZAF	1.0145	6.30
RUSTE	1.0240	6.74

Table V.1.b

Root-mean-square values * obtained for 163 selected analyses which depend for their correction mainly on the atomic number effect.

Program	RMS(%)
BAS	2.73
LOS	2.41
ZAF	2.87

*These apply to the ratio between the calculated and the measured k-ratio for a given concentration.

V.2. Description of Programs

The so-called "established" ZAF-procedure ("ZAF") is based on the atomic number correction of Duncumb and Reed[20], the simplified Philibert[24] absorption correction and Reed[27]'s correction for characteristic fluorescence. In our case the ZAF program used is essentially the one purchased from TRACOR Northern and is suitable to work on-line in an automation system coupled to our JEOL Superprobe 733. It is written in Flextran which is an interpreter language and is consequently very easily accessed by the user. The expression for the ionisation potential used in the calculation of the stopping power is that of Berger and Seltzer[30].

As we had a special interest to use the other programs also on-line they were all written in Flextran within the basic framework given by the ZAF-program. Only in the case of the Ruste program could a copy of the original listing (in Fortran) be used as reference; in the other cases this was not made available (Love & Scott) or not suitable (Brown) for reasons mentioned before.

The Love & Scott program (LOS) was entirely made according to the equations published, which means Love and Scott's new atomic number correction[23] and Bishop's[25] absorption correction model with Love and Scott's[26] expression for the mean depth of X-ray production.
The characteristic fluorescence correction in all programs was kept identical to that of the ZAF program; a correction for continuum fluorescence was not included.

In the Ruste program[1-3] the Philibert-Tixier[21] atomic number correction is employed, with Ruste[3]'s expression for the ionisation potential, and the so-called "full" Philibert[24] absorption correction. A number of parameters in this correction have here been made dependent on atomic number and energy, contrary to the original equations.

The BAS program will now be discussed in rather more detail because it is relatively new.
According to Brown et al[28,29] $\phi(\rho z)$ curves can be accurately described by an equation of the type:

$$\phi(\rho z) = \gamma . \left[1 - \frac{\gamma - \phi(o)}{\gamma} . \exp(-\beta \rho z)\right] . \exp\left[-\alpha^2 (\rho z)^2\right] \qquad (1)$$

In this equation the ionisation ϕ as a function of mass depth (ρz) is basically described by the Gaussian expression $\gamma . \exp[-\alpha^2 (\rho z)^2]$ in which γ is a scaling factor and α gives the decay rate with the square of the mass depth. This is illustrated in Fig. V.1 where an example is given for the case of copper at 30 keV. The values of α, β and γ have been calculated with equations (2)-(4). In our previous papers[13,14] we have shown that for the moment the optimum expressions are:

$$\alpha = \frac{1.75.10^5}{E_o^{1.25} . (U_o - 1)^{0.55}} . \left[\frac{\ln(1.166 E_o/J)}{E_c}\right]^{0.5} \qquad (2)$$

$$\beta = 0.4 . \alpha . \frac{Z^{1.7}}{A} . (U_o - 1)^{0.3} \qquad (3)$$

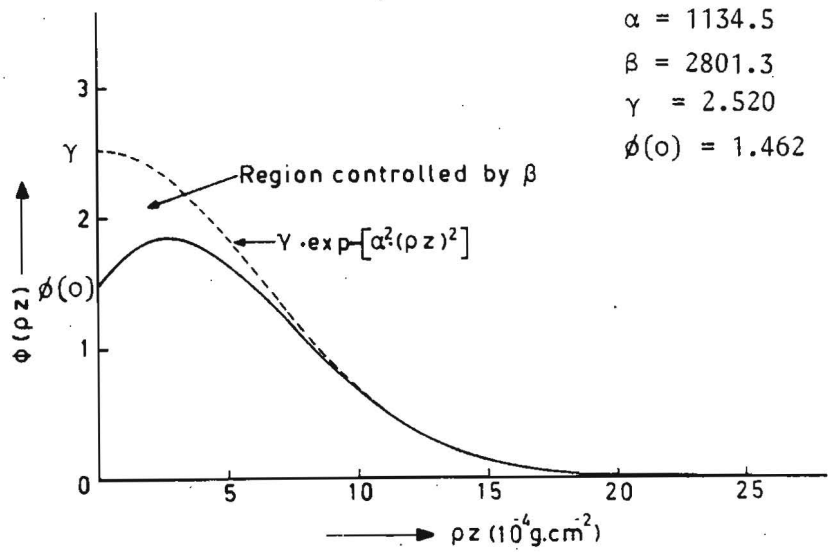

Fig. V.1. Example of a φ(ρz) curve for Copper at 30 keV, as calculated by the BAS program.

$$\gamma = \frac{4.9\pi U_o}{(U_o-1)\ln U_o} \cdot (\ln U_o - 5 + 5U_o^{-0.2}) \cdot \exp(0.001.Z) \qquad (4)$$

in which Z, A and J are the atomic number, atomic weight and ionisation potential for the matrix element in question. The expression for J we use is that of Ruste. E_o is the accelerating voltage, E_c the critical excitation voltage and U_o the overvoltage ratio (E_o/E_c) for the X-ray line in question. For a compound specimen (sp) the value of $(\alpha_i)_{sp}$ is obtained as follows[13]:

$$(\alpha_i)^2_{sp} = \frac{\bar{A}}{\bar{Z}} \cdot \Sigma\, C_j \frac{Z_j}{A_j} \cdot \alpha^2_{ij} \qquad (5)$$

in which $\bar{A}$ and $\bar{Z}$ are the weight fraction averaged atomic weight and number of the specimen; A_j and Z_j those of the matrix element j and C_j its weight fraction. α_{ij} is the quantity that describes α for element i-radiation in interaction with element j of the matrix. The values of

β and γ for a compound are obtained by inserting $\bar{A}$ and $\bar{Z}$ into eq. (3) and (4). Normally the combined [ZA]-correction factor is calculated by multiplying eq. (1) by the absorption term $\exp(-\chi\rho z)$ (in which $\chi = \frac{\mu}{\rho} \cdot \text{cosec}\ \theta$, $\frac{\mu}{\rho}$ is the mass absorption coefficient and θ is the take-off angle) for specimen (sp) and standard (st) and integrating (numerically) the product for all mass depths between zero and infinity, followed by a division.

At present, however, we prefer to carry out the integration with and without the absorption term which gives us the [ZA] and [Z] factors separately. A simple division then makes the [A]-factor visible.

We have shown previously[13] that the time-consuming process of numerical integration of eq. (1) can be avoided by writing:

$$Z = \frac{[\gamma-(\gamma-\phi(o)) \cdot R(\frac{\beta}{2\alpha})]_{st}}{[\gamma-(\gamma-\phi(o)) \cdot R(\frac{\beta}{2\alpha})]_{sp}} \cdot \frac{\alpha_{sp}}{\alpha_{st}} \qquad (6)$$

and:

$$ZA = \frac{[\gamma \cdot R(\frac{\chi}{2\alpha}) - (\gamma-\phi(o)) \cdot R(\frac{\beta+\chi}{2\alpha})]_{st}}{[\gamma \cdot R(\frac{\chi}{2\alpha}) - (\gamma-\phi(o) \cdot R(\frac{\beta+\chi}{2\alpha})]_{sp}} \cdot \frac{\alpha_{sp}}{\alpha_{st}} \qquad (7)$$

in which R is a fifth-order polynomial used in the approximation of the error function which comes in when the integrals are solved in closed form through a Laplace transformation. R is described by:

$$R = a_1 t + a_2 t^2 + a_3 t^3 + a_4 t^4 + a_5 t^5$$

with $t = 1/(1+px)$ and $p = 0.3275911$

$a_1 = 0.254829592$ $\quad a_2 = -0.284496736$

$a_3 = 1.421413741$ $\quad a_4 = -1.453152027$

$a_5 = 1.061405429$

The input value for x is $\beta/2\alpha$, $\chi/2\alpha$ or $(\beta+\chi)/2\alpha$, respectively.

Please note that *Z* and *A* are defined here by the relation:

$C = k.Z.A.F$

(C is weight fraction, k is intensity ratio) in accordance with the original ZAF program of TRACOR.

V.3. Use of the Data Files

The performance of a correction program is usually tested by subjecting it to a large number of analyses after which the results are treated statistically (see e.g. Table V.1). The usual approach is that for a given concentration in the test file the intensity ratio k' is calculated and compared to the actually measured k-ratio, which in fact means that the program is run backwards, thus avoiding the iterative procedure normally necessary. The k'/k values are usually displayed in a histogram showing the number of analyses as a function of k'/k and the shape of the histogram, together with the relative root-mean-square deviation (r.m.s. value) are used as a final judgement of success. This procedure has, in our case, been applied to the analyses of the metal lines in the carbides. The complete file, representing 145 measured k-ratios between 4 and 30 kV, is given in appendix C.1. An inspection of this file shows that it contains a number of quantities which are normally calculated by the program, like mass absorption coefficients and critical excitation voltages. These are now imposed upon the program, as it is forced to take these quantities from the test file. These values are taken from the recent work of Henke[16]. Note that the metal k-ratios in appendix C.1. are based on smoothed data obtained from the curves in Fig. IV.6.a-o. In the case of the carbon analyses a somewhat different procedure has been used. Here the normal iterative procedure was preferred (measured k-ratio input; concentration output). and the metal content was simply calculated by difference. In this case, however, as the mass absorption coefficients for C-K_α radiation were still a matter of discussion and in fact represented a vital issue as mentioned in Chapter I, different sets of mass absorption coefficients were stored in separate files on floppy disk and could be selected by the operation of a switch in the program. Full details on the test file representing 117 carbon analyses, are given in Appendix C.2. The Carbon k-ratios (Area k-ratios!) have not been smoothed.

V.4. Results

V.4.1. Metal Analyses

The results obtained with the four programs in the case of the metal k-ratios (appendix C.1.) are graphically represented in Fig. V.2. As it turns out the ZAF program seems to be the most satisfactory for this rather particular type of file, particular in the sense that in the vast majority of cases only a very small atomic number correction is necessary. With the exception of boron at higher kV's absolutely no demand is being made upon the absorption

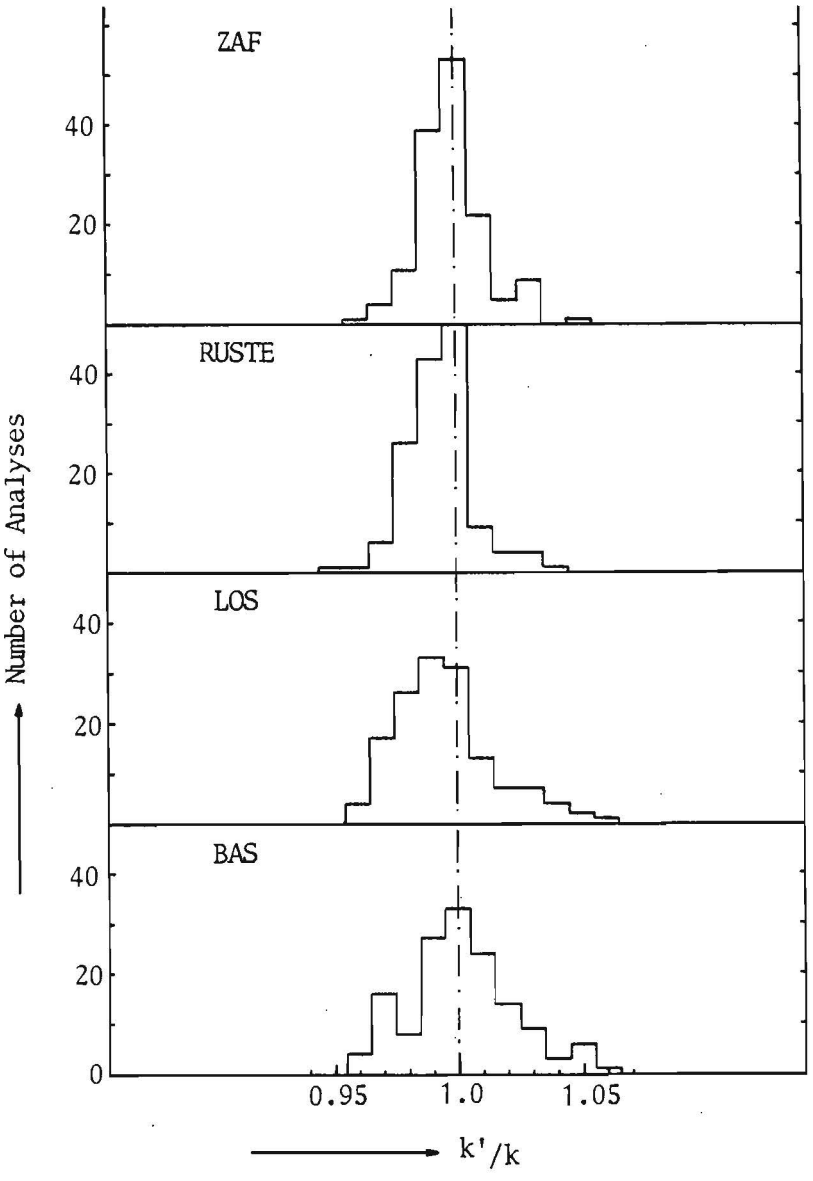

Fig. V.2. Histograms showing the results of the 4 correction programs for 145 metal analyses between 4 and 30 kV. Note that in this specific case only a very small (in most cases smaller than 5%) atomic number correction is required.
k' is the calculated and k the measured k-ratio.

correction. The resulting r.m.s. value is 1.4% (Table V.2), which is almost matched by the RUSTE program. Nevertheless it is clear that the application of Ruste's expression for the ionisation potential leads to a slight deterioration in the results. The LOS and BAS programs on the

Table V.2.

RMS values and averages obtained with four correction programs for 145 metal analyses in binary carbides between 4 and 30 kV.

Program	Average	RMS(%)
ZAF	0.9989	1.4
RUSTE	0.9934	1.5
LOS	0.9948	2.0
BAS	1.0014	2.1

average lead to comparable results. It is remarkable though that in the LOS program a small bias can be noticed, which is quite similar to the one observed earlier[14] when the performances of the programs were compared on the testfile containing 441 analyses of a widely varying nature. Moreover, it is quite interesting to note that the figure of merit in the present case is in a completely reversed order when compared to the data in Table V.1.b. In the latter case the atomic number effects were considerably larger and were, unfortunately, usually accompanied by rather larger absorption effects than in the present case. This may serve as an example that it is very hard to make firm statements on the performance of correction programs, especially if the test file used is of a rather specific nature.

As far as the BAS program is concerned it must be remarked that the present file contains a relatively large number of analyses at low overvoltage ratios. It has been stated before[13,14] that this program is more sensitive to low overvoltage ratios than others; as a consequence, somewhat better results would have been obtained if only analyses at $U_o > 1.5$ would have been carried out. A final remark can be made on the analyses of TiC (see III.1); all programs agree closely on the composition given in Table III.1.

V.4.2. Carbon Analyses

It is rather more difficult to assess the performance of the programs for the carbon analyses, mainly because of two reasons:

- In the first place the carbon measurements have been carried out with respect to a complex standard (Fe_3C) and this may obscure to a certain extent any malfunctioning of a particular program as the calculations are in this case performed through the primary calculation of a correction factor (k ratio of Fe_3C with respect to an imaginary carbon standard). The measured k-ratio of a carbide MeC (Me=metal) relative to Fe_3C is then multiplied by this factor after which the program converts the imaginary k-ratio (MeC/C) into concentration. One could argue that in such a procedure one does not have to rely so heavily on the proper functioning of the program as the total amount of correction is only a fraction of that required with respect to a carbon standard. Thus it is perfectly conceivable that both in the carbide MeC as well as in the standard Fe_3C appreciable errors might be made; yet the final result could turn out to be acceptable as these errors could well be divided out in taking the ratio. To a certain extent these remarks also apply to a carbon standard, of course.

- A further complicating factor is the uncertainty in the mass absorption coefficients which contributes just as much to the final uncertainty in the result as the performance of the program as we will show later on. The effect is noticeable in two ways: First in a way that it renders the absorption in a carbide MeC uncertain, second in a way that the absorption coefficient of C-K_α in Fe plays a major role as this comes in through the calculation of the correction factor for Fe_3C and is therefore implicitely contained in all final k-ratios (MeC/C).

It was, therefore, considered vital to measure the (Area)k-ratio of C-K_α in Fe_3C relative to a glassy carbon standard, in order to check the performance of the programs in this crucial first step. The results are shown in Fig. V.3. The calculated k-ratios of the BAS program agree perfectly up to 12-15 kV. In this case our own mass absorption coefficients (m.a.c.'s) have been used; inspection of Table II.1 shows, however, that the differences between the sets of Ruste[1], Henke[16] and our set can here be neglected.

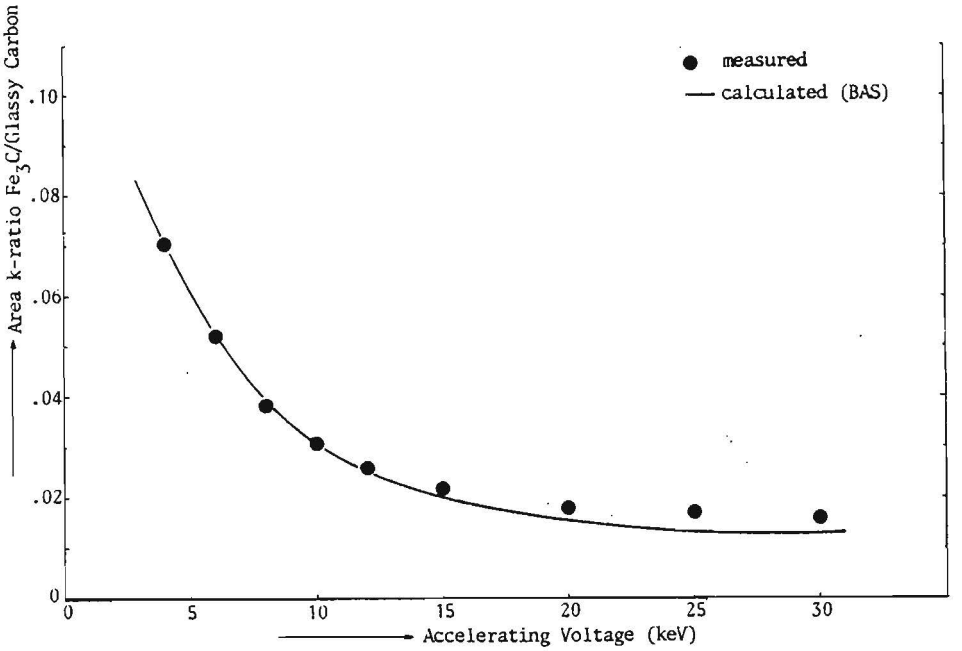

Fig. V.3. Measured Area k-ratio for Carbon in Fe_3C relative to glassy carbon, as compared to the results calculated by the BAS program.

The good results obtained up to 15 kV do not come completely as a surprise because a comparison of $\phi(\rho z)$ curves generated by our BAS program and those calculated by Monte-Carlo procedures (Fig. V.4.) came out very promising. Note, by the way, the very small fraction of generated intensity which is finally emitted from Fe_3C. This shows the extreme importance of the proper shape of the $\phi(\rho z)$ curve for low (up to 2 units) values of ρz. For most practical purposes the curve could just as well be drawn horizontal after 3 units!

Beyond 15 kV increasingly too low values are calculated by the BAS program and this can mainly be attributed to the program's failure to predict the proper $\phi(\rho z)$ curve in carbon at such high overvoltage ratios any longer. In fact, the present set of equations does not allow the peak to be laid deep enough in the specimen.

This is corroborated by the observation that the rise in relative intensity in glassy carbon (Appendix B.1.) is fairly well predicted; beyond the maximum however, the equations (2)-(4) in V.2. can no longer be relied upon as they fail to predict the proper decay. Nevertheless, as Fig. V.3. shows, the measured k-ratios agree perfectly with the calculated correction factors up to about 15 kV, which can be interpreted in a way that all other carbides

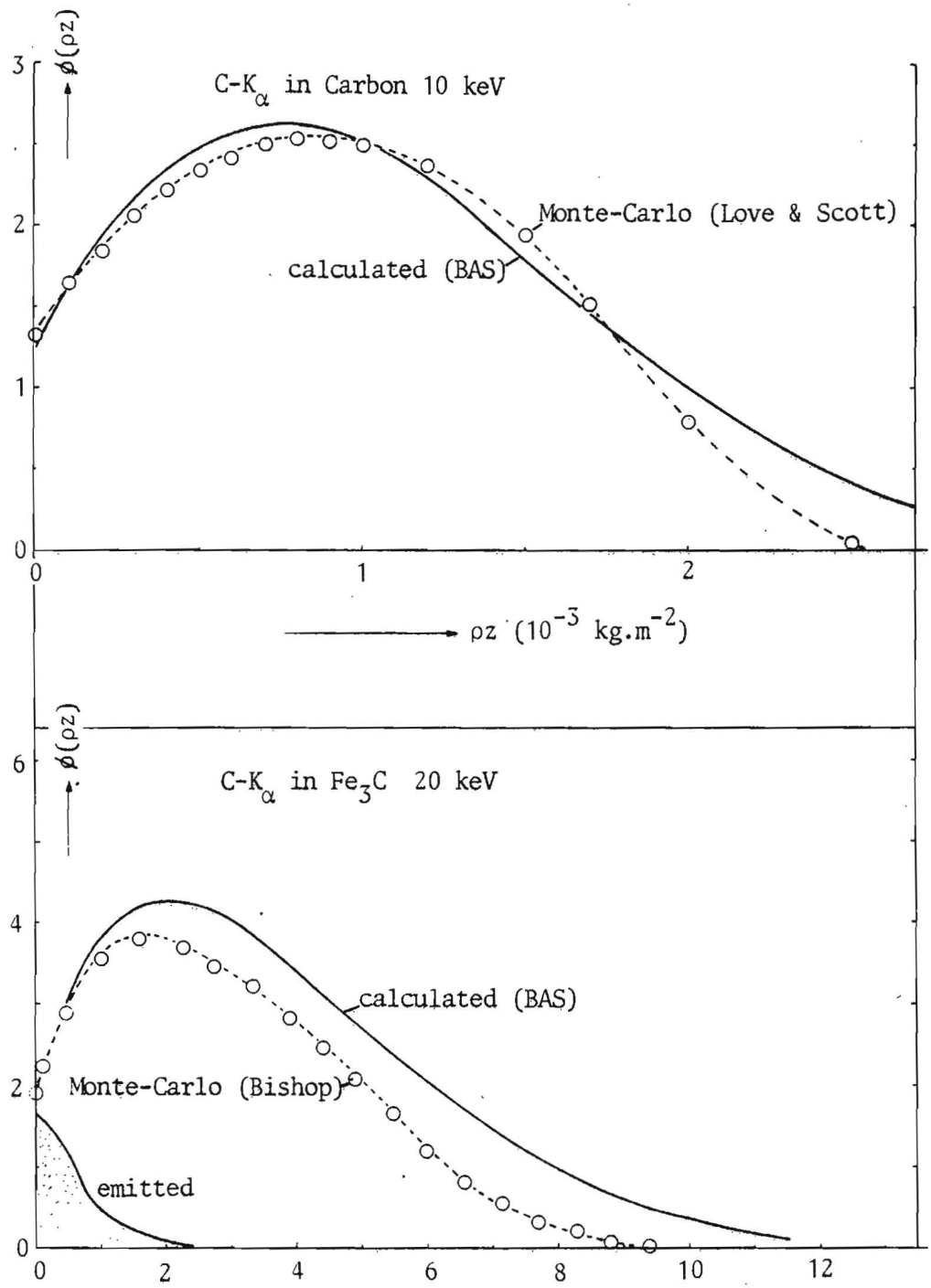

Fig. V.4. φ(ρz) curves calculated by the BAS program for Carbon-K_α in Carbon at 10 kV (Top) and Carbon-K_α in Fe_3C (bottom) as compared to the results of Monte-Carlo calculations.

could just as well have been measured relative to glassy carbon in the range between 4 and 15 kV!
As it turns out the RUSTE program is second best in this range, giving somewhat too low (about 5%) values, followed by the LOS program with too high (up to about 10%) values. The ZAF program, finally, was the least satisfactory: up to 8 kV 6% too low values, between 8 and 15 kV 8-10% too high values, good results at 20 kV and suddenly 18% too low again at higher kV's.
Beyond 15 kV the LOS program performs best, followed by the RUSTE, BAS and ZAF programs. It must be noticed, however, that this is not the range one would usually measure carbon in.

After this very important first step final sets of calculations were carried out for the complete file of carbon measurements, mainly using the three most recent sets of m.a.c.'s (see Table II.1.): that of Ruste[1] (1979), Henke (1982) and our own set.
The results for the BAS program are represented in histograms in Fig. V.5.a-c. It is evident that the use of Henke's newest set of m.a.c.'s gives a very significant improvement in the results which is both noticeable in the

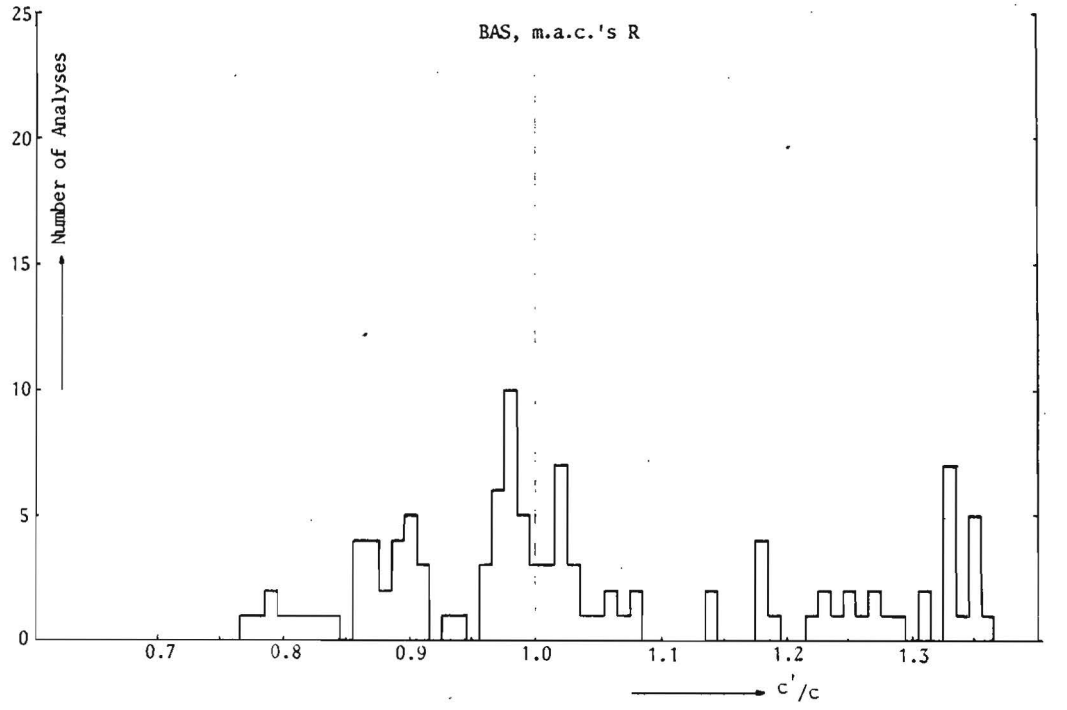

Fig. V.5.a. Histogram showing the results obtained with the BAS program for 117 carbon analyses between 4 and 30 keV when Ruste[1]'s m.a.c.'s are used

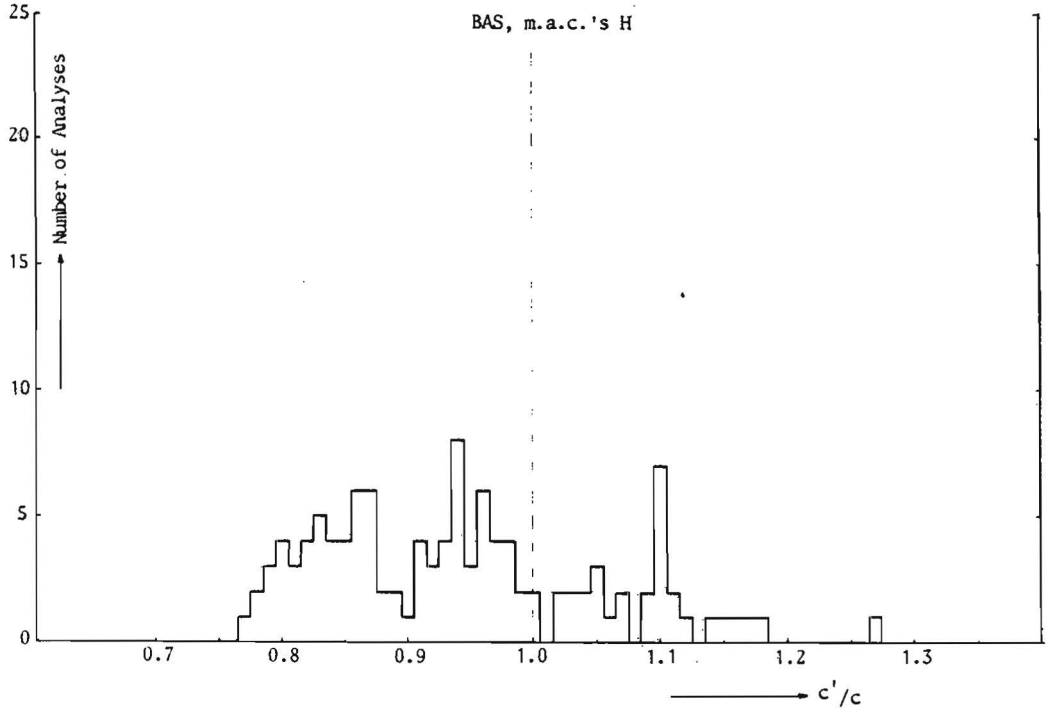

Fig. V.5. b. As a, however, Henke[16]'s m.a.c.'s have been used.

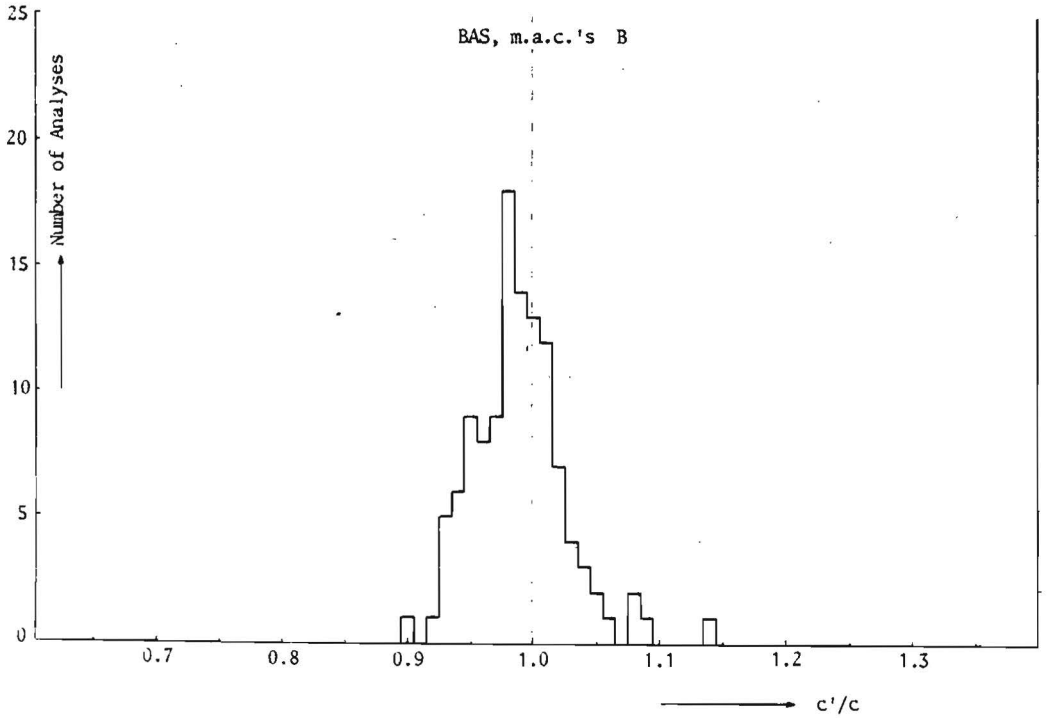

Fig. V.5. c. As a, with the m.a.c.'s of the present investigation.

r.m.s. values (Table V.3.) as well as from the shapes of the histograms. As all programs show more or less significant improvements it must be concluded that Henke's newest set is obviously better than Ruste's set.

Table V.3.

Root-mean-square values* (%) for various correction programs using different sets of mass absorption coefficients.
(117 carbon analyses between 4 and 30 keV).

m.a.c.'s / Program	Ruste[1]	Henke[16]	Present work (BAS)
BAS	16.78	10.85	3.69
LOS	14.19	11.33	8.98
RUSTE	12.56	10.65	11.94
ZAF	19.40	15.27	17.86

*These apply to the ratio between the calculated and nominal concentration for a measured k-ratio.

Table V.4.

Averages obtained with various correction programs using different sets of mass absorption coefficients (117 carbon analyses between 4 and 30 keV).

m.a.c.'s / Program	Ruste[1]	Henke[16]	Present Work (BAS)
BAS	1.045	0.942	0.988
LOS	1.009	0.914	0.958
RUSTE	0.991	0.894	0.946
ZAF	1.042	0.929	0.989

The use of our own set leads to almost spectacular results for the BAS program and to a further improvement for the LOS program, while the RUSTE and ZAF program are somewhat indifferent. This brings us back again to the problem of the m.a.c.'s.

As was shown already in IV.3. a lot of justification in proposing a new and consistent set of m.a.c.'s was found in the application of the "Thin Film" model to the measured k-ratios at high kV's. A further justification can be found in Fig. V.6.a-m, where the calculated concentrations are represented as a function of kV. In the majority of cases the results are almost independent of kV, showing more or less horizontal lines which merely shift up and down with the use of different m.a.c.'s. This is most noticeable in the cases of TiC, VC, ZrC, NbC, TaC and VC. A final justification for our new set of m.a.c.'s can be found in the following reasoning:

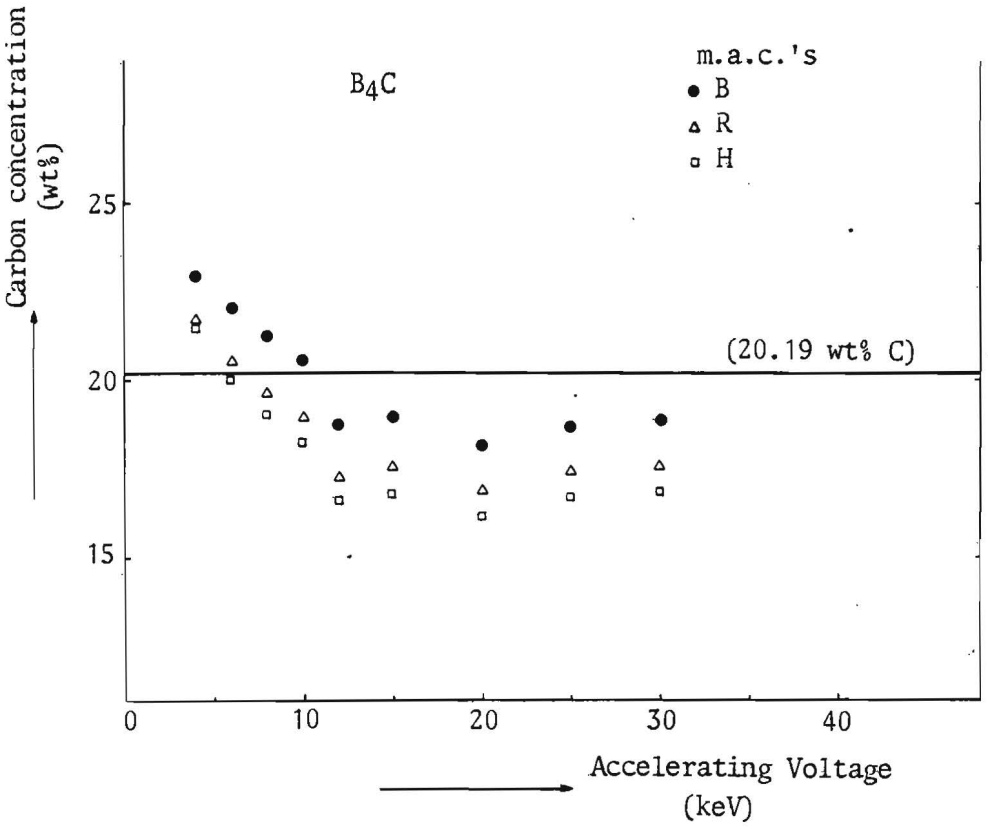

Fig. V.6.a-m Results obtained with the BAS program for carbon analyses in 13 binary carbides using three sets of m.a.c.'s: H = Henke[16], R = Ruste[1], B = present work.

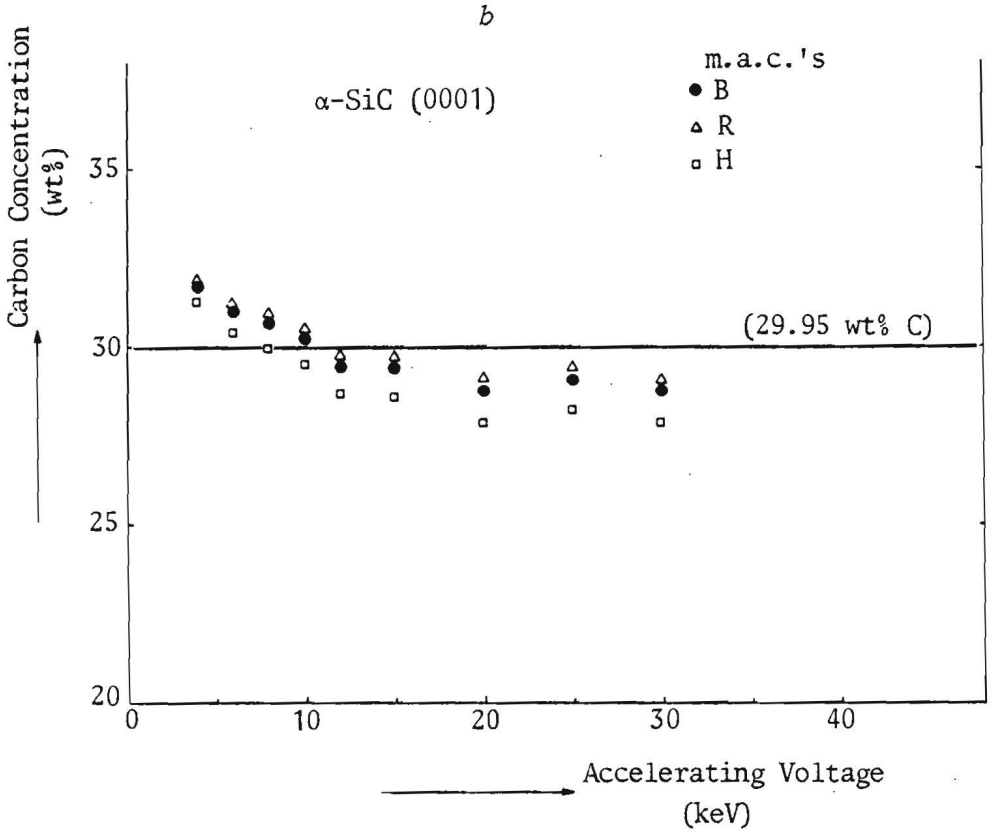
b
α-SiC (0001)
m.a.c.'s
B
R
H
(29.95 wt% C)
Carbon Concentration (wt%)
35
30
25
20
0
10
20
30
40
Accelerating Voltage (keV)

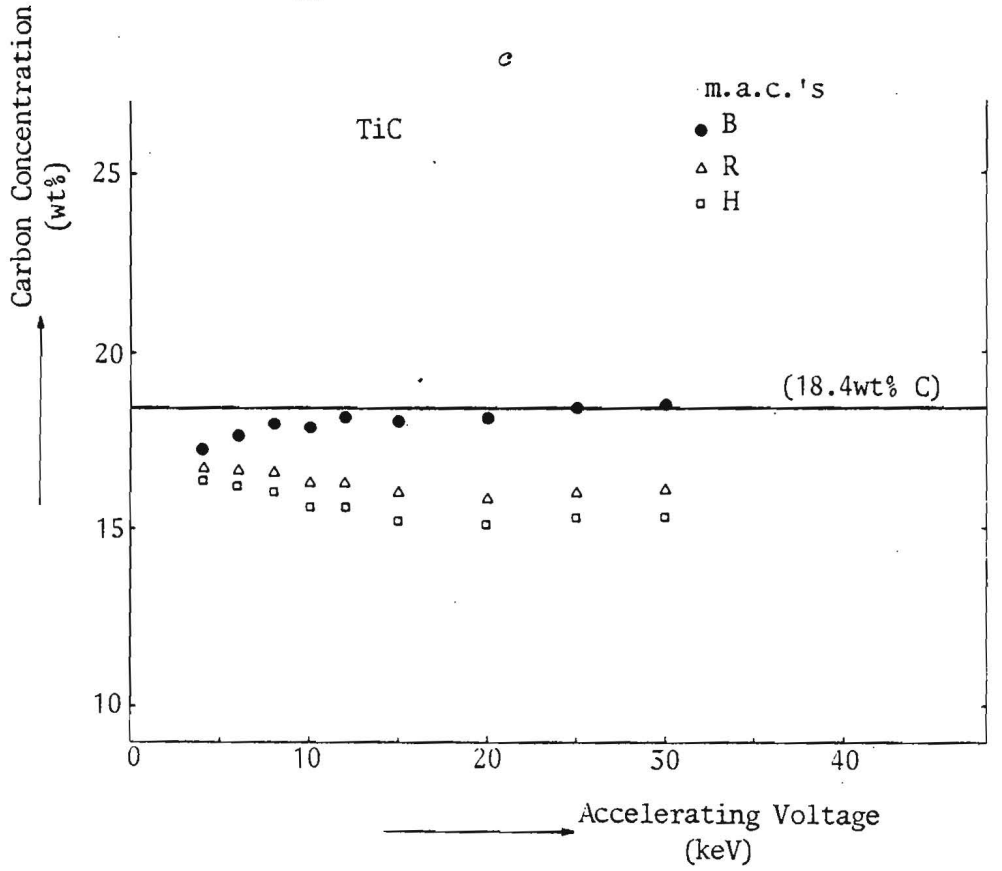
c
TiC
m.a.c.'s
B
R
H
(18.4wt% C)
Carbon Concentration (wt%)
25
20
15
10
0
10
20
30
40
Accelerating Voltage (keV)

Fig. V.6.

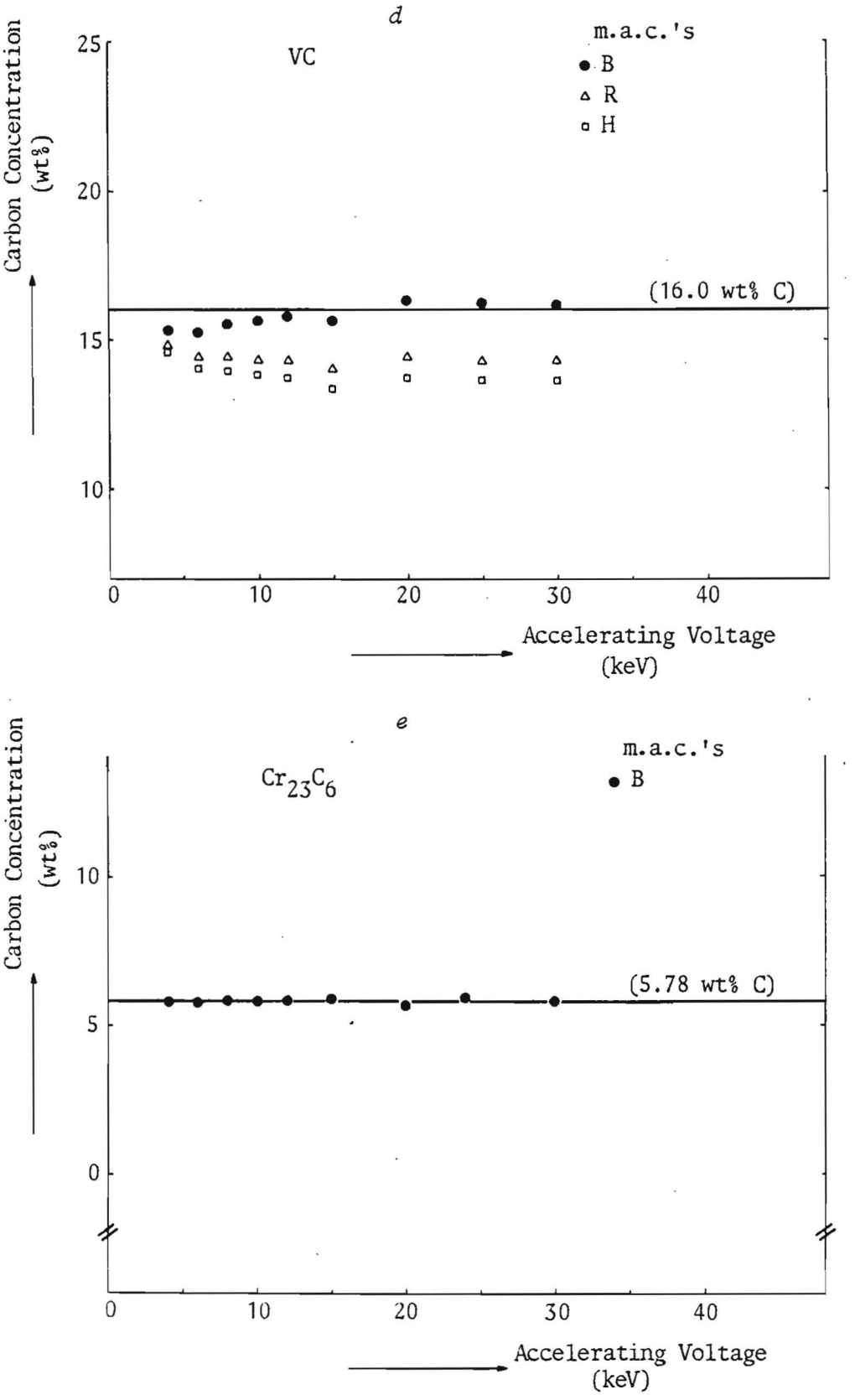
d
VC
m.a.c.'s
B
R
H
Carbon Concentration (wt%)
25
20
15
10
(16.0 wt% C)
0
10
20
30
40
Accelerating Voltage (keV)
e
$Cr_{23}C_6$
m.a.c.'s
B
Carbon Concentration (wt%)
10
5
0
(5.78 wt% C)
0
10
20
30
40
Accelerating Voltage (keV)

Fig. V.6.

f

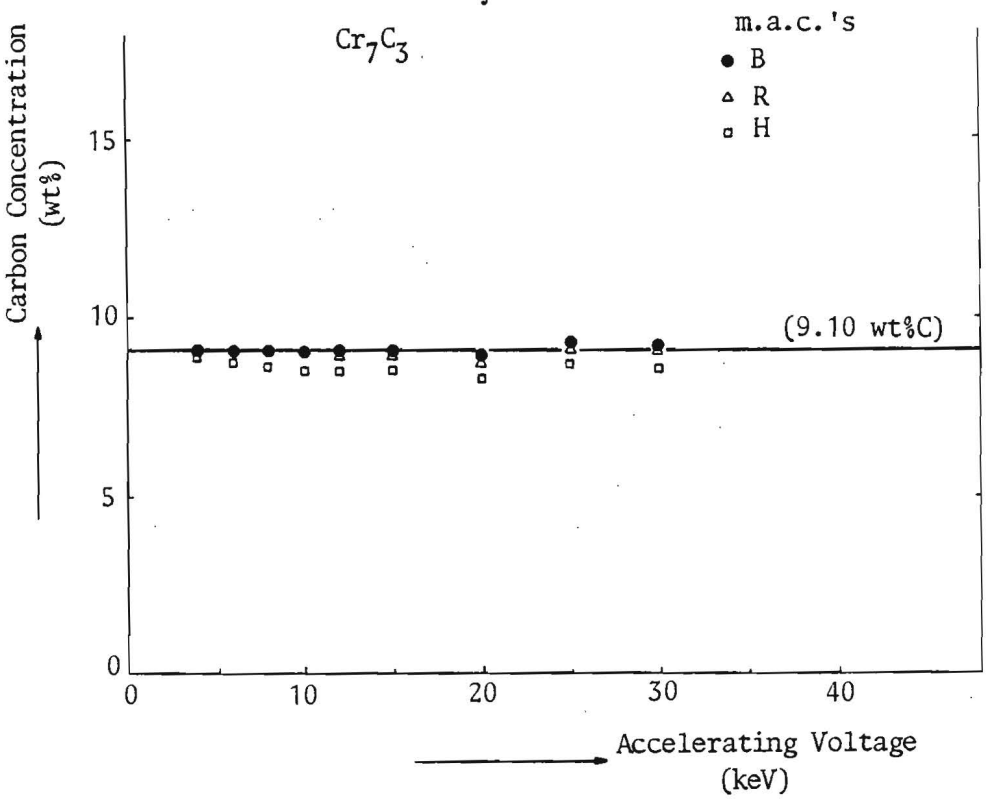
Cr_7C_3
m.a.c.'s
B
R
H
Carbon Concentration (wt%)
15
10
5
0
(9.10 wt%C)
0
10
20
30
40
Accelerating Voltage (keV)

g

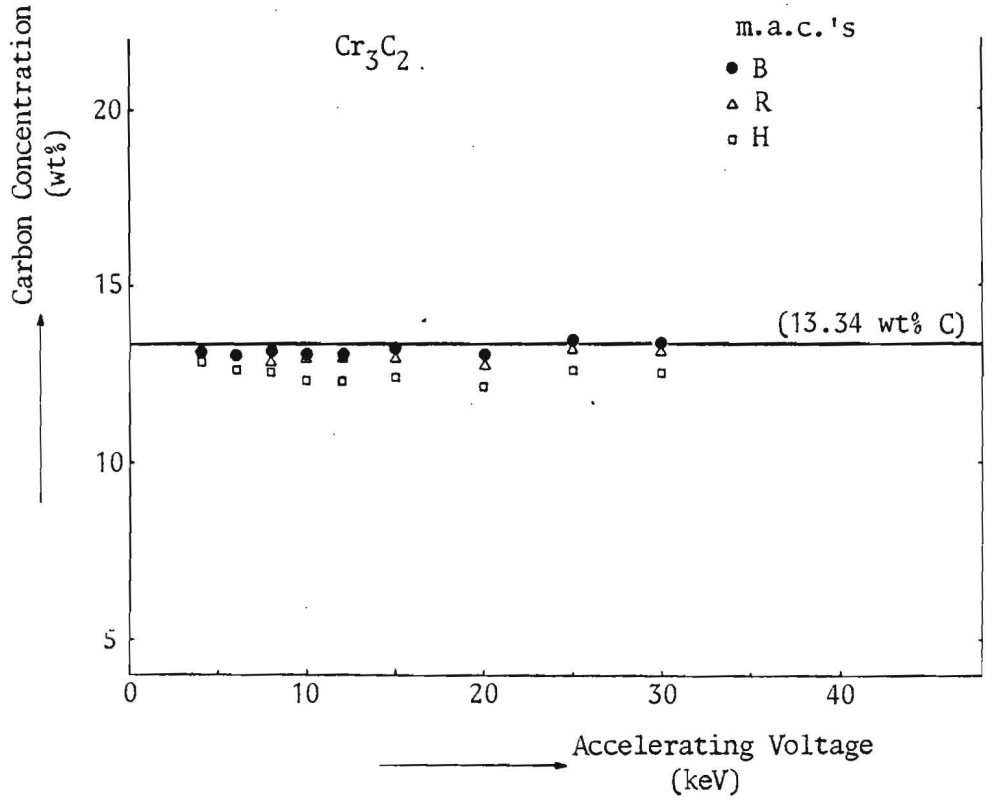
Cr_3C_2
m.a.c.'s
B
R
H
Carbon Concentration (wt%)
20
15
10
5
0
(13.34 wt% C)
0
10
20
30
40
Accelerating Voltage (keV)

Fig. V.6.

h

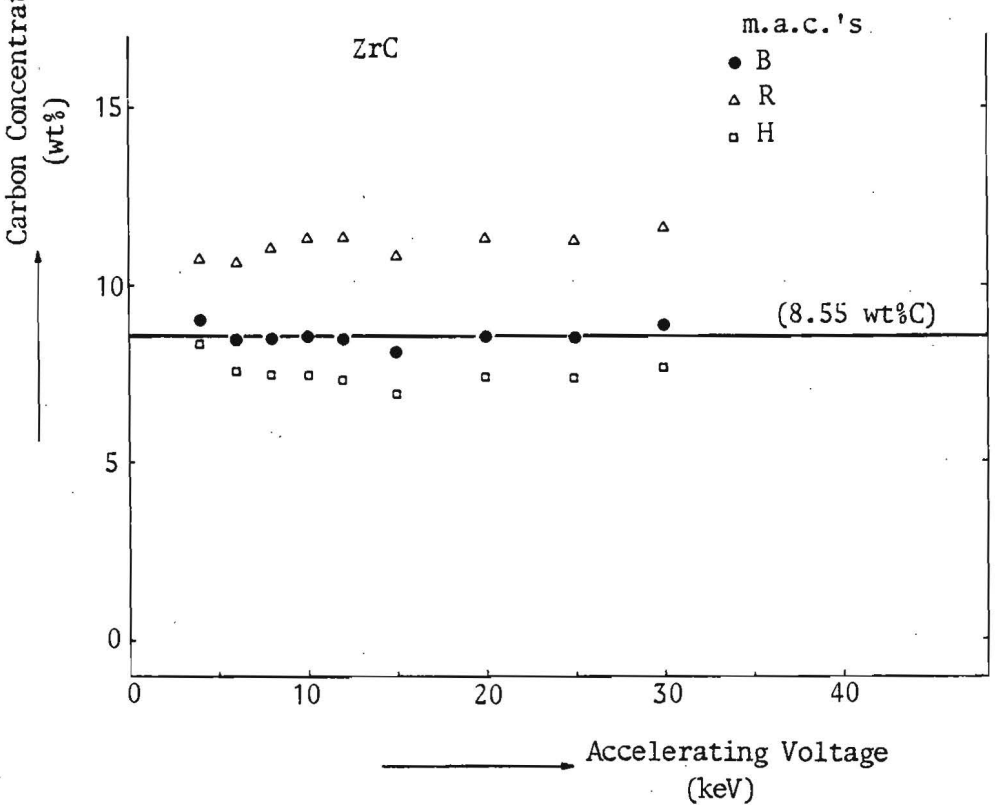
ZrC
m.a.c.'s
B
R
H
Carbon Concentration (wt%)
15
10
5
0
(8.55 wt%C)
0
10
20
30
40
Accelerating Voltage (keV)

i

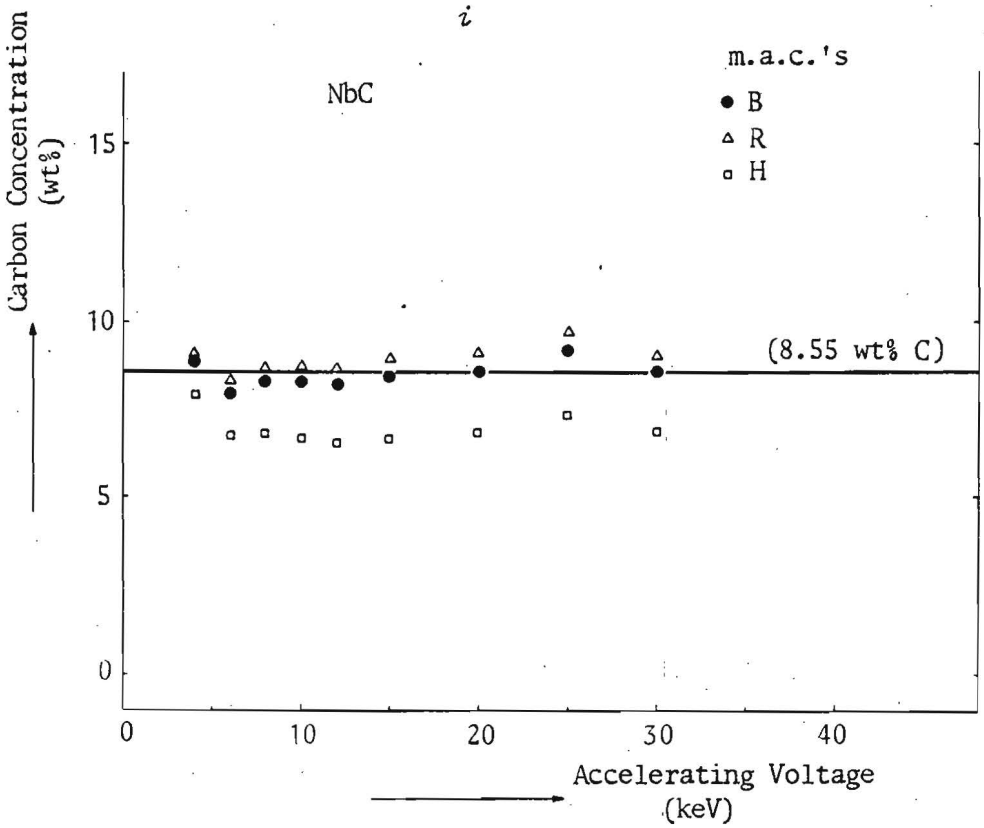
NbC
m.a.c.'s
B
R
H
Carbon Concentration (wt%)
15
10
5
0
(8.55 wt% C)
0
10
20
30
40
Accelerating Voltage (keV)

Fig. V.6.

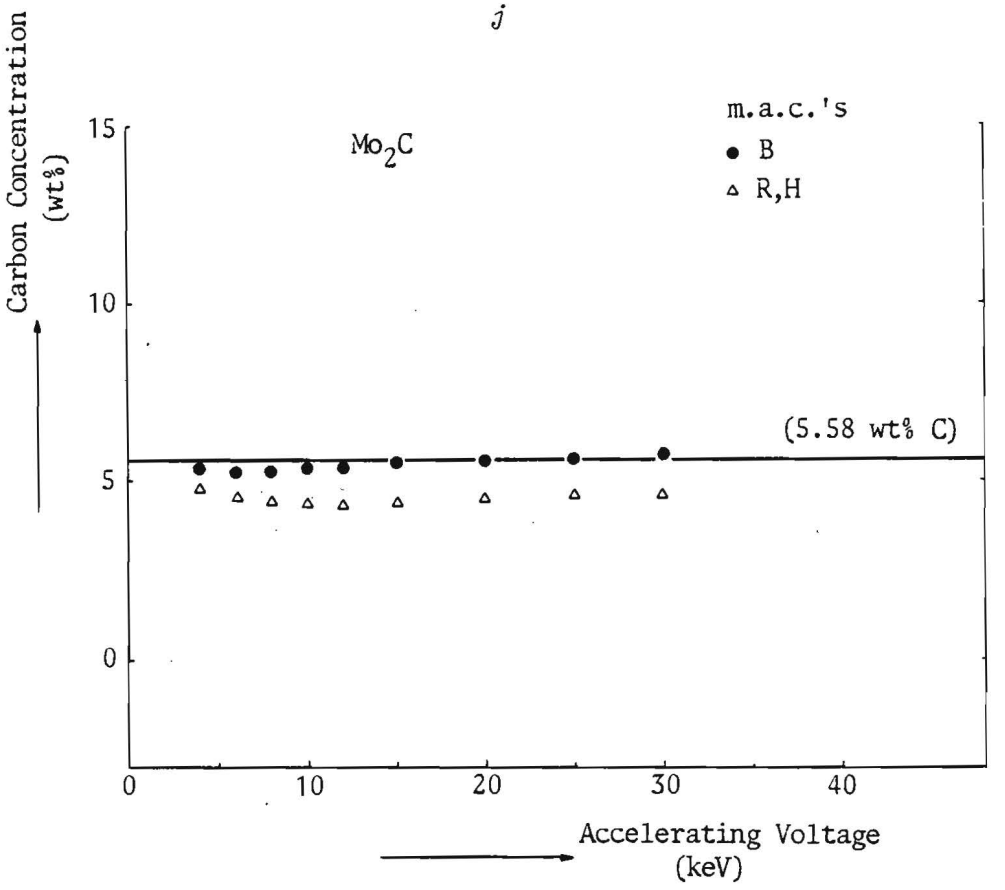
j
Carbon Concentration (wt%)
15
10
5
0
Mo_2C
m.a.c.'s
B
R,H
(5.58 wt% C)
0
10
20
30
40
Accelerating Voltage (keV)

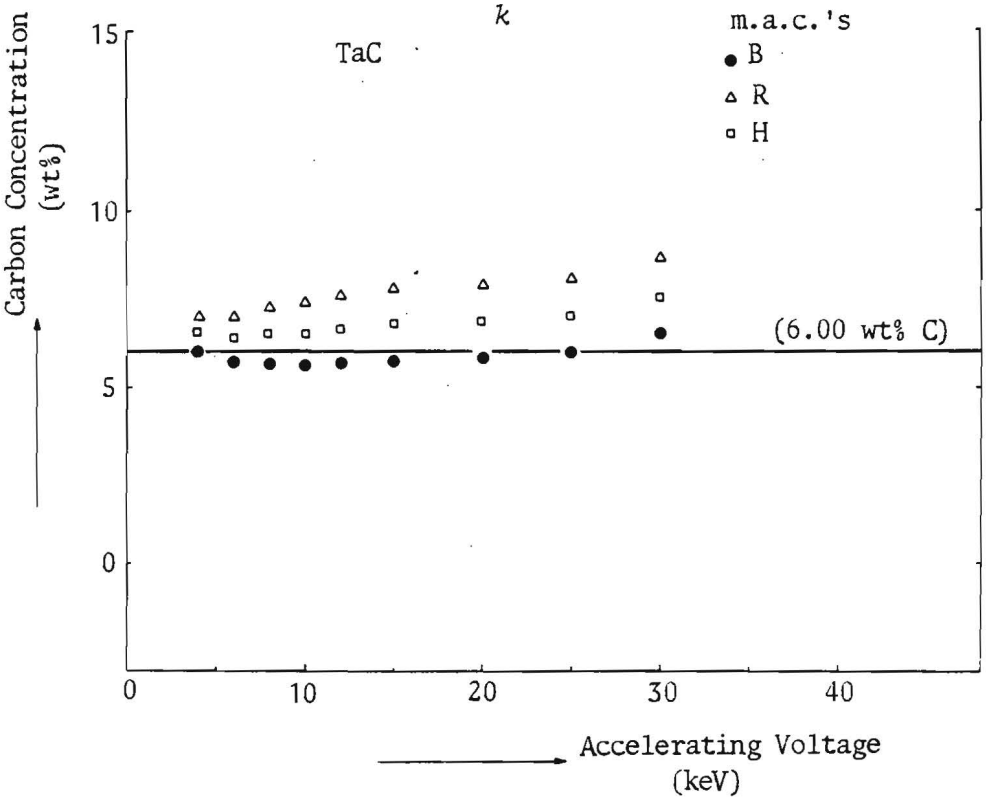
k
Carbon Concentration (wt%)
15
10
5
0
TaC
m.a.c.'s
B
R
H
(6.00 wt% C)
0
10
20
30
40
Accelerating Voltage (keV)

Fig. V.6.

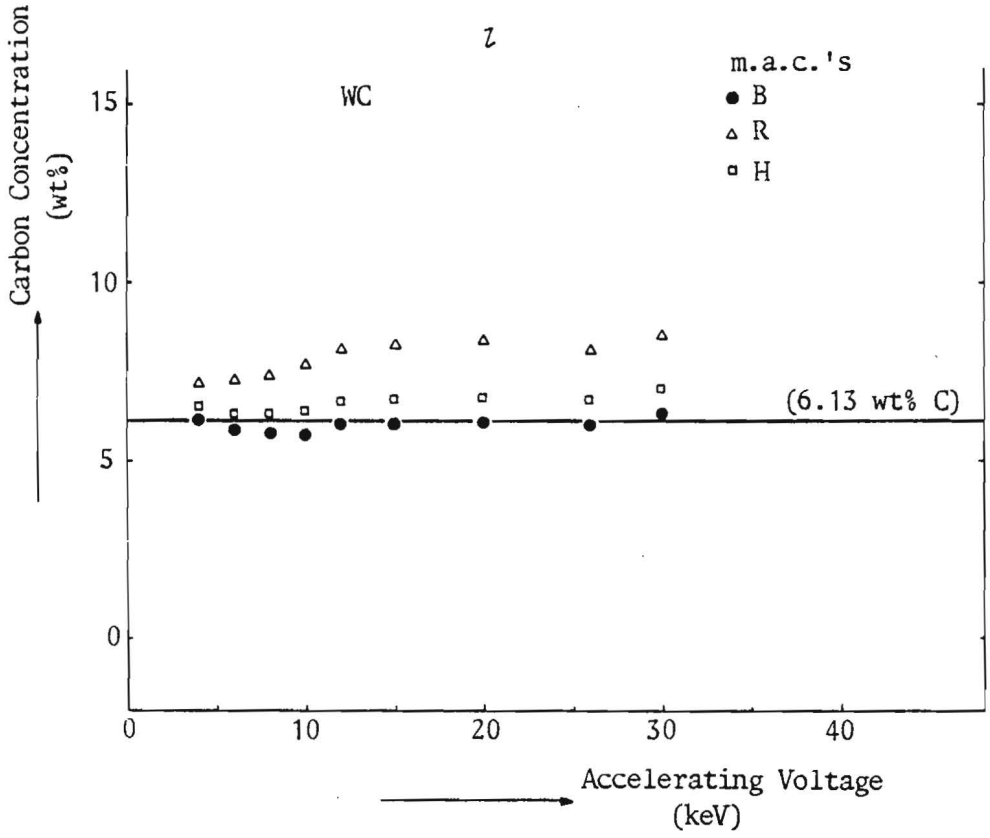
l
WC
m.a.c.'s
B
R
H
Carbon Concentration (wt%)
15
10
5
0
(6.13 wt% C)
0
10
20
30
40
Accelerating Voltage (keV)

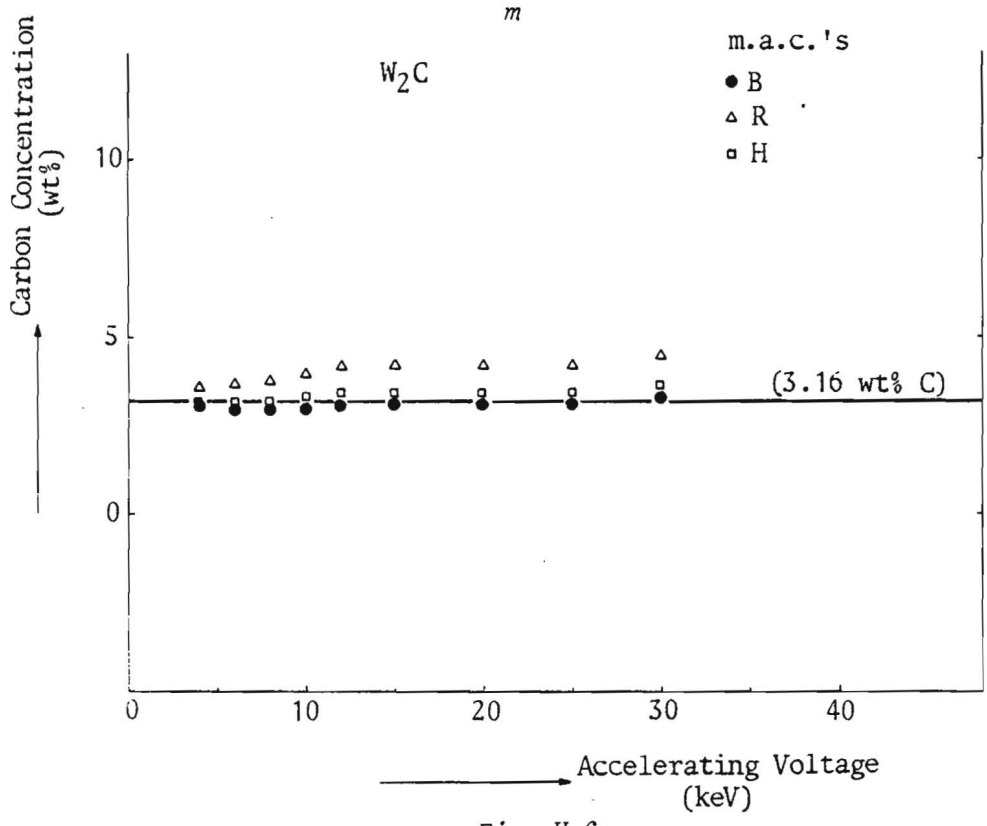
m
W_2C
m.a.c.'s
B
R
H
Carbon Concentration (wt%)
10
5
0
(3.16 wt% C)
0
10
20
30
40
Accelerating Voltage (keV)

Fig. V.6.

It has been established that up to 15 kV the BAS program works perfectly for Fe_3C with respect to carbon (see Fig. V.3), either with Ruste's or Henke[16]'s set. Now, if this is the case, one would expect the program to work equally well for $Cr_{23}C_6$, as all equations used are explicitely or implicitely based on functions of atomic number and/or weight, and the elements Cr and Fe are almost neighbours in the periodic system. As it turns out the results for $Cr_{23}C_6$ are indeed very good for either set of m.a.c.'s; the results cannot be made distinguishable in Fig. V.6.e. This being the case, one would in turn expect very good results for Cr_7C_3 and Cr_3C_2, which is indeed the case for Ruste's m.a.c.'s. Moving one step back in the periodic system brings us to V, in which case suddenly 10-12% too low values are obtained (see Fig. V.6.d). In our opinion this makes no sense; obviously the m.a.c. for C-K_α radiation in V is much too low. For TiC even larger deviations are found. This is the more surprising as the systems Ti-C and V-C require the least correction of all binary carbides investigated: an absorption factor of only about 2 at 4 kV, which one would expect even the ZAF program to be able to cope with. In complete agreement with this reasoning is that the LOS program which came out 10% too high between 4 and 10 kV for Fe_3C gives better results for TiC and VC. Similar reasoning can be applied to the sequence ZrC, NbC and Mo_2C which show remarkable fluctuations in the results (See Fig. V.6.h-j). NbC comes out very well with Ruste's m.a.c.'s while ZrC comes out much too high and Mo_2C too low; whereas with our set results are obtained which are almost independent of kV.

If the m.a.c. is plotted as a function of wavelength, as is done for the example of Zr in Fig. V.7, it becomes immediately obvious why there is such a large scatter in the reported values. The wavelength of C-K_α radiation is always very close to the M5 edge of these metals and the m.a.c.'s have to be determined in a strongly curved area of the curve. This is not the case for Ti and V, in which case it can only be remarked that the values reported by Henke[16] are still the same as those from Henke and Ebisu (1974). Apparently no evidence for revised values has since then been obtained.

A complete survey of our new set of m.a.c.'s, as compared to the other sets can be found in Fig. V.8. Note that our values beyond atomic number 26 (Fe) are only estimates, based on extrapolations of the curve between Ti and Fe. It is further interesting to note that our values for

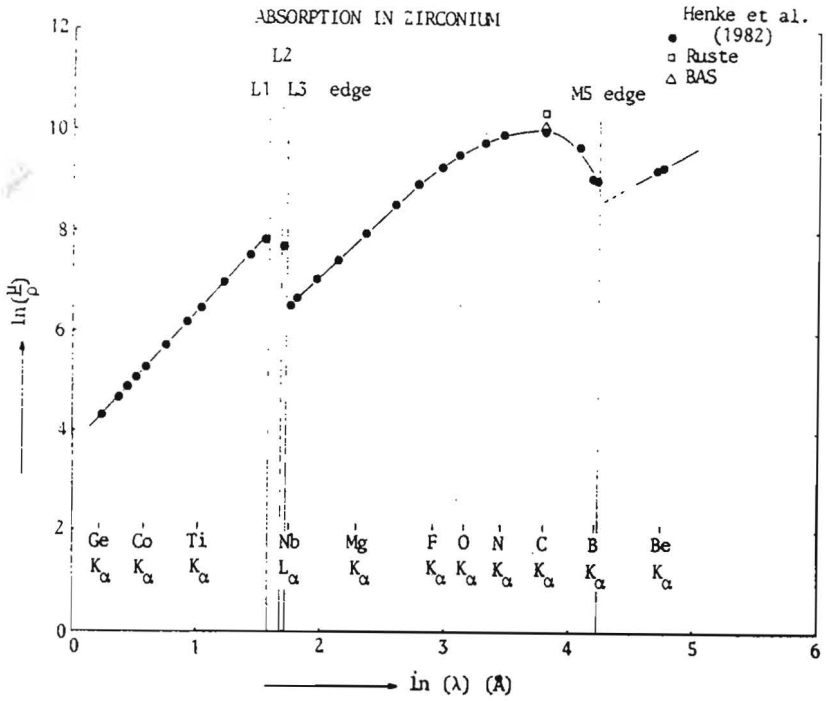

Fig. V.7. Variation of mass absorption coefficient with wavelength in Zirconium Note the strongly curved region close to the M_5-edge where the m.a.c. for C-K_α has to be determined. Quite similar curves apply to Nb and Mo.

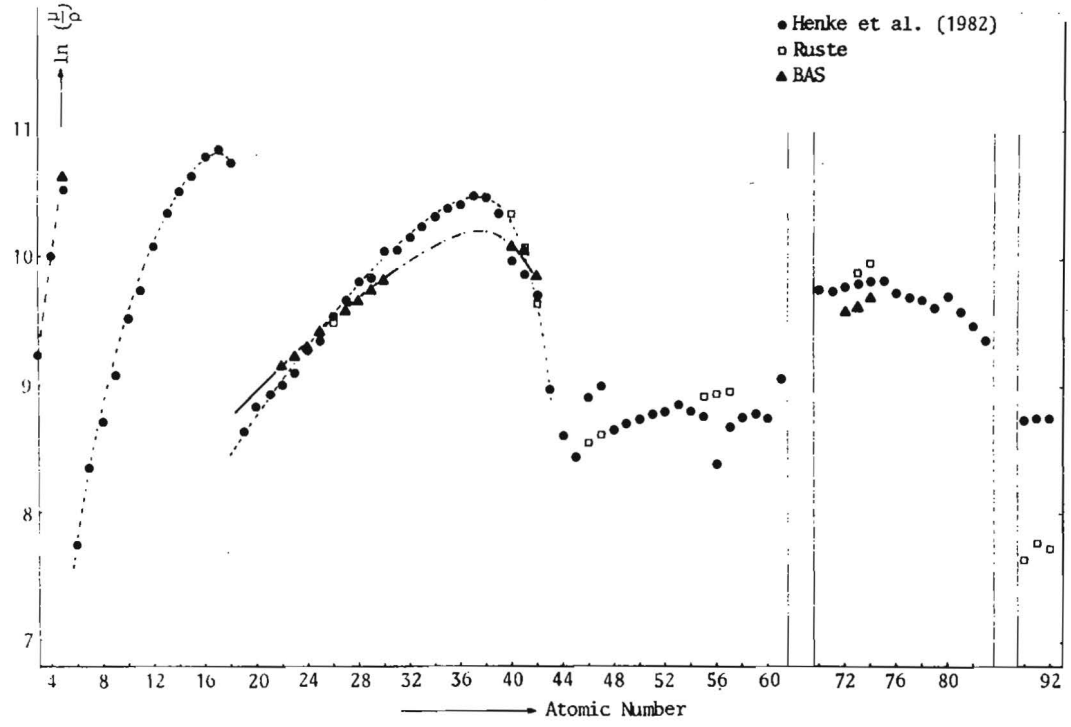

Fig. V.8. Variation of m.a.c. for Carbon-K_α radiation with the atomic number of the absorber. Values of 3 sources for specific elements are compared. Note that our values in the region 26 < Z < 40 rely only upon extrapolation from lower atomic numbers.

Ta and W have a tendency to take away much of the discontinuity in Henke's values and perhaps provide a better connection with the atomic numbers beyond 76.

V.4.3. Final test in the Titanium-Carbon system

As already mentioned in Chapter III, we had a special interest in the Ti-C system for a number of reasons. It was, therefore, of utmost importance to us to be absolutely sure about the composition of the TiC specimen, used in the present investigation. It was dediced to test our measuring procedures and our value of the m.a.c. for C in Ti on two two-phased Ti-C alloys: one containing the maximum possible Carbon-content (19.66 wt% C at 2770 ^{o}C) according to the most recent phase diagram[18] and one containing the minimum Carbon content (10.55 wt%C at 1650^{o}C).
These alloys were prepared by repeated argon-arc melting. As could be expected on the basis of the phase diagram the carbon-rich specimen contained primary TiC, in equilibrium with graphite. The Ti-rich specimens contained TiC in equilibrium with Ti. The application of our measuring procedure to these specimens yielded values of 19.60 and 10.28 wt% Carbon, respectively, which are within 2.5% relative of the expected values. Since then a number of diffusion experiments have been performed in the Ti-C system and in no cases concentrations have been measured that are outside the reported homogeneity range of TiC.
In our opinion these experiments prove beyond any reasonable doubt that both our procedures as well as our value of the m.a.c. for C-K_{α} in Ti is correct.

Summarizing Chapter V we could say that it is apparently possible to measure carbon quantitatively with a relative accuracy of better than 3.7% over the range between 4 and 30 kV. If this range would be restricted to between 8 and 12 kV, which we personally prefer for reasons discussed before, this figure would undoubtedly be much better still.

References

1. J. Ruste, J. Microsc. Spectrosc. Electron., 4 (1979), 123.
2. J. Ruste and M. Gantois, J. Phys. D: Appl. Phys., 8 (1975) 872.
3. J. Ruste and C. Zeller, C.R. Acad. Sc. Paris, 284, serie B (1977) 507.
4. W. Weisweiler, Microchim. Acta. 1982/2, 145.
5. W. Weisweiler, Microchim. Acta. 1975I, 611.
6. W. Weisweiler, Microchim. Acta. 1975II, 179.
7. W. Weisweiler, Arch. Eisenhüttenwes. 49 (1978), 555.
8. G. Love, M.G.C. Cox and V.D. Scott, J. Phys. D: Appl. Phys., 7 (1974) 2131.
9. E. Kohlhaas and F. Scheiding, Arch. Eisenhüttenwes., 41 (1970), 97.
10. D. Fornwalt and A. Manzione, Norelco Reporter, 13 (1966), 39.
11. T. Shiraiwa and N. Fujino, Jap. J. Appl. Phys., 9 (1970),976
12. P. Duncumb and D.A. Melford, IVth Conference on X-ray Optics and Micro-analysis, R. Castaing Ed., Hermann, Paris (1966), 240.
13. G.F. Bastin, F.J.J. van Loo and H.J.M. Heijligers, X-ray Spec., 13 (1984) 91.
14. G.F. Bastin, H.J.M. Heijligers and F.J.J. van Loo, Scanning, 6, (1984), 58
15. B.L. Henke and E.S. Ebisu, Adv. in X-ray Analysis, 17 (1974) 150.
16. B.L. Henke et al., Atomic Data and Nuclear Data Tables, 27 (1982), 1.
17. J.E. Holliday in "The Electron Microprobe", T.D. McKinley, K.F.J. Heinrich, D.B. Wittry, Eds., John Wiley & Sons, New-York (1966), 3.
18. E.K. Storms, "The Refractory Carbides", J.L. Margrave, Ed., Academic Press, New York, 1967.
19. G. Love, M.G. Cox and V.D. Scott, J. Phys. D: Appl. Phys., 11 (1978), 23.
20. P. Duncumb and S.J.B. Reed in: Quantitative Electron Probe Micro-Analysis, K.F.J. Heinrich, Ed., NBS Spec. Publ. No. 298, (1968) 133.
21. J. Philibert and R. Tixier in: Quantitative Electron Probe Micro-Analysis, K.F.J. Heinrich, Ed., NBS Spec. Publ. No. 298, (1968) 13.
22. D.R. Beaman and J.A. Isasi in: Electron Beam Microanalysis, A.S.T.M. Spec. Techn. Publ. 506 (1972).
23. G. Love, M.G. Cox and V.D. Scott, J. Phys. D: Appl. Phys. 11 (1978) 7.
24. J. Philibert, in Proc. 3rd Int. Symp. on X-ray Optics and X-ray Microanalysis, H.H. Pattee, V.E. Cosslett and E. Engström, Eds., Acad. Press, New York (1963), 379.
25. H.E. Bishop, J. Phys. D: Appl. Phys. 7 (1974) 2009.
26. G. Love and V.D. Scott, J. Phys. D: Appl. Phys., 11 (1978) 1369.
27. S.J.B. Reed, Brit. J. Appl. Phys., 16 (1965) 913.
28. R.H. Packwood and J.D. Brown, X-ray Spec., 10 (1981) 138.
29. J.D. Brown and R.H. Packwood, X-ray Spec., 11 (1982) 187.
30. M.J. Berger and S.M. Seltzer, Nucl. Ser. Rep. No. 39, NAS-NRC Publ. No. 1133 (Washington D.C.; Nat. Acad. Sci), (1964) 205.

B_4C (20.19 wt% C)

kV	Beam Current (nA)		Gross Peak Intensities (cps/nA)				Backgrounds (cps/nA)[1]				Peak k-ratios	
	$B\text{-}K_\alpha$	$C\text{-}K_\alpha$	$B\text{-}K_\alpha$		$C\text{-}K_\alpha$		$B\text{-}K_\alpha$		$C\text{-}K_\alpha$		$B\text{-}K_\alpha$	$C\text{-}K_\alpha$
			B	B_4C	Fe_3C	B_4C	B	B_4C	Fe_3C	B_4C		
4	200	100	17.86	13.63	4.02	5.17	0.25	0.18	0.29	0.48	0.7636±0.0110	1.2593±0.0455
6	150	200	25.51	19.53	4.78	4.88	0.31	0.27	0.32	0.67	0.7644±0.0119	0.9424±0.0232
8	100	200	31.12	22.66	4.69	4.04	0.36	0.30	0.30	0.70	0.7271±0.0110	0.7604±0.0207
10	100	250	27.56	20.01	4.35	3.40	0.29	0.23	0.30	0.73	0.7253±0.0122	0.6581±0.0290
12	100	250	26.94	18.64	4.01	2.83	0.27	0.21	0.29	0.76	0.6910±0.0112	0.5560±0.0375
15	64	300	26.39	17.95	3.34	2.37	0.22	0.20	0.26	0.67	0.6784±0.0127	0.5516±0.0303
20	98	300	21.58	14.33	2.61	1.82	0.20	0.17	0.24	0.54	0.6624±0.0216	0.5418±0.0254
25	100	300	17.43	11.42	2.06	1.53	0.17	0.11	0.21	0.44	0.6554±0.0096	0.5895±0.0189
30	100	300	14.16	9.38	1.77	1.33	0.13	0.11	0.23	0.37	0.6610±0.0108	0.6194±0.0155

[1]Background for carbon measured at position of carbon peak and composed on basis of weight fraction of constituent element (See II.1); That of B measured at ± 20 mm on either side of the peak and interpolated.

P.H.A. settings: $B\text{-}K_\alpha$ Counter H.T. 1700 Volt; Lower Level 0.6 Volt; Window: open; Gain 64x7.0

$C\text{-}K_\alpha$ " " " " ; " " 0.6 Volt; " : 5.0 Volt; Gain 64x5.0.

$B\text{-}K_\alpha$ and $C\text{-}K_\alpha$ both on Stearate.

SiC (29.95 wt% C)

kV	Beam current (nA)		Gross Peak Intensities (cps/nA)				Backgrounds (cps/nA)[1]				Peak k-ratios	
	Si-K_α	C-K_α	Si-K_α		C-K_α		Si-K_α		C-K_α		Si-K_α	C-K_α
			Si	SiC	Fe_3C	SiC	Si	SiC	Fe_3C	SiC		
4	30	100	138.52	93.80	4.02	12.01	0.53	0.42	0.29	0.42	0.6767±0.0041	3.1139±0.0292
6	10	200	389.58	266.64	4.78	11.80	1.55	0.88	0.32	0.52	0.6849±0.0055	2.5268±0.0193
8	3	200	699.97	486.91	4.69	10.02	2.08	1.67	0.30	0.55	0.6953±0.0056	2.1778±0.0182
10	3	250	1045.15	714.41	4.35	8.48	2.55	2.00	0.30	0.55	0.6833±0.0048	1.9583±0.0142
12	3	250	1419.78	958.27	4.01	7.16	3.16	2.33	0.29	0.52	0.6748±0.0040	1.7863±0.0157
15	1	300	1959.87	1328.21	3.34	5.80	4.86	3.50	0.26	0.47	0.6776±0.0061	1.7270±0.0163
20	1	300	2890.11	1947.95	2.61	4.37	6.54	5.00	0.24	0.38	0.6738±0.0048	1.6862±0.0184
25	1	300	3546.72	2370.56	2.06	3.58	6.96	6.00	0.21	0.31	0.6680±0.0047	1.7647±0.0192
30	1	300	4222.37	2800.89	1.77	3.01	12.52	8.50	0.23	0.26	0.6633±0.0040	1.7812±0.0204

[1]Background for carbon measured at position of Carbon Peak and composed on basis of weight fraction of constituent element (see II.1.); That of Si measured at ± 5 mm on either side of the peak and interpolated.

P.H.A. Settings: Si-K_α Counter 1600 Volt; Lower Level 0.6 Volt; Window: open ; Gain 32x4.4

C-K_α " 1700 " ; " " 0.6 " ; " : 5.0 Volt; " 64x5.0

Si-K_α on TAP; C-K_α on Stearate

TiC (18.40 wt% C)

kV	Beam Current (nA)		Gross Peak Intensities (cps/nA)				Backgrounds (cps/nA)[1]				Peak k-ratios	
			Ti-K_α		C-K_α		Ti-K_α		C-K_α		Ti-K_α	C-K_α
	Ti-K_α	C-K_α	Ti	TiC	Fe_3C	TiC	Ti	TiC	Fe_3C	TiC		
4	--	300	--	--	4.03	14.74	--	--	0.29	0.31	--------	3.8627±0.0923
6	100	250	22.30	17.19	4.77	19.97	0.21	0.21	0.32	0.37	0.7783±0.0046	4.3993±0.0421
8	30	250	134.13	106.27	4.66	21.91	0.59	0.51	0.30	0.40	0.7920±0.0048	4.9305±0.0348
10	15	250	295.06	236.80	4.37	21.85	1.00	1.20	0.30	0.38	0.8012±0.0040	5.2727±0.0832
12	10	200	361.62	284.49	3.90	20.70	1.01	0.80	0.29	0.37	0.7867±0.0040	5.6309±0.0808
15	10	230	645.47	514.25	3.29	18.17	1.55	1.37	0.26	0.34	0.7965±0.0032	5.8780±0.0744
20	3	250	1183.32	939.26	2.55	14.36	2.25	1.73	0.24	0.30	0.7938±0.0048	6.0919±0.1268
25	3	300	1778.80	1419.98	2.06	11.73	3.11	2.98	0.21	0.27	0.7980±0.0040	6.1990±0.0834
30	2	300	2337.98	1889.57	1.79	9.81	4.58	3.25	0.22	0.24	0.8084±0.0040	6.1131±0.0886

[1]Background for Carbon measured at position of Carbon Peak and composed on basis of weight fraction of constituent element (see II.1.); that of Ti measured at ± 5 mm on either side of the peak and interpolated.

P.H.A. Settings: Ti-K_α Counter 1600 Volt; Lower Level 0.6 Volt; Window: open; Gain: 64x6.5.
C-K_α " 1700 Volt; " " 0.6 Volt; " : 5.0 Volt; " : 64x5.0.

Ti-K_α on PET, C-K_α on Stearate

VC (16.00 wt% C)

kV	Beam Current (nA)		Gross Peak Intensities (cps/nA)				Backgrounds (cps/nA)[1]				Peak k-ratios	
	$V\text{-}K_\alpha$	$C\text{-}K_\alpha$	$V\text{-}K_\alpha$		$C\text{-}K_\alpha$		$V\text{-}K_\alpha$		$C\text{-}K_\alpha$		$V\text{-}K_\alpha$	$C\text{-}K_\alpha$
			V	VC	Fe_3C	VC	V	VC	Fe_3C	VC		
4	--	300	--	--	4.03	12.09	--	--	0.29	0.30	-------	3.1547±0.0349
6	100	250	10.93	8.65	4.77	15.70	0.27	0.23	0.32	0.35	0.7901±0.0087	3.4447±0.0600
8	30	250	136.62	111.30	4.66	16.88	0.88	0.77	0.30	0.37	0.8143±0.0049	3.7867±0.0478
10	15	250	343.37	275.13	4.37	16.89	1.56	1.07	0.30	0.38	0.8018±0.0040	4.0560±0.0702
12	10	200	520.26	421.40	3.90	15.72	1.62	1.20	0.29	0.35	0.8102±0.0040	4.2567±0.1021
15	10	230	955.24	781.15	3.29	13.57	2.39	2.00	0.26	0.31	0.8177±0.0033	4.3718±0.0631
20	3	250	1837.25	1514.71	2.55	11.06	4.02	3.03	0.24	0.26	0.8246±0.0041	4.6763±0.1108
25	3	300	2808.73	2313.20	2.06	8.78	5.63	5.13	0.21	0.24	0.8234±0.0040	4.6182±0.1481
30	2	300	3748.70	3129.41	1.79	7.33	7.79	5.00	0.22	0.22	0.8352±0.0033	4.5470±0.1133

[1]Background for Carbon measured at position of Carbon Peak and composed on basis of weight fraction of constituent element (See II.1.); that of V measured at ±5mm on either side of the peak and interpolated.

P.H.A. Settings: $V\text{-}K_\alpha$: Counter 1600 Volt; Lower Level 0.6 Volt; Window: Open ; Gain: 64x6.5.
$C\text{-}K_\alpha$: " 1700 Volt; " " 0.6 Volt; " : 5.0Volt ; Gain: 64x5.0.

$V\text{-}K_\alpha$ on PET; $C\text{-}K_\alpha$ on Stearate

$Cr_{23}C_6$ (5.78 wt% C)

kV	Beam current (nA)		Gross Peak Intensities (cps/nA)				Backgrounds (cps/nA)[1]				Peak k-ratios	
	Cr-K_α	C-K_α	Cr-K_α		C-K_α		Cr-K_α		C-K_α		Cr-K_α	C-K_α
			Cr	$Cr_{23}C_6$	Fe_3C	$Cr_{23}C_6$	Cr	$Cr_{23}C_6$	Fe_3C	$Cr_{23}C_6$		
4	--	200	---	---	3.33	3.88	--	--	0.23	0.32	-----	1.1495±0.0206
6	--	300	---	---	4.08	4.97	--	--	0.23	0.35	-----	1.1969±0.0114
8	30	300	107.85	100.04	3.99	5.14	1.20	1.10	0.22	0.36	0.9276±0.0047	1.2657±0.0184
10	17.5	300	313.19	290.11	3.78	5.00	2.17	2.23	0.21	0.34	0.9256±0.0049	1.3054±0.0146
12	10	300	530.22	490.48	3.43	4.66	2.50	2.55	0.20	0.32	0.9246±0.0053	1.3417±0.0172
15	5	300	1011.80	945.32	2.89	4.02	5.77	3.64	0.17	0.29	0.9343±0.0035	1.3711±0.0140
20	2	300	2326.19	2163.70	2.07	2.79	7.34	7.40	0.17	0.26	0.9299±0.0085	1.3293±0.0161
25	1.5	300	3134.80	2909.08	1.58	2.24	8.50	8.20	0.14	0.23	0.9279±0.0029	1.3939±0.0170
30	1	300	4342.17	4030.09	1.34	1.82	11.19	10.51	0.14	0.19	0.9280±0.0028	1.3533±0.0184

[1]Background for Carbon measured at position of Carbon Peak and composed on basis of weight fraction of constituent element (See II.1.); that of Cr measured at ± 5mm on either side of the peak and interpolated.

P.H.A. Settings: Cr-K_α : Counter 1600 Volt; Lower Level: 0.6 Volt; Window: open; Gain 64x6.0.
C-K_α : " 1700 Volt; " " : 1.0 Volt; " : 2.0Volt; Gain 64x5.0.

Cr-K_α on PET; C-K_α on Stearate

Cr_7C_3 (9.10 wt% C)

kV	Beam current (nA)		Gross Peak Intensities (cps/nA)				Backgrounds (cps/nA)[1]				Peak k-ratios	
	Cr-K_α	C-K_α	Cr-K_α		C-K_α		Cr-K_α		C-K_α		Cr-K_α	C-K_α
			Cr	Cr_7C_3	Fe_3C	Cr_7C_3	Cr	Cr_7C_3	Fe_3C	Cr_7C_3		
4	--	200	--	--	3.33	5.90	--	--	0.23	0.32	-----	1.8012±0.0328
6	--	300	--	--	4.08	7.65	--	--	0.23	0.36	-----	1.8926±0.0140
8	30	300	97.52	85.79	3.99	7.92	1.30	1.18	0.22	0.37	0.8793±0.0053	2.0008±0.0163
10	30	300	284.62	251.40	3.78	7.67	2.27	2.00	0.21	0.35	0.8833±0.0044	2.0524±0.0191
12	10	300	544.99	483.53	3.43	7.15	3.41	3.20	0.20	0.33	0.8869±0.0045	2.1104±0.0218
15	5	300	1048.30	926.34	2.89	6.17	5.41	5.16	0.17	0.30	0.8833±0.0044	2.1620±0.0162
20	1	300	2102.89	1870.99	2.07	4.33	7.72	7.50	0.17	0.26	0.8930±0.0049	2.1376±0.0312
25	1	300	3249.67	2927.13	1.58	3.45	14.25	11.50	0.14	0.23	0.9013±0.0045	2.2337±0.0280
30	1	300	4432.69	4113.83	1.34	2.82	15.85	15.00	0.14	0.19	0.8936±0.0049	2.1820±0.0249

[1] Background for Carbon measured at position of Carbon Peak and composed on basis of weight fraction of constituent element (See II.1.); that of Cr measured at ± 5 mm on either side of the peak and interpolated.

P.H.A. Settings: Cr-K_α : Counter H.T. 1600 Volt; Lower Level: 0.6 Volt; Window: open; Gain 64x4.5.
C-K_α : " " 1700 Volt; " " : 1.0 Volt; " : 2.0 Volt; Gain 64x5.0.

Cr-K_α on PET; C-K_α on Stearate

Cr_3C_2 (13.30 wt% C)

kV	Beam current (nA)		Gross Peak Intensities (cps/nA)				Backgrounds (cps/nA)[1]				Peak k-ratios	
	$Cr\text{-}K_\alpha$	$C\text{-}K_\alpha$	$Cr\text{-}K_\alpha$		$C\text{-}K_\alpha$		$Cr\text{-}K_\alpha$		$C\text{-}K_\alpha$		$Cr\text{-}K_\alpha$	$C\text{-}K_\alpha$
			Cr	Cr_3C_2	Fe_3C	Cr_3C_2	Cr	Cr_3C_2	Fe_3C	Cr_3C_2		
4	--	200	---	---	3.33	8.15	---	---	0.23	0.33	-----	2.5265±0.0758
6	--	300	---	---	4.08	10.71	---	---	0.23	0.36	-----	2.6859±0.0175
8	30	300	107.85	89.35	3.99	11.19	1.20	1.00	0.22	0.37	0.8284±0.0072	2.8662±0.0178
10	17.5	300	313.19	261.48	3.78	10.86	2.17	1.87	0.21	0.36	0.8347±0.0046	2.9442±0.0192
12	10	300	550.22	434.41	3.43	10.17	2.50	2.47	0.20	0.34	0.8185±0.0050	3.0414±0.0206
15	5	300	1011.80	847.81	2.89	8.87	3.77	3.18	0.17	0.30	0.8379±0.0051	3.1546±0.0284
20	2	300	2326.19	1965.34	2.07	6.25	7.34	8.00	0.17	0.27	0.8441±0.0042	3.1444±0.0394
25	1.5	300	3134.80	2647.98	1.58	4.93	8.50	8.53	0.14	0.23	0.8470±0.0033	3.2559±0.0350
30	1	300	4342.17	3667.91	1.34	4.04	11.19	11.26	0.14	0.20	0.8443±0.0021	3.1912±0.0335

[1] Background for Carbon measured at position of Carbon Peak and composed on basis of weight fraction of constituent element (See II.1); that of Cr measured at ± 5 mm on either side of the peak and interpolated.

P.H.A. Settings: $Cr\text{-}K_\alpha$: Counter 1600 Volt; Lower Level: 0.6 Volt; Window: open; Gain: 64x6
$C\text{-}K_\alpha$: " 1700 Volt; " " : 1.0 Volt; " : 2.0Volt;Gain: 64x5

$Cr\text{-}K_\alpha$ on PET; $C\text{-}K_\alpha$ on Stearate.

Fe_3C (6.67 wt% C)

kV	Beam Current (nA)	Gross Peak Intensities (cps/nA)		Background (cps/nA)[1]		Peak k-ratio
		Fe-K_α		Fe-K_α		
		Fe	Fe_3C	Fe	Fe_3C	
8	300	6.42	5.64	0.10	0.10	0.8925±0.0071
10	100	38.50	35.45	0.21	0.22	0.9200±0.0046
12	50	93.80	87.06	0.39	0.36	0.9282±0.0046
15	30	205.71	190.25	0.64	0.56	0.9250±0.0037
20	15	442.40	407.03	0.90	0.95	0.9179±0.0035
25	15	713.91	670.58	1.50	1.34	0.9394±0.0028
30	10	1009.98	939.16	1.56	1.93	0.9294±0.0028

[1]Background for Fe measured at±5 mm on either side of the peak and interpolated

P.H.A. Setting: Counter 1600 Volt; Lower Level: 0.6 Volt; Window: open; Gain: 32x7.

Fe-K_α on LiF.

ZrC (8.55 wt% C)

kV	Beam current (nA)		Gross Peak Intensities (cps/nA)				Backgrounds (cps/nA)[1]				Peak k-ratios	
	$Zr\text{-}L_\alpha$	$C\text{-}K_\alpha$	$Zr\text{-}L_\alpha$		$C\text{-}K_\alpha$		$Zr\text{-}L_\alpha$		$C\text{-}K_\alpha$		$Zr\text{-}L_\alpha$	$C\text{-}K_\alpha$
			Zr	ZrC	Fe_3C	ZrC	Zr	ZrC	Fe_3C	ZrC		
4	100	200	6.47	5.81	2.98	4.62	0.03	0.03	0.23	0.33	0.8971±0.0068	1.5608±0.0022
6	100	300	19.28	17.38	3.60	4.58	0.10	0.07	0.23	0.39	0.9024±0.0060	1.2421±0.0240
8	100	300	35.04	31.61	3.58	4.19	0.13	0.10	0.22	0.41	0.9027±0.0034	1.1236±0.0260
10	100	300	49.92	45.37	3.34	3.74	0.17	0.17	0.21	0.41	0.9087±0.0038	1.0643±0.0257
12	--	300	--	--	3.02	3.29	--	--	0.20	0.41	----------	1.0195±0.0237
15	100	300	91.67	83.21	2.42	2.53	0.32	0.31	0.17	0.39	0.9075±0.0044	0.9533±0.0537
20	30	300	125.09	114.49	1.86	2.09	0.42	0.37	0.17	0.36	0.9154±0.0010	1.0248±0.0236
25	50	300	160.52	146.25	1.53	1.77	0.51	0.46	0.14	0.31	0.9111±0.0065	1.0474±0.0337
30	50	300	171.26	154.85	1.30	1.57	0.54	0.52	0.14	0.27	0.9040±0.0052	1.1221±0.0399

[1] Background for Carbon measured at position of Carbon Peak and composed on basis of weight fraction of constituent element (See II.1.); that of Zr measured at ± 5 mm on either side of the peak and interpolated.

P.H.A. Settings: $Zr\text{-}L_\alpha$: Counter H.T. 1600 Volt; Lower Level: 0.6 Volt; Window: open ; Gain: 128x7.4.

$C\text{-}K_\alpha$: " " 1700 Volt; " " : 1.0 Volt; " : 2.0 Volt; Gain: 64x5.

$Zr\text{-}L_\alpha$ on PET; $C\text{-}K_\alpha$ on Stearate.

NbC (8.55 wt% C)

kV	Beam current (nA)		Gross Peak Intensities (cps/nA)				Backgrounds (cps/nA)[1]				Peak k-ratios	
	$Nb\text{-}L_\alpha$	$C\text{-}K_\alpha$	$Nb\text{-}L_\alpha$		$C\text{-}K_\alpha$		$Nb\text{-}L_\alpha$		$C\text{-}K_\alpha$		$Nb\text{-}L_\alpha$	$C\text{-}K_\alpha$
			Nb	NbC	Fe_3C	NbC	Nb	NbC	Fe_3C	NbC		
4	150	200	7.02	6.20	2.98	4.24	0.04	0.03	0.23	0.32	0.8840±0.0088	1.4283±0.0149
6	200	300	23.46	20.50	3.60	4.07	0.09	0.08	0.23	0.34	0.8738±0.0044	1.1064±0.0250
8	150	300	43.63	38.83	3.58	3.91	0.14	0.13	0.22	0.40	0.8899±0.0036	1.0440±0.0260
10	100	300	62.22	55.81	3.34	3.45	0.22	0.18	0.21	0.38	0.8973±0.0038	0.9830±0.0296
12	--	300	---	---	3.02	3.04	--	---	0.20	0.40	-----	0.9380±0.0222
15[X]	30	300	110.68	99.70	2.42	2.50	0.35	0.26	0.17	0.37	0.9013±0.0054	0.9466±0.0353
20	20	300	151.81	137.66	1.86	1.99	0.48	0.37	0.17	0.32	0.9072±0.0054	0.9858±0.0220
25	20	300	183.35	167.45	1.53	1.79	0.52	0.45	0.14	0.29	0.9134±0.0055	1.0819±0.0303
30	20	300	203.86	187.51	1.30	1.47	0.63	0.56	0.14	0.28	0.9199±0.0046	1.0249±0.0682

[1] Background for Carbon measured at position of Carbon Peak and composed on basis of weight fraction of constituent element (see II.1); that of Nb measured at ± 5 mm on either side of the peak and interpolated.

P.H.A. Settings: $Nb\text{-}L_\alpha$: Counter H.T. 1600 Volt; Lower Level: 0.6 Volt; Window: Open; Gain 128x8

$C\text{-}K_\alpha$: " " 1700 Volt; " " : 1.0 Volt; " : 2.0 Volt; Gain: 64x5

[X] From 15 kV on : $Nb\text{-}L_\alpha$: " " 1600 Volt; " " : 1.25 Volt; " : 1.5 Volt; Gain:128x7.4

$Nb\text{-}L_\alpha$ on PET; $C\text{-}K_\alpha$ on Stearate

Mo_2C (5.58 wt% C)

kV	Beam Current (nA)		Gross Peak Intensities (cps/nA)				Background (cps/nA)[1]				Peak k-ratios	
	Mo-L_α	C-K_α	Mo-L_α		C-K_α		Mo-L_α		C-K_α		Mo-L_α	C-K_α
			Mo	Mo_2C	Fe_3C	Mo_2C	Mo	Mo_2C	Fe_3C	Mo_2C		
4	150	200	7.49	6.73	2.98	2.80	0.04	0.04	0.23	0.29	0.8981±0.0089	0.9156±0.0170
6	150	300	26.23	24.04	3.00	3.06	0.10	0.09	0.23	0.32	0.9166±0.0091	0.8124±0.0200
8	30	300	49.05	45.05	3.58	2.88	0.13	0.17	0.22	0.33	0.9175±0.0082	0.7575±0.0180
10	30	300	71.88	66.43	3.34	2.64	0.30	0.23	0.21	0.35	0.9249±0.0065	0.7335±0.0070
12	10	300	95.17	88.04	3.02	2.38	0.40	0.40	0.20	0.35	0.9248±0.0100	0.7178±0.0203
15	5	300	128.68	120.22	2.42	1.96	0.45	0.45	0.17	0.32	0.9340±0.0126	0.7262±0.0193
20	5	300	180.25	168.93	1.86	1.55	0.53	0.60	0.17	0.30	0.9366±0.0103	0.7420±0.0195
25	5	300	216.78	203.28	1.53	1.34	0.87	0.90	0.14	0.27	0.9415±0.0095	0.7694±0.0374
30	5	300	242.70	229.57	1.30	1.17	0.93	0.90	0.14	0.26	0.9458±0.0085	0.7885±0.0345

[1] Background for Carbon measured at position of Carbon Peak and composed on basis of weight fraction of constituent element (See II.1); that of Mo measured at ± 5 mm on either side of the peak and interpolated.

P.H.A. Settings: Mo-L_α : Counter H.T.: 1600 Volt; Lower Level: 0.5 Volt; Window: open; Gain 128x5

C-K_α : " " : 1700 Volt; " " : 1.0 Volt; " : 2.0 Volt; Gain 64x5.

Mo-L_α on PET; C-K_α on Stearate.

TaC (6.00 wt%C)

kV	Beam Current (nA)		Gross Peak Intensities (cps/nA)				Backgrounds (cps/nA)[1]				Peak k-ratios	
			Ta-M_α		C-K_α		Ta-M_α		C-K_α			
	Ta-M_α	C-K_α	Ta	TaC	Fe_3C	TaC	Ta	TaC	Fe_3C	TaC	Ta-M_α	C-K_α
4	300	200	6.07	5.39	2.97	3.27	0.04	0.04	0.23	0.19	0.8865±0.0071	1.1264±0.0180
6	300	300	14.52	12.79	3.61	3.55	0.11	0.09	0.23	0.22	0.8873±0.0044	0.9846±0.0104
8	200	300	23.49	20.71	3.60	3.43	0.16	0.15	0.22	0.24	0.8812±0.0044	0.9430±0.0114
10	100	300	30.96	27.33	3.39	3.14	0.19	0.18	0.21	0.24	0.8824±0.0053	0.9131±0.0121
12	100	300	38.67	34.55	2.96	2.76	0.25	0.23	0.20	0.22	0.8933±0.0045	0.9182±0.0114
15	66.8	300	48.75	43.75	2.60	2.48	0.31	0.26	0.17	0.22	0.8979±0.0067	0.9328±0.0118
20	20	300	60.06	54.94	2.03	1.99	0.35	0.32	0.17	0.20	0.9148±0.0105	0.9592±0.0158
25	10	300	65.43	60.07	1.61	1.65	0.29	0.42	0.14	0.17	0.9157±0.0121	1.0048±0.0160
30	50	300	71.61	65.87	1.31	1.47	0.65	0.63	0.14	0.17	0.9194±0.0067	1.1049±0.0168

	Ta-L_α	Ta-L_α		Ta-L_α		Ta-L_α
12	100	23.03	20.15	1.73	1.59	0.8715±0.0042
15	66.8	90.43	81.19	2.84	2.60	0.8973±0.0045
20	20	250.82	226.79	4.65	4.18	0.9045±0.0040
25	10	427.91	383.67	6.85	6.19	0.8965±0.0045
30	5	609.42	558.16	9.03	8.08	0.9162±0.0047

[1]Background for Carbon measured at position of Carbon Peak and composed on basis of weight fraction of constituent element (See II.1). that of Ta measured at ± 5 mm on either side of the peak and interpolated.

P.H.A. Setting: Ta-M_α: Counter H.T.: 1600 Volt; Lower Level: 0.5 Volt; Window: 3.0 Volt; Gain : 64x6
Ta-L_α: " 1600 Volt; " 0.5 Volt; " open ; Gain: 32x5.8
C-K_α: " 1700 Volt; " 1.0 Volt; " 2.0 Volt; Gain: 64x5

Ta-M_α on PET, Ta-L_α on LiF, C-K_α on Stearate.

Ta_2C (3.00 wt%)

kV	Beam Current (nA)		Gross Peak Intensities (cps/nA)				Backgrounds (cps/nA)[1]				Peak k-ratios	
	$Ta\text{-}M_\alpha$	$C\text{-}K_\alpha$	$Ta\text{-}M_\alpha$		$C\text{-}K_\alpha$		$Ta\text{-}M_\alpha$		$C\text{-}K_\alpha$		$Ta\text{-}M_\alpha$	$C\text{-}K_\alpha$
			Ta	Ta_2C	Fe_3C	Ta_2C	Ta	Ta_2C	Fe_3C	Ta_2C		
4	300	--	6.00	5.63	--	--	0.04	0.04	--	--	0.9383±0.0157	---
6	300	--	14.52	13.58	--	--	0.11	0.09	--	--	0.9360±0.0100	---
8	200	--	23.49	22.07	--	--	0.16	0.15	--	--	0.9395±0.0116	---
10	100	--	30.96	29.08	--	--	0.19	0.17	--	--	0.9452±0.0051	---
12	100	--	38.67	36.77	--	--	0.25	0.23	--	--	0.9511±0.0039	---
15	50	--	49.14	46.92	--	--	0.36	0.36	--	--	0.9544±0.0060	---
20	20	--	60.06	57.65	--	--	0.35	0.40	---	--	0.9588±0.0222	---
25	10	--	65.43	63.97	--	--	0.29	0.35	--	--	0.9766±0.0116	---
30	50	--	71.61	69.19	--	--	0.65	0.63	--	--	0.9662±0.0081	---
	$Ta\text{-}L_\alpha$		$Ta\text{-}L_\alpha$				$Ta\text{-}L_\alpha$				$Ta\text{-}L_\alpha$	
12	100	--	23.03	21.56	--	--	1.73	1.59	--	--	0.9376±0.0100	---
15	50	--	91.08	81.45	--	--	2.76	2.73	--	--	0.9440±0.0069	---
20	20	--	250.82	236.17	--	--	4.65	4.55	--	--	0.9409±0.0024	---
25	10	--	427.91	403.88	--	--	6.85	6.44	--	--	0.9439±0.0047	---
30	5	--	609.42	586.78	--	--	9.03	8.36	--	--	0.9634±0.0060	---

[1]Background for Ta measured at ± 5 mm on either side of the peak and interpolated.

P.H.A. Settings: $Ta\text{-}M_\alpha$: Counter H.T.: 1600 Volt; Lower Level 0.5 Volt; Window: 3.0 Volt; Gain: 64x6

$Ta\text{-}L_\alpha$: " : 1600 Volt; " 0.5 Volt; " : open Gain: 32x5.8

$Ta\text{-}M_\alpha$ on PET; $Ta\text{-}L_\alpha$ on LiF

WC (6.13 wt% C)

kV	Beam Current (nA)		Gross Peak Intensities (cps/nA)				Backgrounds (cps/nA)[1]				Peak k-ratios	
	$W\text{-}M_\alpha$	$C\text{-}K_\alpha$	$W\text{-}M_\alpha$		$C\text{-}K_\alpha$		$W\text{-}M_\alpha$		$C\text{-}K_\alpha$		$W\text{-}M_\alpha$	$C\text{-}K_\alpha$
			W	WC	Fe_3C	WC	W	WC	Fe_3C	WC		
4	300	200	6.37	5.43	2.97	3.23	0.05	0.04	0.23	0.22	0.8524±0.0068	1.0982±0.0271
6	100	300	15.26	13.28	3.61	3.45	0.10	0.09	0.23	0.23	0.8700±0.0078	0.9510±0.0237
8	300	300	24.63	21.75	3.60	3.27	0.14	0.13	0.22	0.25	0.8829±0.0035	0.8928±0.0265
10	100	300	33.12	29.25	3.39	2.99	0.20	0.18	0.21	0.24	0.8831±0.0053	0.8671±0.0271
12	50	300	37.08	34.08	2.96	2.69	0.19	0.18	0.20	0.22	0.9178±0.0073	0.8951±0.0285
15	30	300	51.90	46.97	2.60	2.39	0.33	0.31	0.17	0.21	0.9048±0.0072	0.8990±0.0277
20	15	300	64.90	59.59	2.03	1.90	0.57	0.55	0.17	0.19	0.9178±0.0100	0.9163±0.0409
25	15	300	70.95	66.91	1.61	1.56	0.57	0.55	0.14	0.20	0.9429±0.0094	0.9253±0.0394
30	10	300	73.19	68.79	1.31	1.38	0.80	0.73	0.14	0.21	0.9402±0.0111	0.9966±0.0414
	$W\text{-}L_\alpha$		$W\text{-}L_\alpha$				$W\text{-}L_\alpha$				$W\text{-}L_\alpha$	
12	50	--	18.83	16.08	--	--	1.92	1.63	--	--	0.8544±0.0110	---
15	30	--	85.50	75.42	--	--	2.98	2.94	--	--	0.8783±0.0061	---
20	15	--	249.19	224.35	--	--	4.97	4.87	--	--	0.8987±0.0053	---
25	15	--	436.30	397.21	--	--	7.16	6.95	--	--	0.9094±0.0036	---
30	10	--	624.62	572.79	--	--	10.29	9.20	--	--	0.9174±0.0037	---

[1] Background for Carbon measured at position of Carbon Peak and composed on basis of weight fraction of constituent element (See II.1); that of W measured at ±5 mm on either side of the peak and interpolated.

P.H.A. Settings: $W\text{-}M_\alpha$: Counter H.T. 1600 Volt; Lower Level: 0.6 Volt; Window: open; Gain: 128x7.8
$W\text{-}L_\alpha$: " 1600 Volt; " 0.6 Volt; " : open; Gain: 32x5
$C\text{-}K_\alpha$: " 1700 Volt; " 1.0 Volt; " : 2.0 Volt; Gain: 64x5

$W\text{-}M_\alpha$ on PET; $W\text{-}L_\alpha$ on LiF
$C\text{-}K_\alpha$ on Stearate

W_2C (3.16 wt% C)

kV	Beam current (nA)		Gross Peak Intensities (cps/nA)				Backgrounds (cps/nA)[1]				Peak k-ratios	
	$W\text{-}M_\alpha$	$C\text{-}K_\alpha$	$W\text{-}M_\alpha$		$C\text{-}K_\alpha$		$W\text{-}M_\alpha$		$C\text{-}K_\alpha$		$W\text{-}M_\alpha$	$C\text{-}K_\alpha$
			W	W_2C	Fe_3C	W_2C	W	WC	Fe_3C	W_2C		
4	300	200	6.37	5.59	2.97	1.64	0.05	0.04	0.23	0.22	0.8786±0.0070	0.5205±0.0115
6	100	300	15.26	13.76	3.61	1.75	0.10	0.09	0.23	0.22	0.9017±0.0081	0.4529±0.0076
8	300	300	24.63	22.72	3.60	1.67	0.14	0.14	0.22	0.24	0.9219±0.0037	0.4236±0.0105
10	100	300	33.12	30.89	3.39	1.55	0.20	0.19	0.21	0.23	0.9326±0.0056	0.4144±0.0079
12	50	300	37.08	35.48	2.96	1.38	0.19	0.20	0.20	0.21	0.9564±0.0077	0.4247±0.0090
15	30	300	51.90	48.73	2.60	1.23	0.33	0.40	0.17	0.20	0.9372±0.0075	0.4258±0.0087
20	15	300	64.90	61.74	2.03	1.00	0.57	0.59	0.17	0.19	0.9505±0.0095	0.4335±0.0130
25	15	300	70.95	68.91	1.61	0.85	0.57	0.73	0.14	0.19	0.9687±0.0097	0.4443±0.0111
30	10	300	73.19	71.30	1.31	0.78	0.80	0.69	0.14	0.21	0.9754±0.0117	0.4842±0.0111
	$W\text{-}L_\alpha$		$W\text{-}L_\alpha$				$W\text{-}L_\alpha$				$W\text{-}L_\alpha$	
12	50	--	18.83	17.12	--	--	1.92	1.74	--	--	0.9094±0.0117	---
15	30	--	85.50	79.75	--	--	2.98	2.95	--	--	0.9307±0.0065	---
20	15	--	249.19	234.97	--	--	4.97	5.13	--	--	0.9411±0.0056	---
25	15	--	436.30	415.87	--	--	7.16	7.41	--	--	0.9518±0.0038	---
30	10	--	624.62	597.45	--	--	10.29	9.90	--	--	0.9564±0.0038	---

[1] Background for Carbon measured at position of Carbon Peak and composed on basis of weight fraction of constituent element (See III.); that of W measured at ± 5 mm on either side of the peak and interpolated.

P.H.A. Settings: $W\text{-}M_\alpha$: Counter H.T.: 1600 Volt; Lower Level: 0.6 Volt; Window: open; Gain: 128x7.8
$W\text{-}L_\alpha$: " 1600 Volt; " 0.6 Volt; " open; Gain: 32x5
$C\text{-}K_\alpha$: " 1700 Volt; " 1.0 Volt; " 2.0Volt;Gain: 64x5

Appendix B.1.

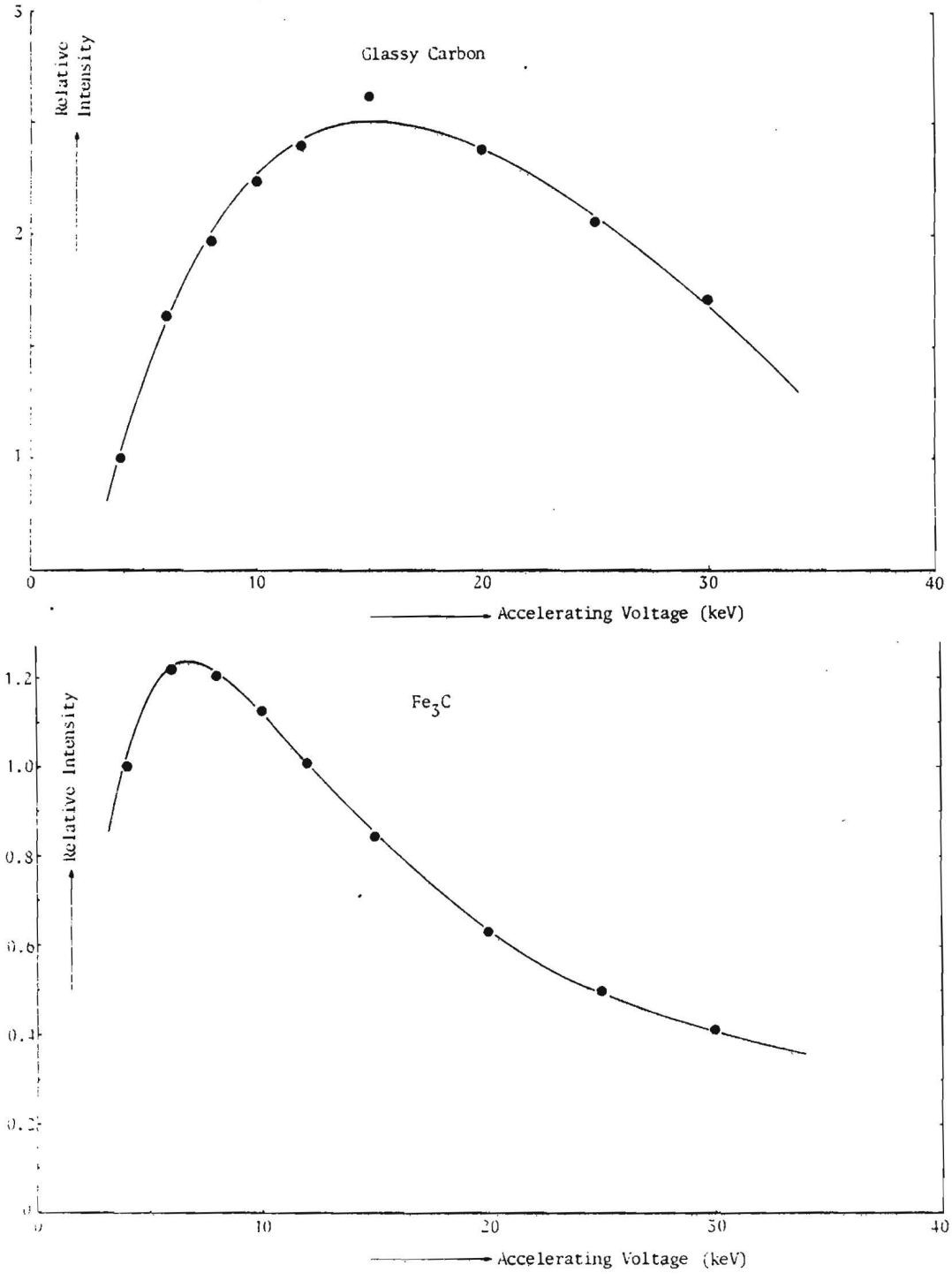

Relative Carbon-K_α intensities in Glassy Carbon and Fe_3C as a function of Accelerating Voltage.

Appendix B.2.

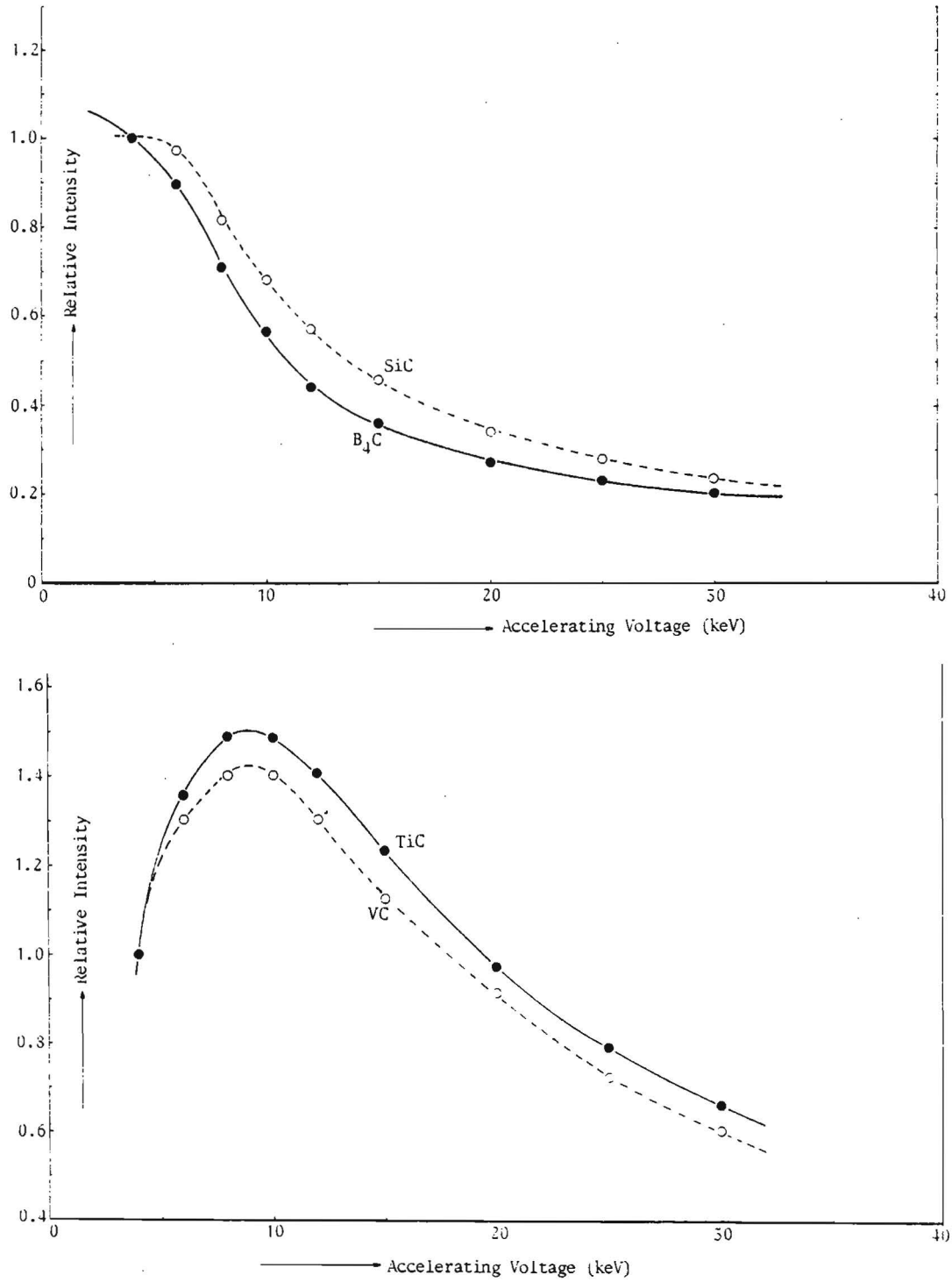

Relative Carbon-K_α intensities in B_4C, SiC, TiC and VC as a function of Accelerating Voltage.

Appendix B.3.

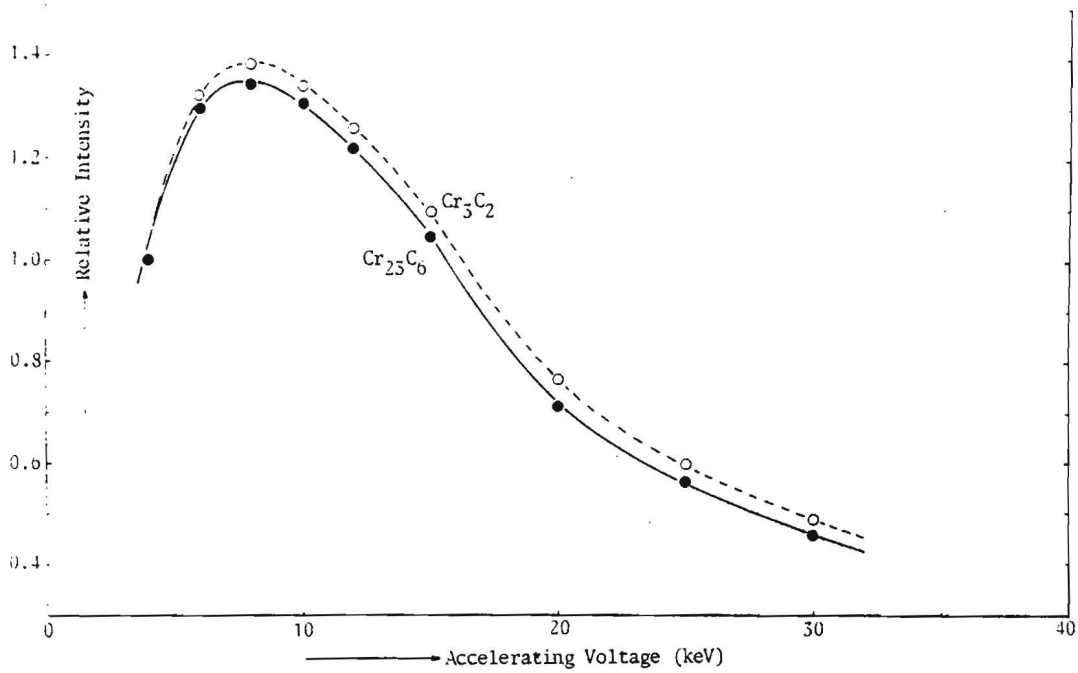

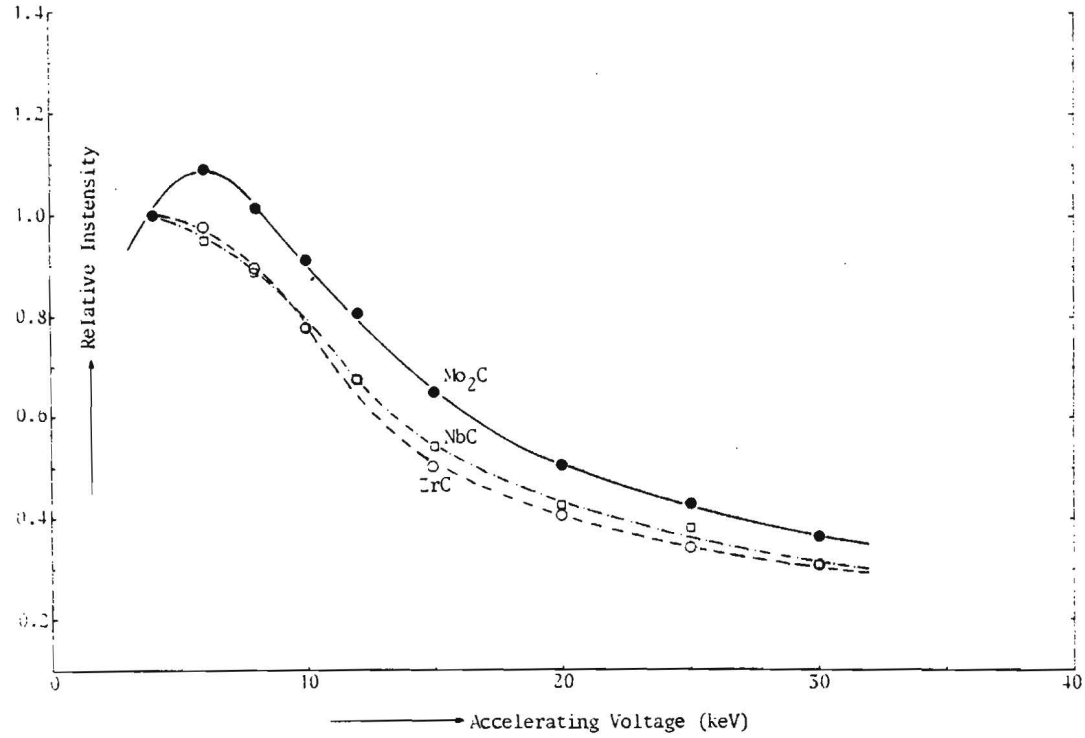

Relative Carbon-K_α intensities in $Cr_{23}C_6$, Cr_3C_2, ZrC, NbC and Mo_2C as a function of Accelerating Voltage.

Appendix B.4.

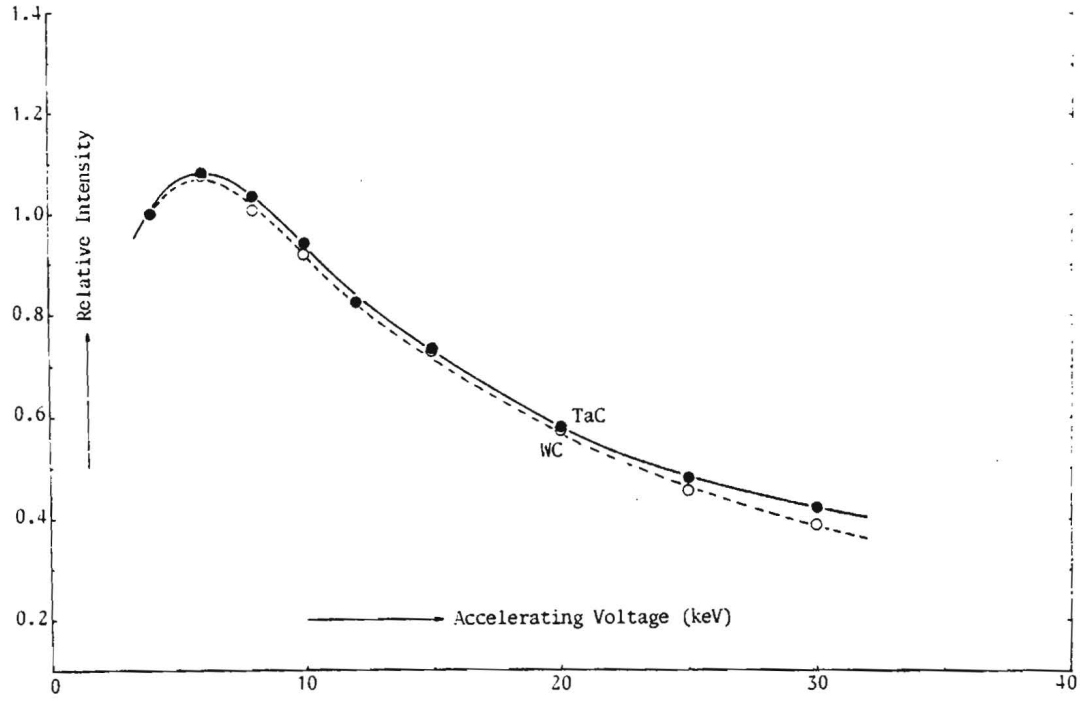

Relative Carbon-K_α intensities in TaC and WC as a function of Accelerating Voltage.

Appendix C.1.

Legend:

1 = atomic number of metal
2 = atomic number of carbon
3 = mass abs. coeff. of metal line in metal
4 = mass abs. coeff. of metal line in carbon
5 = critical excitation voltage of metal line
6 = weight fraction of metal
7 = k-ratio (smoothed!) of metal
8 = accelerating voltage (keV)
9 = take-off angle (deg.)
10 = type of metal line (K = 0, L = 1, M = 2)
11 = type of carbon line(≡K)

1	2	3	4	5	6	7	8	9	10	11
5	6	3350	6350	0.1880	0.7981	0.7754	4	40	0	0
5	6	3350	6350	0.1880	0.7981	0.7510	6	40	0	0
5	6	3350	6350	0.1880	0.7981	0.7297	8	40	0	0
5	6	3350	6350	0.1880	0.7981	0.7109	10	40	0	0
5	6	3350	6350	0.1880	0.7981	0.6960	12	40	0	0
5	6	3350	6350	0.1880	0.7981	0.6795	15	40	0	0
5	6	3350	6350	0.1880	0.7981	0.6630	20	40	0	0
5	6	3350	6350	0.1880	0.7981	0.6565	25	40	0	0
5	6	3350	6350	0.1880	0.7981	0.6549	30	40	0	0
14	6	350	455	1.8399	0.7005	0.6799	4	40	0	0
14	6	350	455	1.8399	0.7005	0.6798	6	40	0	0
14	6	350	455	1.8399	0.7005	0.6789	8	40	0	0
14	6	350	455	1.8399	0.7005	0.6787	10	40	0	0
14	6	350	455	1.8399	0.7005	0.6779	12	40	0	0
14	6	350	455	1.8399	0.7005	0.6762	15	40	0	0
14	6	350	455	1.8399	0.7005	0.6730	20	40	0	0
14	6	350	455	1.8399	0.7005	0.6681	25	40	0	0
14	6	350	455	1.8399	0.7005	0.6630	30	40	0	0
22	6	108	26	4.9650	0.8159	0.7831	6	40	0	0
22	6	108	26	4.9650	0.8159	0.7861	8	40	0	0
22	6	108	26	4.9650	0.8159	0.7887	10	40	0	0
22	6	108	26	4.9650	0.8159	0.7909	12	40	0	0
22	6	108	26	4.9650	0.8159	0.7938	15	40	0	0
22	6	108	26	4.9650	0.8159	0.7980	20	40	0	0
22	6	108	26	4.9650	0.8159	0.8012	25	40	0	0
22	6	108	26	4.9650	0.8159	0.8033	30	40	0	0
23	6	95	20	5.4639	0.8399	0.7951	6	40	0	0
23	6	95	20	5.4639	0.8399	0.8013	8	40	0	0
23	6	95	20	5.4639	0.8399	0.8064	10	40	0	0
23	6	95	20	5.4639	0.8399	0.8111	12	40	0	0
23	6	95	20	5.4639	0.8399	0.8161	15	40	0	0
23	6	95	20	5.4639	0.8399	0.8220	20	40	0	0
23	6	95	20	5.4639	0.8399	0.8264	25	40	0	0
23	6	95	20	5.4639	0.8399	0.8295	30	40	0	0
24	6	83	15	5.9889	0.9431	0.9252	8	40	0	0
24	6	83	15	5.9889	0.9431	0.9257	10	40	0	0
24	6	83	15	5.9889	0.9431	0.9259	12	40	0	0
24	6	83	15	5.9889	0.9431	0.9261	15	40	0	0
24	6	83	15	5.9889	0.9431	0.9265	20	40	0	0
24	6	83	15	5.9889	0.9431	0.9270	25	40	0	0

Appendix C.1. (Continued)

1	2	3	4	5	6	7	8	9	10	11
24	6	83	15	5.9889	0.9431	0.9277	30	40	0	0
24	6	83	15	5.9889	0.9089	0.8790	8	40	0	0
24	6	83	15	5.9889	0.9089	0.8819	10	40	0	0
24	6	83	15	5.9889	0.9089	0.8841	12	40	0	0
24	6	83	15	5.9889	0.9089	0.8874	15	40	0	0
24	6	83	15	5.9889	0.9089	0.8918	20	40	0	0
24	6	83	15	5.9889	0.9089	0.8949	25	40	0	0
24	6	83	15	5.9889	0.9089	0.8971	30	40	0	0
24	6	83	15	5.9889	0.8665	0.8310	8	40	0	0
24	6	83	15	5.9889	0.8665	0.8321	10	40	0	0
24	6	83	15	5.9889	0.8665	0.8357	12	40	0	0
24	6	83	15	5.9889	0.8665	0.8385	15	40	0	0
24	6	83	15	5.9889	0.8665	0.8421	20	40	0	0
24	6	83	15	5.9889	0.8665	0.8454	25	40	0	0
24	6	83	15	5.9889	0.8665	0.8478	30	40	0	0
26	6	69	9	7.1110	0.9332	0.9171	8	40	0	0
26	6	69	9	7.1110	0.9332	0.9193	10	40	0	0
26	6	69	9	7.1110	0.9332	0.9215	12	40	0	0
26	6	69	9	7.1110	0.9332	0.9239	15	40	0	0
26	6	69	9	7.1110	0.9332	0.9270	20	40	0	0
26	6	69	9	7.1110	0.9332	0.9290	25	40	0	0
26	6	69	9	7.1110	0.9332	0.9303	30	40	0	0
40	6	778	284	2.2229	0.9144	0.8980	4	40	1	0
40	6	778	284	2.2229	0.9144	0.9010	6	40	1	0
40	6	778	284	2.2229	0.9144	0.9032	8	40	1	0
40	6	778	284	2.2229	0.9144	0.9054	10	40	1	0
40	6	778	284	2.2229	0.9144	0.9070	12	40	1	0
40	6	778	284	2.2229	0.9144	0.9087	15	40	1	0
40	6	778	284	2.2229	0.9144	0.9094	20	40	1	0
40	6	778	284	2.2229	0.9144	0.9100	25	40	1	0
40	6	778	284	2.2229	0.9144	0.9109	30	40	1	0
41	6	726	239	2.3709	0.9144	0.8750	4	40	1	0
41	6	726	239	2.3709	0.9144	0.8821	6	40	1	0
41	6	726	239	2.3709	0.9144	0.8880	8	40	1	0
41	6	726	239	2.3709	0.9144	0.8929	10	40	1	0
41	6	726	239	2.3709	0.9144	0.8969	12	40	1	0
41	6	726	239	2.3709	0.9144	0.9021	15	40	1	0
41	6	726	239	2.3709	0.9144	0.9087	20	40	1	0
41	6	726	239	2.3709	0.9144	0.9134	25	40	1	0
41	6	726	239	2.3709	0.9144	0.9175	30	40	1	0
42	6	684	202	2.5230	0.9441	0.9059	4	40	1	0
42	6	684	202	2.5230	0.9441	0.9127	6	40	1	0
42	6	684	202	2.5230	0.9441	0.9182	8	40	1	0
42	6	684	202	2.5319	0.9441	0.9224	10	40	1	0
42	6	684	202	2.5230	0.9441	0.9263	12	40	1	0
42	6	684	202	2.5230	0.9441	0.9312	15	40	1	0
42	6	684	202	2.5230	0.9441	0.9373	20	40	1	0
42	6	684	202	2.5230	0.9441	0.9417	25	40	1	0
42	6	684	202	2.5230	0.9441	0.9457	30	40	1	0
73	6	1274	464	1.7430	0.9400	0.8764	4	40	2	0
73	6	1274	464	1.7430	0.9400	0.8814	6	40	2	0
73	6	1274	464	1.7430	0.9400	0.8861	8	40	2	0
73	6	1274	464	1.7430	0.9400	0.8905	10	40	2	0
73	6	1274	464	1.7430	0.9400	0.8942	12	40	2	0
73	6	1274	464	1.7430	0.9400	0.8999	15	40	2	0
73	6	1274	464	1.7430	0.9400	0.9087	20	40	2	0
73	6	1274	464	1.7430	0.9400	0.9162	25	40	2	0
73	6	1247	464	1.7430	0.9400	0.9219	30	40	2	0
73	6	159	4	9.8769	0.9400	0.8819	12	40	1	0
73	6	159	4	9.8769	0.9400	0.8885	15	40	1	0
73	6	159	4	9.8769	0.9400	0.8979	20	40	1	0
73	6	159	4	9.8769	0.9400	0.9059	25	40	1	0
73	6	159	4	9.8769	0.9400	0.9129	30	40	1	0
73	6	1274	464	1.7430	0.9699	0.9342	4	40	2	0
73	6	1274	464	1.7430	0.9699	0.9389	6	40	2	0
73	6	1274	464	1.7430	0.9699	0.9428	8	40	2	0
73	6	1274	464	1.7430	0.9699	0.9461	10	40	2	0
73	6	1274	464	1.7430	0.9699	0.9490	12	40	2	0
73	6	1274	464	1.7430	0.9699	0.9539	15	40	2	0

Appendix C.1. (Continued)

1	2	3	4	5	6	7	8	9	10	11
73	6	1274	464	1.7430	0.9699	0.9602	20	40	2	0
73	6	1274	464	1.7430	0.9699	0.9659	25	40	2	0
73	6	1274	464	1.7430	0.9699	0.9701	30	40	2	0
73	6	159	4	9.8769	0.9699	0.9347	12	40	1	0
73	6	159	4	9.8769	0.9699	0.9406	15	40	1	0
73	6	159	4	9.8769	0.9699	0.9452	20	40	1	0
73	6	159	4	9.8769	0.9699	0.9503	25	40	1	0
73	6	159	4	9.8769	0.9699	0.9543	30	40	1	0
74	6	1164	420	1.8139	0.9386	0.8559	4	40	2	0
74	6	1164	420	1.8139	0.9386	0.8711	6	40	2	0
74	6	1164	420	1.8139	0.9386	0.8823	8	40	2	0
74	6	1164	420	1.8139	0.9386	0.8909	10	40	2	0
74	6	1164	420	1.8139	0.9386	0.8986	12	40	2	0
74	6	1164	420	1.8139	0.9386	0.9081	15	40	2	0
74	6	1164	420	1.8139	0.9386	0.9211	20	40	2	0
74	6	1164	420	1.8139	0.9386	0.9327	25	40	2	0
74	6	1164	420	1.8139	0.9386	0.9428	30	40	2	0
74	6	151	4	10.1999	0.9386	0.8557	12	40	1	0
74	6	151	4	10.1999	0.9386	0.8781	15	40	1	0
74	6	151	4	10.1999	0.9386	0.8975	20	40	1	0
74	6	151	4	10.1999	0.9386	0.9092	25	40	1	0
74	6	151	4	10.1999	0.9386	0.9177	30	40	1	0
74	6	1164	420	1.8139	0.9699	0.8865	4	40	2	0
74	6	1164	420	1.8139	0.9699	0.9059	6	40	2	0
74	6	1164	420	1.8139	0.9699	0.9177	8	40	2	0
74	6	1164	420	1.8139	0.9699	0.9272	10	40	2	0
74	6	1164	420	1.8139	0.9699	0.9349	12	40	2	0
74	6	1164	420	1.8139	0.9699	0.9442	15	40	2	0
74	6	1164	420	1.8139	0.9699	0.9567	20	40	2	0
74	6	1164	420	1.8139	0.9699	0.9668	25	40	2	0
74	6	1164	420	1.8139	0.9699	0.9756	30	40	2	0
74	6	151	4	10.1999	0.9699	0.9153	12	40	1	0
74	6	151	4	10.1999	0.9699	0.9290	15	40	1	0
74	6	151	4	10.1999	0.9699	0.9431	20	40	1	0
74	6	151	4	10.1999	0.9699	0.9521	25	40	1	0
74	6	151	4	10.1999	0.9699	0.9580	30	40	1	0
0	0	0	0	0.0000	0.0000	0.0000	0	0	0	0
0	0	0	0	0.0000	0.0000	0.0000	0	0	0	0

Appendix C.2.

Legend:

1-7 See Appendix C.1.

8 = Area k-ratio for C-K_α rel. to Fe_3C (not smoothed!)

9 = accelerating voltage (keV)

10 = take-off angle

11 = type of metal line (K = 0, L = 1, M = 2)
(Carbon line is always K_α)

1	2	3	4	5	6	7	8	9	10	11
5	6	3350	6350	0.1880	0.7981	0.7755	1.3197	4	40	0
5	6	3350	6350	0.1880	0.7981	0.7510	0.9876	6	40	0
5	6	3350	6350	0.1880	0.7981	0.7298	0.7969	8	40	0
5	6	3350	6350	0.1880	0.7981	0.7110	0.6897	10	40	0
5	6	3350	6350	0.1880	0.7981	0.6960	0.5827	12	40	0
5	6	3350	6350	0.1880	0.7981	0.6795	0.5781	15	40	0
5	6	3350	6350	0.1880	0.7981	0.6630	0.5678	20	40	0
5	6	3350	6350	0.1880	0.7981	0.6565	0.6178	25	40	0
5	6	3350	6350	0.1880	0.7981	0.6550	0.6491	30	40	0
14	6	350	455	1.8400	0.7005	0.6800	2.6811	4	40	0
14	6	350	455	1.8400	0.7005	0.6798	2.1756	6	40	0
14	6	350	455	1.8400	0.7005	0.6790	1.8751	8	40	0
14	6	350	455	1.8400	0.7005	0.6787	1.6861	10	40	0
14	6	350	455	1.8400	0.7005	0.6780	1.5380	12	40	0
14	6	350	455	1.8400	0.7005	0.6762	1.4869	15	40	0
14	6	350	455	1.8400	0.7005	0.6730	1.4518	20	40	0
14	6	350	455	1.8400	0.7005	0.6682	1.5194	25	40	0
14	6	350	455	1.8400	0.7005	0.6630	1.5336	30	40	0
22	6	1	1	1.0000	0.8160	0.0000	2.7920	4	40	1
22	6	108	26	4.9650	0.8160	0.7831	3.1798	6	40	0
22	6	108	0	4.9650	0.8160	0.7861	3.5638	8	40	0
22	6	108	0	4.9650	0.8160	0.7888	3.8111	10	40	0
22	6	108	0	4.9650	0.8160	0.7910	4.0700	12	40	0
22	6	108	0	4.9650	0.8160	0.7938	4.2486	15	40	0
22	6	108	0	4.9650	0.8160	0.7980	4.4032	20	40	0
22	6	108	26	4.9650	0.8160	0.8012	4.4806	25	40	0
22	6	108	26	4.9650	0.8160	0.8033	4.4185	30	40	0
23	6	1	1	1.0000	0.8400	0.0000	2.4398	4	40	0
23	6	95	20	5.4640	0.8400	0.7952	2.6641	6	40	0
23	6	95	20	5.4640	0.8400	0.8013	2.9286	8	40	0
23	6	95	20	5.4640	0.8400	0.8065	3.1369	10	40	0
23	6	95	20	5.4640	0.8400	0.8111	3.2921	12	40	0
23	6	95	20	5.4640	0.8400	0.8162	3.3812	15	40	0
23	6	95	20	5.4640	0.8400	0.8220	3.6167	20	40	0
23	6	95	20	5.4640	0.8400	0.8265	3.5717	25	40	0
23	6	95	20	5.4640	0.8400	0.8295	3.5166	30	40	0
24	6	1	1	1.0000	0.9422	0.0000	0.9204	4	40	0
24	6	1	1	1.0000	0.9422	0.0000	0.9584	6	40	0
24	6	83	15	5.9890	0.9422	0.9252	1.0134	8	40	0
24	6	83	15	5.9890	0.9422	0.9257	1.0452	10	40	0
24	6	83	15	5.9890	0.9422	0.9259	1.0743	12	40	0
24	6	83	15	5.9890	0.9422	0.9261	1.0978	15	40	0
24	6	83	15	5.9890	0.9422	0.9265	1.0644	20	40	0
24	6	83	15	5.9890	0.9422	0.9271	1.1161	25	40	0
24	6	83	15	5.9890	0.9422	0.9278	1.0836	30	40	0
24	6	1	1	1.0000	0.9090	0.0000	1.4455	4	40	0
24	6	1	1	1.0000	0.9090	0.0000	1.5188	6	40	0
24	6	83	15	5.9890	0.9090	0.8790	1.6056	8	40	0
24	6	83	15	5.9890	0.9090	0.8819	1.6471	10	40	0
24	6	83	15	5.9890	0.9090	0.8842	1.6936	12	40	0

Appendix C.2. (Continued)

1	2	3	4	5	6	7	8	9	10	11
24	6	83	15	5.9890	0.9090	0.8875	1.7350	15	40	0
24	6	83	15	5.9890	0.9090	0.8918	1.7154	20	40	0
24	6	83	15	5.9890	0.9090	0.8950	1.7925	25	40	0
24	6	83	15	5.9890	0.9090	0.8972	1.7511	30	40	0
24	6	1	1	1.0000	0.8670	0.0000	2.0831	4	40	0
24	6	1	1	1.0000	0.8670	0.0000	2.2145	6	40	0
24	6	83	15	5.9890	0.8670	0.8310	2.3632	8	40	0
24	6	83	15	5.9890	0.8670	0.8332	2.4275	10	40	0
24	6	83	15	5.9890	0.8670	0.8358	2.5076	12	40	0
24	6	83	15	5.9890	0.8670	0.8385	2.6010	15	40	0
24	6	83	15	5.9890	0.8670	0.8422	2.5926	20	40	0
24	6	83	15	5.9890	0.8670	0.8455	2.6845	25	40	0
24	6	83	15	5.9890	0.8670	0.8478	2.6311	30	40	0
40	6	778	284	2.2230	0.9145	0.8981	1.1164	4	40	1
40	6	778	284	2.2230	0.9145	0.9011	0.8885	6	40	1
40	6	778	284	2.2230	0.9145	0.9033	0.8037	8	40	1
40	6	778	284	2.2230	0.9145	0.9055	0.7613	10	40	1
40	6	778	284	2.2230	0.9145	0.9070	0.7292	12	40	1
40	6	778	284	2.2230	0.9145	0.9088	0.6819	15	40	1
40	6	778	284	2.2230	0.9145	0.9095	0.7330	20	40	1
40	6	778	284	2.2230	0.9145	0.9100	0.7492	25	40	1
40	6	778	284	2.2230	0.9145	0.9110	0.8026	30	40	1
41	6	726	239	2.3710	0.9145	0.8750	1.1236	4	40	1
41	6	726	239	2.3710	0.9145	0.8822	0.8704	6	40	1
41	6	726	239	2.3710	0.9145	0.8880	0.8213	8	40	1
41	6	726	239	2.3710	0.9145	0.8930	0.7733	10	40	1
41	6	726	239	2.3710	0.9145	0.8970	0.7379	12	40	1
41	6	726	239	2.3710	0.9145	0.9022	0.7447	15	40	1
41	6	726	239	2.3710	0.9145	0.9088	0.7755	20	40	1
41	6	726	239	2.3710	0.9145	0.9135	0.8511	25	40	1
41	6	726	239	2.3710	0.9145	0.9175	0.8063	30	40	1
42	6	684	202	2.5230	0.9442	0.9060	0.7523	4	40	1
42	6	684	202	2.5230	0.9442	0.9128	0.6675	6	40	1
42	6	684	202	2.5230	0.9442	0.9182	0.6224	8	40	1
42	6	684	202	2.5230	0.9442	0.9225	0.6026	10	40	1
42	6	684	202	2.5230	0.9442	0.9264	0.5897	12	40	1
42	6	684	202	2.5230	0.9442	0.9312	0.5966	15	40	1
42	6	684	202	2.5230	0.9442	0.9373	0.6096	20	40	1
42	6	684	202	2.5230	0.9442	0.9418	0.6321	25	40	1
42	6	684	202	2.5230	0.9442	0.9458	0.6478	30	40	1
73	6	1274	464	1.7430	0.9400	0.8765	1.0899	4	40	2
73	6	1274	464	1.7430	0.9400	0.8815	0.9527	6	40	2
73	6	1274	464	1.7430	0.9400	0.8862	0.9124	8	40	2
73	6	1274	464	1.7430	0.9400	0.8905	0.8835	10	40	2
73	6	1274	464	1.7430	0.9400	0.8943	0.8885	12	40	2
73	6	1274	464	1.7430	0.9400	0.9000	0.9026	15	40	2
73	6	1274	464	1.7430	0.9400	0.9088	0.9281	20	40	2
73	6	1274	464	1.7430	0.9400	0.9162	0.9722	25	40	2
73	6	1274	464	1.7430	0.9400	0.9220	1.0691	30	40	2
74	6	1164	420	1.8140	0.9387	0.8560	1.0693	4	40	2
74	6	1164	420	1.8140	0.9387	0.8712	0.9260	6	40	2
74	6	1164	420	1.8140	0.9387	0.8823	0.8693	8	40	2
74	6	1164	420	1.8140	0.9387	0.8910	0.8443	10	40	2
74	6	1164	420	1.8140	0.9387	0.8987	0.8716	12	40	2
74	6	1164	420	1.8140	0.9387	0.9081	0.8754	15	40	2
74	6	1164	420	1.8140	0.9387	0.9212	0.8922	20	40	2
74	6	1164	420	1.8140	0.9387	0.9328	0.9010	25	40	2
74	6	1164	420	1.8140	0.9387	0.9428	0.9704	30	40	2
74	6	1164	420	1.8140	0.9684	0.8865	0.5315	4	40	2
74	6	1164	420	1.8140	0.9684	0.9060	0.4625	6	40	2
74	6	1164	420	1.8140	0.9684	0.9178	0.4325	8	40	2
74	6	1164	420	1.8140	0.9684	0.9272	0.4231	10	40	2
74	6	1164	420	1.8140	0.9684	0.9350	0.4337	12	40	2
74	6	1164	420	1.8140	0.9684	0.9443	0.4348	15	40	2
74	6	1164	420	1.8140	0.9684	0.9568	0.4426	20	40	2
74	6	1164	420	1.8140	0.9684	0.9668	0.4537	25	40	2
74	6	1164	420	1.8140	0.9684	0.9756	0.4944	30	40	2